Veronika Macher

Adjoint and Fundamental Scalar Fields coupled to Landau-gauge Yang-Mills Theory

Diplomarbeit

zur Erlangung des Magistergrades der Naturwissenschaften

verfasst am Institut für Physik, Fachbereich Theoretische Physik
der Karl-Franzens-Universität Graz

Betreuer: Univ.-Prof. Dr. Reinhard Alkofer

Mitbetreuer: Dr. Axel Maas

Acknowledgements

At this point I want to seize the opportunity to thank everyone who supported me in writing this thesis. First of all I am grateful to my supervisor, Dr. Reinhard Alkofer, who offered me the chance to work on this highly interesting topic of ongoing research.

Next, I want to thank my co-supervisor, Dr. Axel Maas for always finding time for me and never getting tired of answering my questions (often more than once!) as well as explaining physical concepts to me. Without his help I definitly would have been lost in the world of groups and tensor structures.

I am also very thankful to Dr. Markus Q. Huber for helping me a lot with Mathematica and Mag. Tina Herbst for a critical reading of the draft of this thesis and many physical discussions.

The financial support of the Paul-Urban-Stipendienstiftung enabled me to participate in several conferences and workshops. I am really grateful to them for giving me the opportunity to present my work in front of experts in this field.

Apart from physics, I especially want to thank my parents. Over the years they have supported me in every way possible and always motivated me to go on.

I am also grateful to my family and friends who showed interest in my 'freaky' work and patiently listened to my complaints.

Last but not least I want to thank my colleagues and friends at university who made my time there really enjoyable.

Contents

1. Introduction

According to today's belief there are four fundamental forces in nature: gravity and the electromagnetic, weak and strong interactions. The last three can be unified in the so-called standard model of elementary particles, but a complete quantum field theoretical description of gravity yet remains to be formulated. The theory within the standard model describing the strong interaction is called Quantum Chromodynamics (QCD). Despite the fact that it is widely accepted, the theory is not solved yet.

Unlike other forces, e.g. the electromagnetic force, the strong force does not decrease with distance. At very small distances the quarks behave like free particles. This behaviour is called asymptotic freedom and was shown by D. Politzer [1], D. Gross and F. Wilczek [2] in 1973, who were awarded the Nobel prize in 2004.

One of the most intriguing problems within QCD is confinement. This notion refers to the experimental fact that no single quark has ever been observed [3]. We say, the quarks are confined into hadrons, bound states consisting of two or three quarks and antiquarks which form a non-coloured object. The massless particles that are thought to mediate the strong interaction force are called gluons. Like quarks, single gluons have not been seen in experiment so far [3]. This allows us to take a step from the picture of quark confinement to the more general concept of colour confinement: there are no isolated particles in nature with non-vanishing colour charge. As far as theory is concerned, this circumstance still has to be proven. Right now there are different confinement mechanisms on the market, with the Gribov-Zwanziger [4] [5] [6] and the Kugo-Ojima [7] scenarios being the most relevant ones for the correlation functions to be treated here.

It is reasonable to assume that the interaction between quarks is responsible for the confining behaviour of coloured particles. One possible way to access the strong interaction is via the Wegner-Wilson loop [8] [9]. This quantity can be used to define a static quark potential that is convex, monotonically rising, but not rising faster than linearly [10].

Many different ways to calculate the potential have been proposed over the years. The resulting potential itself has some important properties: it is not only gauge group dependent but there is also a dependence on the representation of matter fields under the gauge group in question.

To illustrate this, figure 1.1 shows a schematic plot of the static potential for the gauge group $SU(N)$. The dashed line represents the case of matter in the fundamental representation and shows a linear rise. This means, that the strongly interacting particles are confined because the potential is increasing with the distance between them. However, as far as the adjoint representation is concerned the potential first shows a linear rise, but then it exhibits a flattening. This is associated with string breaking [11] [12].

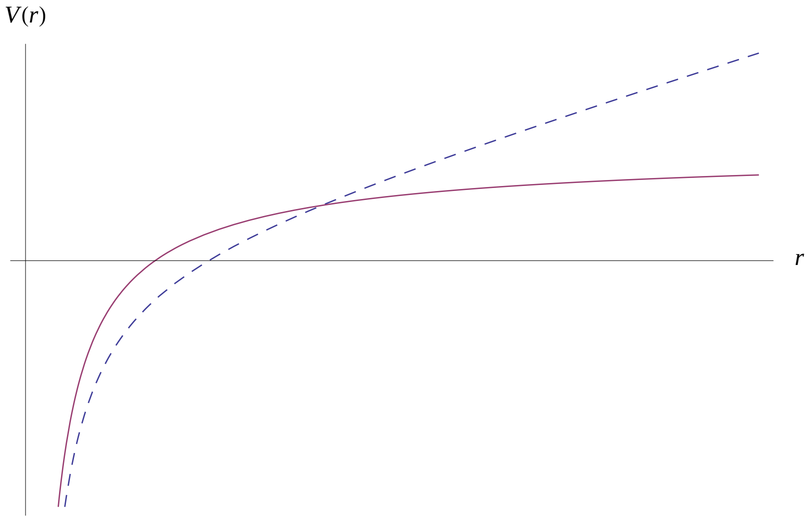

Figure 1.1.: Static potential for $SU(N)$: the dashed line stands for the fundamental and full line for the adjoint case, respectively.

The aim in this thesis was to investigate whether one can see such differences concerning the gauge group and the representation on the level of Greens functions.

To this end the simplest system possible in this context is investigated: charged scalar fields in the fundamental as well as the adjoint representation coupled to a Yang-Mills theory. One is interested in Green functions, which are in general gauge-dependent quantities. Therefore, a gauge fixing has to be done. In this thesis, the Landau gauge was chosen for several reasons: it is a covariant gauge and has been well studied over the years. Additionally, there are also technical advantages like good renormalization properties and the fact that only the minimum number of Lorentz tensor structures in the correlation functions are relevant [13]. These correlation functions can be determined using Dyson-Schwinger equations (DSEs).

As a consequence, the Dyson-Schwinger equations are derived first for both cases. The next step is to perform an infrared powercounting analysis [14] [15] [16] to obtain the infrared, and thus long-distance, behaviour and compare the results for both representations. The main part of this thesis will be a thorough analysis of the colour structure of the diagrams in the DSEs. This will be done in terms of group invariants. Then we apply the results to three specific gauge groups: $SU(2)$, $SU(3)$ and $G(2)$.

Although the confinement problem is fascinating, this is not the only reason to investigate this system. When quantum electrodynamics (QED) is neglected, the fundamental case can also be applied to the Higgs sector. This is due to the fact that the Dyson-Schwinger equations are topologically equivalent in the conifining and the Higgs phase, if the Landau gauge is chosen.

In addition, there is an equivalence between the infinite-temperature limit of a 4-dimensional Yang-Mills theory and 3-dimensional Yang-Mills theory coupled to a massive Higgs field in the adjoint representation [17] [18].

Similarly, a 5-dimensional field theory with a compactified 5^{th} dimension can be reduced to a 4-dimensional one plus a real scalar field. In case of an non-Abelian theory, the scalar is in adjoint representation [19].

The structure of this thesis is as follows: After this introduction the second chapter is about group theory and what consequences arise from coupling a charged scalar field to a Yang-Mills theory in Landau gauge. In the third chapter the methods used, like Dyson-Schwinger equations and the infrared powercounting technique, are discussed. An analysis of the colour structure of the diagrams appearing in the Dyson-Schwinger equations is given in chapter four. The last two chapters contain a discussion of results as well as a summary and an outlook.

2. Yang-Mills Theory Including Adjointly and Fundamentally Charged Scalars

Quantum Chromodynamics is formulated as a local quantum field theory. Generalising the principle of local gauge invariance from the Abelian gauge theories like Quantum Electrodynamics one can construct other non-Abelian theories. This was first done by C. N. Yang and R. Mills [20]. The result is Yang-Mills theory.

2.1. Yang-Mills Theory

To investigate the differences and dependencies mentioned in the introduction let us construct the simplest system suitable for this purpose. We choose to work in Euclidean space-time because of technical advantages [21] and start with the Yang-Mills Lagrangian in a covariant gauge [9]:

$$\mathcal{L} = \frac{1}{2} F^a_{\mu\nu} F^a_{\mu\nu} + \frac{1}{2\zeta} \left(\partial_\mu A^a_\mu \right)^2 + \bar{c}^a \partial_\mu D^{ab}_\mu c^b \tag{2.1}$$

Greek letters refer to Lorentz indices, latin ones to colour indices. ζ is the gauge parameter and for Landau gauge we have $\zeta \to 0$. A^a_ν stands for the gluon fields, $\bar{c}^a$ and c^b represent the anti-ghost and ghost field, respectively. The field strength tensor $F^a_{\mu\nu}$ is defined as

$$F^a_{\mu\nu} = \partial_\mu A^a_\nu - \partial_\nu A^a_\mu - g f^{abc} A^b_\mu A^c_\nu \tag{2.2}$$

and

$$D^{ab}_\mu = \delta^{ab} \partial_\mu + g f^{abc} A^c_\mu \tag{2.3}$$

is the covariant derivative in the adjoint representation. The factor g appearing in the formula denotes the gauge coupling. A derivation of this Lagrangian can be found in standard textbooks on quantum field theory like [9].

Up to now all we have is a pure gauge theory. To include massive particles, we couple a charged, massive scalar field to this Yang-Mills theory. Scalars are spinless bosons and therefore the system including them lacks any internal spin degrees of freedom compared to fermionic matter fields. Thus, the scalars are easier to deal with in calculations than fermions, but as a consequence more diagrams in the DSEs below are created. The full Lagrangian involving the scalar field is given by:

$$\mathcal{L} = \frac{1}{2}F^a_{\mu\nu}F^a_{\mu\nu} + \frac{1}{2\zeta}\left(\partial_\mu A^a_\mu\right)^2 + \bar{c}^a\partial_\mu D^{ab}_\mu c^b + \left(D_{\mu,ij}\Phi_j\right)^\dagger\left(D_{\mu,ik}\Phi_k\right) - m^2\Phi^\dagger_i\Phi_i - \frac{h}{4!}\left(\Phi^\dagger_i\Phi_i\right)^2. \tag{2.4}$$

If the scalar is in the adjoint representation, the covaraint derivatives in the last three terms look like (2.3). For any other (including the fundamental) representation the covariant derivative has a slightly different form:

$$D_{\mu,ij} = \delta_{ij}\partial_\mu - ig\left(\frac{t^a}{2}\right)_{ij} A^a_\mu \tag{2.5}$$

where t^a is the generator of any arbitrary representation but the adjoint. Throughout this thesis, the term 'arbitrary representation' will always exclude the adjoint representation. The scalar field is represented by Φ and its hermitean conjugate by $\Phi^\dagger$. Since we want the Lagrangian to be renormalizable in four space-time dimensions, the last three terms in equation 2.4 are the only allowed possibilities for including scalar fields. There is an expression involving a derivative of the scalar fields, a mass term and a term proportional to Φ^4. The mass of the scalar is given by m and h is a self-coupling between the scalars that has to be distinguished from the gauge coupling g.

2.2. Group Theory: Lie Algebra and Representations

Since the Lagrangian of the system is invariant under a gauge transformation, quantum chromodynamics is a gauge theory. In the case of QCD, the underlying symmetry group is $SU(3)$, which is one of the main sequence Lie groups.

A Lie group is a continuous group. Its infinitesimal group elements can be written down by

$$g(\alpha) = 1 + i\alpha^a t^a + \mathcal{O}\left(\alpha^2\right). \tag{2.6}$$

The Hermitian operators t^a are the generators of the symmetry group while the α^a stand for the group parameters.

The generators t^a of a Lie group form a vector space. This vector space including the commutator as the algebra multiplication is called a Lie algebra. Thus, the generators of a Lie group obey the rule

$$[t^a, t^b] = if^{abc}t^c. \tag{2.7}$$

The factors f^{abc} are named structure constants. They are antisymmetric and, like the generators, they fulfill the Jacobi identity:

$$\left[t^a, \left[t^b, t^c\right]\right] + \left[t^b, \left[t^c, t^a\right]\right] + \left[t^c, \left[t^a, t^b\right]\right] = 0 \tag{2.8}$$

$$f^{ade}f^{bcd} + f^{bde}f^{cad} + f^{cde}f^{abd} = 0. \tag{2.9}$$

For the sake of completeness and because in this thesis also one of the exceptional Lie groups is included, the classification of Lie algebras will be stressed at this point. [1]

In physics one is mostly interested in compact Lie groups, because they have unitary, finite-dimensional representations. By imposing the additional condition that the Lie algebra has to be simple - i.e. no mutually commuting sets of generators within the algebra - the possibilities for a Lie algebra are further restricted. All possible Lie groups can be classified into three families and five exceptions:

- unitary transformations of N-dimensional vectors,
- orthogonal transformations of N-dimensional vectors,
- symplectic transformations of 2N-dimensional vectors,
- five exceptional groups: $G(2), F(4), E(6), E(7), E(8)$.

Our goal is to describe the fields appearing in the Lagrangian of the system. This can be done by using a finite-dimensional unitary representation of the underlying algebra. Since the fact that a Lie algebra represents different groups, e.g. $su(3)$ by $SU(3)$ or $SU(3)/Z(3)$, is not relevant here, it should be noted that these terms are used synonymously, as it is common language use in this field.

Roughly speaking, a finite-dimensional representation is a mapping of the group on a set of matrices in a vector space. Any arbitrary reducible representation can be written as a sum of irreducible representations. The basic irreducible representations are also called fundamental representations and for $SU(N)$ it is an N-dimensional complex vector. Another irreducible representation that can be constructed for every Lie algebra is the adjoint representation, which consists of the generators of the algebra. The structure constants correspond to the representation matrices:

$$\left(t_A^b\right)_{ac} = i f^{abc}. \tag{2.10}$$

At this point some other properties and representation-dependent quantities that are relevant in this work will be introduced.

The generators of a Lie algebra are Hermitian and traceless:

$$\left(t^a\right)^\dagger = t^a, \tag{2.11}$$

$$\left(t^a\right)_{ii} = 0. \tag{2.12}$$

Next, the relation

$$\left(t^a\right)_{ij} \left(t^b\right)_{ji} = Tr\{t^a t^b\} = \delta_{ab} T_R \tag{2.13}$$

yields an index constant T_R for every representation that can be fixed by the normalization chosen. Here, the choice for the index constant is

$$T_R = \frac{1}{2}. \tag{2.14}$$

[1] For more information on Lie groups and group theory in general the reader may consult [22] [23] [24] or similar textbooks on group theory.

The operator

$$t^2 = t^a t^a \tag{2.15}$$

commutes with all generators of the group. This is valid for any simple Lie algebra. t^2 is called the quadratic Casimir operator and is proportional to the unit matrix. From now on it will be denoted by C_R (C_A) for an arbitrary (adjoint) representation.

Similarly, the dimension of the representations are given by the expressions N_R and N_A for arbitrary and adjoint representation, respectively. There is also a useful relation between the Casimir operator for an arbitrary representation and the index constant:

$$N_R C_R = N_A T_R. \tag{2.16}$$

There are other invariant tensors that can be constructed via so-called symmetrized traces STr for each representation R [25]:

$$d_R^{i_1...i_n} = STr\{t_R^{i_1}...t_R^{i_n}\} = \frac{1}{n!}\sum_n Tr\{t_R^{i_{\pi(1)}}...t_R^{i_{\pi(n)}}\}. \tag{2.17}$$

In this expression for symmetrized traces one is summing over all permutations of the indices $i_1...i_n$. One can have one of the indices fixed on a position and permute the ones left. It is sufficient to consider only symmetrized traces since every trace over a number of generators can be written as a completely symmetric trace plus terms of lower order in the generators. These lower order terms can also be expressed in terms of symmetrized traces. In this thesis, $n = 4$ will be the highest occurring number of indices.

The last quantities needed for the evaluation of the colour factors are given by

$$d33 = \left(d_R^{abc}\right)^2 \tag{2.18}$$

as well as

$$d44 = \left(d_R^{abcd}\right)^2 \tag{2.19}$$

and

$$d444 = d^{abcd} d^{cdef} d^{efab}. \tag{2.20}$$

These are group dependent numbers. Their explicit values for the gauge groups we are interested in are given in chapter 5 along with the values of the other group invariants.

In chapter 4, where the analysis of the colour structure is presented, the colour structure of each diagram will first be calculated in terms of these five group invariants C_A, C_R, N_A, N_R, and T_R, as well as $d33$ and $d44$. After that, they will be replaced by their values for specific groups.

2.3. The Static Potential

The simplest way to observe confinement in a theory is to describe the interaction between the colour sources with the help of an attractive potential. Since QCD is a relativistic field theory, the strong interaction is associated with the creation of particles. This phenomenon cannot be described by a potential. This problem can be avoided by introducing infinite masses for the quarks in QCD. In that case, there will be no quark-antiquark pair creation because all the kinetic degrees of freedom of the quarks are frozen. The case of static quarks is also called the quenched case.

When speaking of a potential, one should thus always be aware of the fact that the interaction can only be interpreted as a potential, if static quarks are involved.

In the following the derivation of a potential between a quark-antiquark pair $q\bar{q}$ in a colour-singlet state is sketched. For details of the calculation itself the reader can consult [8] , where this formalism is also applied to QED as an instructive example. In order to define such a confining potential one starts with the Wilson loop:

$$U(\mathcal{C}) = \mathcal{P}\left[\exp\left(ig\int_{\mathcal{C}} dx^{\mu} A_{\mu}^{a}(x)\frac{t^{a}}{2}\right)\right], \tag{2.21}$$

where $\mathcal{C}$ is a closed curve in space and $\mathcal{P}$ is the path ordering operator. $A_{\mu}^{a}(x)$ denotes the gauge field and t^a a generator.

In general, the Wilson loop is a complex quantity, but its expectation value is real because of charge invariance. It represents a finite parallel displacement along the path $\mathcal{C}$.

The next step is to consider the vacuum expectation value of the Wilson loop:

$$W(\mathcal{C}) = \langle Tr\{U(\mathcal{C})\}\rangle = \frac{1}{Z}\int D[\mathbf{A}]Tr\{U(\mathcal{C})\}\exp\left(-S_E(\mathbf{A})\right) \tag{2.22}$$

wherein Z is given by:

$$Z = \int D[\mathbf{A}]\exp\left(-S_E(\mathbf{A})\right). \tag{2.23}$$

These integrals can be evaluated using the path integral formalism. S_E denotes the Euclidean action. The Wilson loop $U(\mathcal{C})$ as well as its expectation value $W(\mathcal{C})$ are gauge-invariant quantities.

In order to calculate the static potential $V(\mathbf{r})$, the path $\mathcal{C}$ is chosen as a planar closed curve. In this manner we arrive at an expression for $V(\mathbf{r})$:

$$V(\mathbf{r}) = \lim_{t\to\infty}\frac{\log W\left(\mathcal{C}(\mathbf{r},t)\right)}{t}, \tag{2.24}$$

in which $\mathcal{C}$ is written in terms of its space and time extent $\mathbf{r}$ and t.

The Wilson criterion for quark confinement follows from the interpretation of the expectation value (2.23) as a potential [8]. It states that if $W(\mathcal{C})$ for similarly shaped paths $\mathcal{C}$ decreases exponentially with the minimal surface area $A(\mathcal{C}) = \mathbf{r}t$ enclosed by $\mathcal{C}$, the theory is confining:

$$W(\mathcal{C}) \propto \exp\left(-\sigma A(\mathcal{C})\right) \qquad\qquad \text{for large } C \tag{2.25}$$

This is considered as a criterion for confinement because in that case a confining potential follows from (2.23) for large paths:

$$V(\mathbf{r}) \approx \sigma \mathbf{r} \qquad\qquad \text{for } \mathbf{r} \to \infty. \tag{2.26}$$

σ is called string constant and its estimated value in QCD is between $(400\text{ MeV})^2$ and $(450\text{ MeV})^2$.

Let us now have a closer look at the properties of the static potential. Using quantum field theoretical arguments it can be proven that the potential cannot rise faster than linearly [10]. Convexity is a consequence of the reflection positivity of gauge-invariant Euclidean n-point functions, so we have:

$$V''(\mathbf{r}) \geq 0. \tag{2.27}$$

Since the potential is also bounded from below, convexity also implies that $V(\mathbf{r})$ is monotonically rising with the distance:

$$V'(\mathbf{r}) \geq 0. \tag{2.28}$$

To illustrate this setting, schematic plots for different gauge groups and representations are shown on the following pages. Starting with the groups $SU(N)$, figure 2.1 depicts the potential for the fundamental representation. Aside from the Coulomb like part near the origin, it shows a linear rise. Thus, the quarks (or any coloured objects in the same representation) are confined by the potential that increases with the distance.

The adjoint case for $SU(N)$ can be seen in figure 2.2. Again, it starts with a Coulomb part but for larger distance the linear rise changes and a flattening of the potential occurs. This behaviour is associated with string breaking, a phenomenon that is explained as follows: The electric flux between two colour sources is squeezed into a thin, effectively one-dimensional flux tube. This flux tube is also referred to as string. At large distances this string can break via particle-antiparticle pair creation because this is energetically more favourable. Still, the quarks are confined because even if the string is breaking, the quarks immediately form bound states with the newly created dynamical quarks or gluons in the quenched case.

The gauge groups of primary interest in this work are $SU(2)$, $SU(3)$ and $G(2)$. As mentioned before, $SU(3)$ is the underlying symmetry group of QCD. $SU(2)$-Yang-

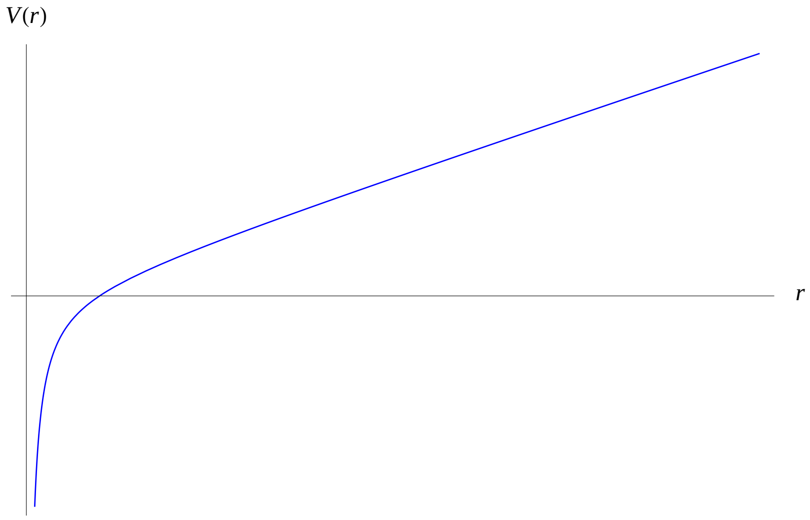

Figure 2.1.: Static potential for $SU(N)$ with matter in the fundamental representation.

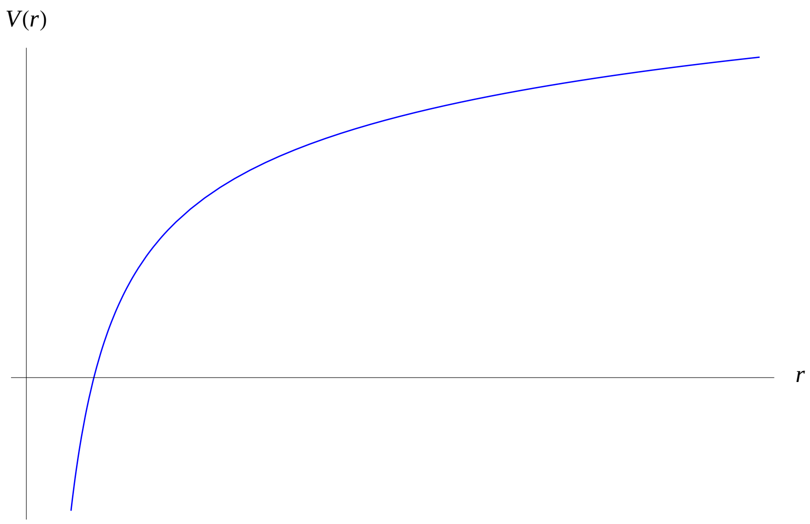

Figure 2.2.: Static potential for $SU(N)$ with matter in the adjoint representation.

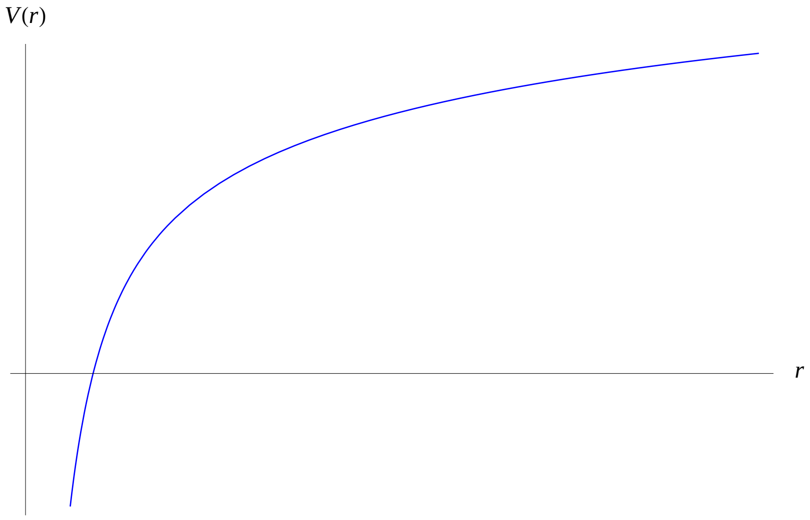

Figure 2.3.: Static potential for $G(2)$ with matter in the adjoint and fundamental representation.

Mills theory has been studied extensively on the lattice and is also the underlying group of the weak isospin. Since $G(2)$ is relatively unknown, a few statements about this group are in order. As stated in the previous chapter, the group $G(2)$ is one of the five exceptional Lie groups that are not part of the main families $SO(N)$, $SU(N)$ and $Sp(n)$. $G(2)$ is a subgroup of $SO(7)$, is generated by a non-Abelian, compact Lie algebra of rank 2 and has 14 generators. The dimension of the fundamental and adjoint representation of this group are 7 and 14, respectively.

Looking at the static potential for $G(2)$, figure 2.3, there is no difference between the adjoint and the fundamental representation. In both cases the potential shows the same behaviour as for $SU(N)$ in adjoint representation: the potential flattens at large distances [26]. Again, this corresponds to string breaking. The reason for this is, that for $G(2)$ gluons can screen quarks. More on this behaviour will follow below.

So why are we interested in this particular group?

The reason is that there is an important structural difference between $SU(N)$ and $G(2)$. The group $G(2)$ has a trivial center. The center of a group is the subgroup of elements in the group that commute with all others. In case of $G(2)$ this is just the identity. For $SU(N)$, the center is $Z(N)$.

In $SU(3)$ Yang-Mills theory confinement is often associated with the center [11]. At low temperatures the center symmetry is unbroken. Therefore, the static quarks and anti-quarks are confined by a string. On the other hand, at high temperatures the symmetry breaks spontaneously. This is called the deconfined phase.

Investigating the gauge group $G(2)$, one can see the triviality of the center has consequences on how confinement is realized. In $G(2)$ Yang-Mills theory, strings confining two $G(2)$ "quarks" can break via the creation of dynamical "gluons".

Thus, one static $G(2)$ "quark" can be screened by three $G(2)$ "gluons" [26]. This is similar to QCD, where a string connecting a quark-antiquark pair can break due to the creation of another quark-antiquark pair. It should be emphasized that like QCD, $G(2)$ Yang-Mills theory is expected to show colour confinement [26] [12].

The possible connection between center symmetry and confinement serves as a motivation for this thesis. However, this issue will not be discussed further in this context since it is not relevant for the technical details of the calculations. For more detailed information the reader is referred to [11] and [27].

At this point, it should be reemphasized that the behaviour of the potential explained before is only true for the quenched case. To avoid confusion, the meaning of 'quenched' in this context is discussed further. In this work, the term 'quenched' refers to the fact that contributions from the sea of particles will be ignored. Speaking in terms of the Dyson-Schwinger equations below, all diagrams containing closed scalar loops will be excluded in the quenched case.

There are no dynamical scalars available in this approximation, therefore, string breaking via the creation of scalar particle-antiparticle pairs is not possible. This leads to the linear rise of the $SU(N)$ potential in fundamental representation. The flattening of the $SU(N)$ potential at large r in adjoint representation is due to the screening of the matter field via dynamical gluons [11] [12]. The same mechanism is responsible for the behaviour of the $G(2)$ potential in both representations, only the number of gluons needed to screen a $G(2)$ matter field is different from the case of $SU(N)$, it is three [26].

Looking at the unquenched case, where contributions from the sea of (scalar) particles are allowed, the potential for the groups mentioned before in both representations exhibits a flattening at large distances. This is due to the fact that the string breaks either via the screening of the matter field by a number of dynamical gluons or via scalar particle-antiparticle pair creation.

3. Methods

Over the years many methods and procedures have been developed to analyse the strong interaction. For example, perturbation theory is and has been successfully applied to QCD, however this only works assuming the coupling constant is small at high ehergies. This is perfectly valid at small distances (i.e. at high momenta), where the quarks are asymptotically free. On the other hand, in the low-momentum range perturbation theory breaks down. Therefore, to gain insight in the infrared behaviour of the theory we have to rely on other techniques. To name a few of them, lattice calculations prove to be very useful [8] [28] as well as functional approaches like renormalization group equations (RGE) [29] and Dyson-Schwinger equations [30]. The latter are used in this thesis.

3.1. Dyson-Schwinger-Equations

Since we are dealing with a quantum field theory, our goal is to get information about the Green functions. The Dyson-Schwinger equations (DSEs) are the quantum equations of motion for Green functions. This formalism was first presented by F.J. Dyson [31] and J.S. Schwinger [32], who developed the concept independently. Dyson-Schwinger equations are a non-perturbative tool, hence one can cover the whole momentum regime of QCD. In particular, one is able to investigate the infrared behaviour of the theory [30].

The formalism is based on the idea that the integral over a total derivative of the generating functional vanishes:

$$\int D[\psi] \frac{d}{d\psi_i} e^{-S[\psi]+\psi_i J_i} = 0. \tag{3.1}$$

For the sake of simplicity all Lorentz, colour and representation indices have been absorbed into the index i. J_i is the source of an arbitrary field ψ_i. $S[\psi]$ is the action of the theory:

$$S = \int d^4x \mathcal{L}. \tag{3.2}$$

This leads to the following equation:

$$-\left.\frac{\delta S}{\delta \psi_i}\right|_{\psi_i=\Psi_i+\Delta^J_{ij}\frac{\delta}{\delta\Psi_j}} + \frac{\delta \Gamma}{\delta \Psi_i} = 0 \tag{3.3}$$

where Ψ_i denotes the averaged fields in the presence of the sources and Δ^J_{ij} is a

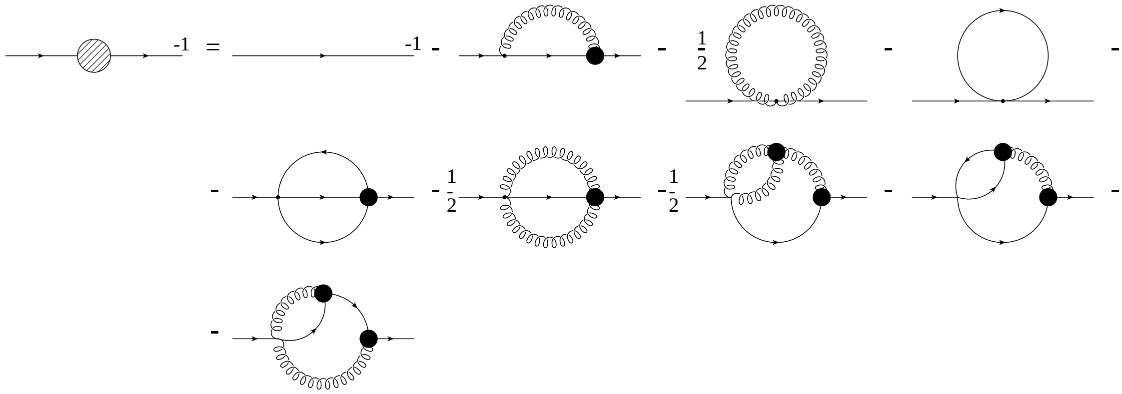

Figure 3.1.: Scalar propagator DSE: The full line represents a scalar field, the spring line a gluon and a dashed line a ghost. Black dots stand for dressed vertices and propagators. Note, that all internal propagators in the diagrams are dressed but the black dots have been omitted for the sake of visual clarity.

general propagator of the generic field ψ. At this point, also mixed propagators can occur. In the theories investigated here, these will vanish when we set the external sources to zero. From the latter equation one can derive the so-called generating equations for particles via taking the functional derivative with respect to a ghost, gluon or scalar.

In the next step we have to take functional derivatives again to get the equations of motions for the Green functions. In principal this calculation can be done by hand, but when going to higher Greens functions it gets very messy due to the number of terms and fields involved. Therefore, all DSEs in this thesis were derived with the Mathematica package DoDSE [33].

The Dyson-Schwinger equation of the scalar propagator in figure 3.1 serves as an illustrative example. On the left hand side there is the dressed scalar propagator. The bare propagator is the first diagram appearing on the right hand side, next is a diagram with a gluon loop and the last two diagrams of the first row are a gluon and a scalar tadpole diagram. The remaining diagrams are of 2-loop order. All inner propagators are dressed propagators. The (truncated) DSEs of the other propagators and vertices appearing in this thesis can be found in appendix A.

3.2. Powercounting Technique

In this section the infrared powercounting technique [34] [35] [36] [14] [15] will be summarized. For a more detailed information I refer the reader to the PhD thesis of M.Q. Huber [37] which does not only contain a thorough review of this tool but also illustrative examples where the powercounting is applied to various cases.

The infrared powercounting technique allows us to investigate the full system of Dyson-Schwinger equations (or renormalization group equations) via inequalities of so-called infrared exponents. Without applying any truncation we are able to convert an infinitely large system of coupled integral equations to an infinite number of inequalities between so-called infrared exponents. Many of these inequalities are superfluous, so they can be ignored. The remaining ones form a rather small finite set that contains supposedly all the information about the infrared behaviour of the theory.

For a Landau-gauge Yang-Mills theory coupled to a scalar field two different kinds of such solutions have been obtained with the help of DSEs: the scaling and the decoupling solution. The first one is characterized by scaling relations between the critical infrared exponents. The decoupling solution is characterized by a constant gluon propagator at zero momentum and a tree-level like ghost propagator. Only the scaling solution leads to IR enhanced n-point functions. A general bound on the IREs necessary for quark confinement is satisfied in both types of solution [38]. We stay with the scaling solution, since it is much simpler. Note that the selection of the scaling or the decoupling solution is likely just a pure gauge choice [13] [39].

Since we are interested in the infrared behaviour of the Yang-Mills theory, we have to investigate the full non-perturbative Green functions as stated in the previous section. For simplicity we start with looking at the 2-point functions. The propagators can be parameterized as follows:

$$\Delta_{ij}(p) = P_{ij}\frac{Z\left(p^2\right)}{p^2}, \tag{3.4}$$

wherein $Z\left(p^2\right)$ is a dressing function while P_{ij} contains all the colour and Lorentz structure of the specific Green function. In the infrared region for the dressing function $Z\left(p^2\right)$ a power law ansatz is made:

$$Z^{IR}\left(p^2\right) = C \cdot \left(p^2\right)^{\delta} \qquad \text{for } p^2 \to 0 \tag{3.5}$$

where C is a constant factor and δ denotes the infrared exponent (IRE). If $\delta < 0$ the propagator is infrared enhanced. Propagators with more than one dressing function can be treated as several propagators with one dressing function each. A generalization for vertices (that usually need many dressing functions due to their tensor structure) is also possible [15].

When all momenta go to zero at the symmetric point, this is called the uniform limit and only this case will be taken into consideration in this section.

Since all momenta in the integrals of the n-point functions turn then into external momenta because of dimensional reasons, it is sufficient to work only on the level of IREs. In order to have a scaling solution, we have to assume that none of the important contributions vanish because of cancellations.

Having stated the above conditions, we can proceed with the infrared power-counting. We start with the formula for the infrared exponent of an arbitrary l-loop diagram ν in d dimensions [16]:

$$\begin{aligned}\delta_\nu =& l\frac{d}{2} + \sum_i n^{x_i}\left(\delta_{x_i} - 1\right) + \sum_{vert.k\geq 3} n_d^{x_{i_1}\ldots x_{i_r}}\left(\delta_{x_{i_1}\ldots x_{i_r}} + c^{x_{i_1}\ldots x_{i_r}}\right)\\ &+ \sum_{vert.k\geq 3} n_b^{x_{i_1}\ldots x_{i_r}} c^{x_{i_1}\ldots x_{i_r}} - c^\nu.\end{aligned} \tag{3.6}$$

The fields are represented by a set $\{x_r\}, r = 1, ..., R$ where R denotes the number of fields in the action. The factor n_{x_i} stands for the number of internal propagators in the diagram, δ_{x_i} for their infrared exponents. The vertices are denoted in a similar fashion: $n_b^{x_{i_1}\ldots x_{i_r}}$ and $n_d^{x_{i_1}\ldots x_{i_r}}$ are the numbers of dressed and bare vertices of type $x_{i_1}...x_{i_r}$. The variable $c^{x_{i_1}\ldots x_{i_r}}$ stands for the canonical dimension of the vertices.

This formula can be rewritten in terms of the number of external legs m_{x_i}. This replaces the dependence on internal propagators. The details of this calculation can be found in the appendix of [16], here I will only present the result in d dimensions:

$$\begin{aligned}\delta_\nu =& \left(\frac{d}{2} - 2\right)\left(1 - \frac{1}{2}\sum_i m^{x_i}\right) - \frac{1}{2}\sum_i m^{x_i}\delta_{x_i}\\ &+ \sum_{vert.r\geq 3} n_d^{x_{i_1}\ldots x_{i_r}}\left(\left(\frac{d}{4} - 1\right)(u-2) + \delta_{x_{i_1}\ldots x_{i_r}} + \frac{1}{2}\sum_i k_{x_i}^{x_{i_1}\ldots x_{i_r}}\delta_{x_i}\right)\\ &+ \sum_{vert.r\geq 3} n_b^{x_{i_1}\ldots x_{i_r}}\left(\left(\frac{d}{4} - 1\right)(u-2) + \frac{1}{2}\sum_i k_{x_i}^{x_{i_1}\ldots x_{i_r}}\delta_{x_i}\right)\end{aligned} \tag{3.7}$$

where $k_{x_i}^{x_{i_1}\ldots x_{i_r}}$ represents the number of times a leg of the field x_i occurs in the vertex $x_{i_1}...x_{i_r}$ and $u = \sum_i k_{x_i}^{x_{i_1}\ldots x_{i_r}}$.

Based on the fact that a diagram on the right-hand side cannot be more divergent than the one on the left-hand side, one can derive inequalities for higher n-point functions [16]:

$$\delta_{x_{i_1}\ldots x_{i_r}} + \frac{1}{2}\sum_i k_{x_i}^{x_{i_1}\ldots x_{i_r}}\delta_{x_i} + (u-2)\left(\frac{d}{4} - 1\right) \geq 0. \tag{3.8}$$

The DSEs of primitively divergent n-point functions always contain the bare quantity on the right-hand side of the equation. The coefficients of n_d and n_b are non-negative. The relation $n_b \neq 0$ holds only for primitively divergent vertex functions. Therefore, a primitively divergent interaction $x_{i_1}...x_{i_r}$ obeys the inequality

$$\frac{1}{2}\sum_i \delta_{x_i}k_{x_i}^{x_{i_1}\ldots x_{i_r}} + (u-2)\left(\frac{d}{4} - 1\right) \geq 0 \tag{3.9}$$

These formulas are all we need to investigate the system that was described in chapter 2.

We can now apply the infrared powercounting technique to our Landau gauge Yang-Mills theory including charged scalar fields. The tree-level interactions appearing in the Lagrangian are the ghost-gluon vertex, the 3-gluon and the 4-gluon vertex, the scalar-gluon vertex, the 2-scalar-2-gluon vertex and the 4-scalar vertex. If we use equation (3.9) on every one of them we end up with a set of six inequalities corresponding to the order of the vertices listed above:

$$\frac{1}{2}\delta_{gl} + \delta_{gh} + \left(\frac{d}{4} - 1\right) \geq 0 \tag{3.10}$$

$$\frac{3}{2}\delta_{gl} + \left(\frac{d}{4} - 1\right) \geq 0 \tag{3.11}$$

$$\frac{1}{2}\delta_{gl} + \delta_{s} + \left(\frac{d}{4} - 1\right) \geq 0 \tag{3.12}$$

$$\delta_{gl} + \left(\frac{d}{4} - 1\right) \geq 0 \tag{3.13}$$

$$\delta_{gl} + \delta_{s} + \left(\frac{d}{2} - 2\right) \geq 0 \tag{3.14}$$

$$\delta_{s} + \left(\frac{d}{4} - 1\right) \geq 0. \tag{3.15}$$

The infrared exponents of the gluon, ghost and scalar propagators are denoted by δ_{gl}, δ_{gh} and δ_s, respectively.

From equation (3.11), (3.13) and (3.15) one can immediately see that $\delta_{gl} \geq 0$ and $\delta_s \geq 0$. This renders all other equations superfluous, except one:

$$\frac{1}{2}\delta_{gl} + \delta_{gh} + \left(\frac{d}{4} - 1\right) \geq 0. \tag{3.16}$$

Since we observed before that $\delta_{gl} \geq 0$, the ghost propagator is the only one left that can have an IRE ≤ 0 and therefore be infrared enhanced. In the literature this is usually denoted as

$$\frac{1}{2}\delta_{gl} = -\delta_{gh} + \left(\frac{d}{4} - 1\right) = \kappa + \left(\frac{d}{4} - 1\right). \tag{3.17}$$

For the system in question here there are two qualitatively distinct phases [40] [8]. These are called the confining and the Higgs phase. The Dyson-Schwinger equations for the two phases are topologically equivalent. In this work we take a closer look at the confining phase, but the results obtained in section 4 and appendic C also hold

IREs	δ_s	δ_g	δ_{gh}	δ_{ggh}	δ_{sg}	δ_{3g}	δ_{4g}
decoupling	M_s	0	0	0	0	0	0
partial scaling	M_s	$2\kappa+ +\frac{d}{4}-1$	$-\kappa+ +\frac{d}{4}-1$	0	0	$-3\kappa+ +\frac{d}{4}-1$	$-4\kappa+ +\frac{d}{4}-1$
full scaling	M_s	$2\kappa+ +\frac{d}{4}-1$	$-\kappa+ +\frac{d}{4}-1$	0	$-M_s-\kappa+ +\frac{d}{4}-1$	$-3\kappa+ +\frac{d}{4}-1$	$-4\kappa+ +\frac{d}{4}-1$

Table 3.1.: Infrared exponents in the confining phase.

true in the Higgs phase.

In the following, the definition of a new quantity M_s

$$M_s = \begin{cases} 0, & \text{for a massless scalar: } m^2 = 0 \\ 1, & \text{for a massive scalar: } m^2 > 0 \end{cases} \tag{3.18}$$

turns out to be very helpful, since we can now treat the massless and the massive confining phase simultaneously.

There are three mathematically possible solutions for this system. All of them are listed in Table 3.1 and named according to their scaling properties. In case of the full scaling solution, a scaling behaviour is seen in both the scalar and the pure Yang-Mills sector.

On the other hand, the partial scaling solution also describes a scaling in the pure gauge sector, but the scalar sector decouples.

The third solution stems from fact that the ghost propagator is dominated by its tree-level term and then the ghost equation can be solved trivially. This case corresponds to $\kappa = 0$ and is called the decoupling solution. Since the derivation of (3.17) requires $\kappa < 0$, it can be seen that the decoupling solution is only realized, if the scaling solution is excluded.

Returning to Table 3.1, it shows the values of the infrared exponents for the confining phase. δ_{ggh}, δ_{sg}, δ_{3g} and δ_{4g} stand for the infrared exponents of the ghost-gluon, the scalar-gluon, the 3-gluon and the 4-gluon vertex respectively. The values of IREs of the 2-scalar-2-gluon (δ_{2g2s}) and the 4-scalar vertex (δ_{4s}) cannot be determined simultaneously for the massless and the massive case due to qualitative differences. Since this has no influence on the analysis of the colour structure in the next chapter, further details and results will be omitted here. For a discussion and physical interpretation of this matter the reader is referred to [41] [42].

The infrared powercounting only needs the tree-level interactions given in the Lagrangian. Yet this technique yields an analysis of the full system of DSEs of the system without any truncation necessary. This makes it a powerful tool for identifying the leading diagrams within a DSE or an RGE.

As mentioned before, the ghost propagator is infrared enhanced. In the scalar propagator DSE the bare propagator is leading in the infrared. It was argued in [41] that coupling a scalar field to a Landau gauge Yang-Mills theory does not change the scaling behaviour of the Yang-Mills sector, or the fact that the ghost is dominating in the infrared. Therefore, in all DSEs of pure Yang-Mills vertices the leading diagrams are the ones containing ghost-loops or ghost-boxes.

As far as the 4-scalar vertex and the 2-scalar-2-gluon vertex are concerned, we have to distinguish between massless and massive scalars again.

In the first case, the leading diagram of the 4-scalar vertex is the bare 4-scalar vertex. For the 2-scalar-2-gluon vertex the ghost-triangle diagram as well as a higher order diagram containing a 5-point function and a ghost loop can be identified as the leading contributions [41].

The leading diagrams of the 2-scalar-2-gluon DSE for a massive scalar are the same as in the massless case. In case of the 4-scalar vertex, the leading contributions can again only be found when including 5-point functions.

More details on this distinction will follow in chapter 5.

At this point the results so far are summarized. In the first step, the Dyson-Schwinger equations for both the adjoint and the fundamental system have been derived. As expected, one arrives at the same set of equations for both cases.

In order to find a difference between the two representations, a powercounting analysis was performed. The infrared exponents for both cases have been evaluated and the possible solutions for the system in question have been discussed. Still, the IREs of the adjoint and the fundamental system turn out to be identical and lead to the same solutions and scaling behaviour because the DSEs are topologically identical. Therefore, concerning this issue the infrared powercounting technique does not bear any new results and a different approach is needed to gain insight on that matter.

The only resolution possible at this point is that the different solutions may correspond to different matter fields. However, the validity of this szenario can not be decided on pure infrared analysis grounds.

4. Analysis of the Colour Structure

4.1. Colour Structure of Diagrams

Since the fundamental and the adjoint system not only have the same Dyson - Schwinger equations, but also the infrared powercounting analysis yields the same IREs in both cases, we have to go further. We are looking for a structural difference, so the next logical step is a thorough analysis of the colour structure.

Therefore, one has to go back to the DSEs. Since the DSEs are an infinite tower of equations, a one-loop truncation is applied to keep the system simple. The appearing non tree-level vertices like the 4-ghost vertex are replaced by the structures given at the end of the section. Their explicit form is given at the end of this section. Every diagram containing an n-point function of the order higher than four are ignored and only DSEs up to order four are considered. The consequences can be seen by comparing the truncated scalar propagator DSE in figure 4.1 with figure 3.1.

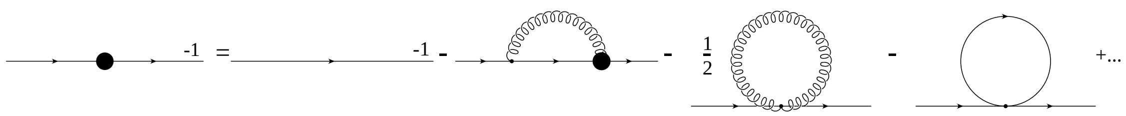

Figure 4.1.: Truncated scalar propagator DSE

All other truncated Dyson-Schwinger equations of the system can be found in appendix A.

Having restricted the DSEs to one-loop diagrams, we can start our analysis of the colour structure of every single diagram. For the tree-level vertices the colour structure can be read off from the DSEs derived before. The example of the ghost-gluon vertex is one of the simplest because both the ghost and the gluon field are in adjoint representation.

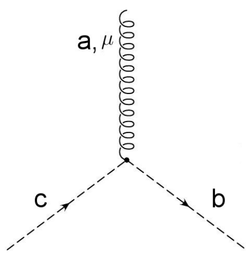

$$\sim igf^{abc}p^\mu$$

Again, the factor g stands for the gauge coupling, f^{abc} are the generators of the adjoint representation and p^{μ} represents the momentum of the anti-ghost.

Vertices involving scalar fields require a little bit more of our attention. Depending on whether we want to calculate the fundamental or the adjoint case, we have to take into account different colour structures.

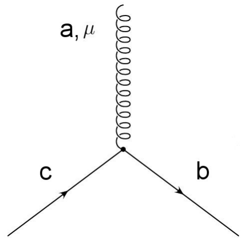

$\sim ig(t^a)_{ij}(q-k)_\mu$ arbitrary representation
$\sim igf^{abc}(q-k)_\mu$ adjoint representation

We do not need to choose a specific representation yet, so at this point $(t^a)_{ij}$ stands for the generator of any arbitrary representation but the adjoint. A complete list of colour structures for tree-level vertices for adjoint and arbitrary representations can be found in appendix B.

Knowing the colour structure of the tree-level vertices provides a starting point for constructing every other diagram. To see how this works we choose the swordfish diagram appearing in the DSE of the scalar-gluon vertex as an example.

At this point another remark about arbitratry representations are in order. In chapter 2 it was stated that every representation but the adjoint is included. Now an additional restriction is made. The theory requires a representation that is sensitive to charge-anticharge particles. For $SU(N)$ this means, only representations with half-integer spin are allowed. Representation with integer spin do not distinguish between this particluar types of particles.

Starting from now, the arbitrary representations are limited to the fundamental representations only in this thesis.

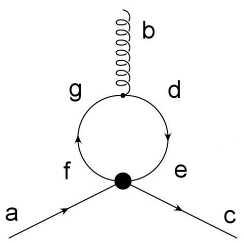

fundamental representation:
$\sim (\delta_{ec}\delta_{af} + \delta_{fe}\delta_{ac}) \times \left(t^b\right)_{dg} \times (\delta_{de}\delta_{fg})$

adjoint representation:
$\sim (\delta_{af}\delta_{ec} + \delta_{ae}\delta_{fc} + \delta_{ac}\delta_{fe}) \times \left(f^{bdg}\right) \times (\delta_{de}\delta_{fg})$

This specific diagram consists of a 4-scalar vertex, a scalar-gluon vertex and two scalar propagators. Consulting appendix B we can see that the first factor stems from the 4-scalar vertex and the second one from the scalar-gluon vertex. There are two expressions for this diagram depending on the representation chosen for the scalar. The third factor containing two Kronecker deltas corresponds to the two inner scalar propagators forming the scalar loop in the diagram.

The colour diagonality of the propagators follows from [43] and has been confirmed in lattice calculations [44] [45] [46].

The imaginary unit and the gauge coupling appearing in appendix B were left out as they factorize from the rest and we are only interested in the colour part of the expression. The same is true for the momentum parts, except for the 4-gluon vertex below.

Some diagrams in the Dyson-Schwinger equations include vertices that have no tree-level contributions: the 4-ghost vertex, the 2-scalar-2-ghost vertex, and the 2-gluon-2-ghost vertex. To obtain an expression for their colour structure, they are approximated by the diagrams containing tree-level vertices given below:

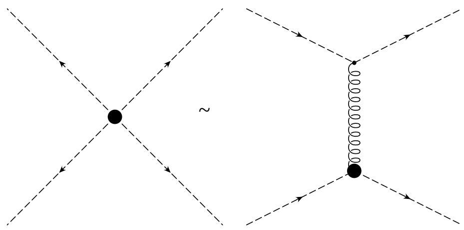

$\sim -g^2 f^{eba} f^{edc}$

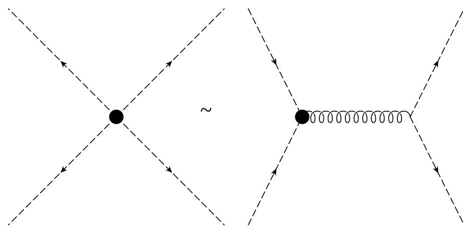

$\sim -g^2 f^{eda} f^{ebc}$

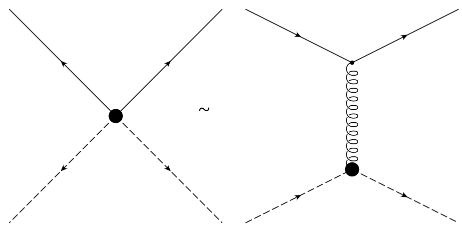

fundamental representation:
$\sim -g^2 f^{eab} \left(t^e\right)_{ab}$

adjoint representation:
$\sim -g^2 f^{eab} f^{ecd}$

There are two possible tree-level diagrams for calculating the colour structure of the 2-gluon-2-ghost vertex. Both are taken into account in this work and will be denoted as L_1 and L_2.

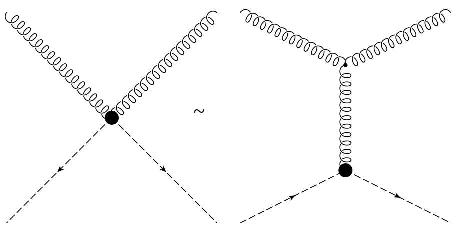

$L_2 \sim -g^2 f^{aed} f^{bce}$

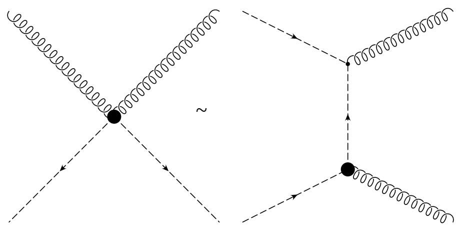

$L_1 \sim g^2 f^{ecd} f^{eab}$

4.2. Colour Structure in Terms of Group Invariants

To keep the discussion more general, we now want to calculate the colour structure of the diagrams constructed before in terms of group invariants. The generators of the adjoint representation are antisymmetric:

$$f^{abc} = -f^{bac} = f^{bca} = -f^{cba} = f^{cab} = -f^{acb}. \tag{4.1}$$

An expression containing two or three structure constants can be reduced to [25]

$$f^{acd} f^{bcd} = C_A \delta^{ab}, \tag{4.2}$$

$$f^{acd} f^{bce} f^{caf} = \frac{1}{2} C_A f^{def}. \tag{4.3}$$

For arbitrary representations there exist similar rules [25]:

$$(t^a)_{ij} (t^a)_{jk} = \delta_{ik} C_R, \tag{4.4}$$

$$(t^a)_{ij} \left(t^b\right)_{ji} = Tr\{t^a t^b\} = \delta_{ab} T_R, \tag{4.5}$$

$$(t^a)_{ij} \left(t^b\right)_{jk} (t^a)_{kl} = \left(C_R - \frac{1}{2} C_A\right) \left(t^b\right)_{li}, \tag{4.6}$$

$$i f^{abc} \left(t^b\right)_{ij} (t^c)_{jk} = \frac{1}{2} C_A (t^a)_{ki}, \tag{4.7}$$

$$(t^a)_{ij} \left(t^b\right)_{jk} (t^c)_{ki} = d^{abc} + \frac{i}{2} f^{abc} T_R. \tag{4.8}$$

As mentioned in chapter 2, C_A and C_R are the Casimir operators of the adjoint and an arbitrary representation, respectively. T_R is an index constant, which is fixed by the normalization.

With the help of these relations each diagram in the Dyson-Schwinger equations for the 3-point vertices can be calculated by hand in reasonable time. This is due to the fact that we restricted the system to one-loop diagrams and the highest n-point functions appearing in these diagrams are of order 4. Therefore there is no expression containing a product of more than three tensor f^{abc} and $(t^a)_{ij}$ and the rules (4.2) - (4.8) can be applied.

Going back to the example of the swordfish diagram we had before, we see that there is indeed a difference in the colour structure depending on which representation for the scalar field we use: in the fundamental case the whole diagram is proportional to the generator of the representation while for the adjoint case the diagram is proportional to zero. This is due to a cancellation because of the antisymmetry of the structure constants.

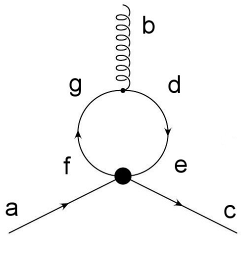

fundamental representation:
$\sim (\delta_{ec}\delta_{af} + \delta_{fe}\delta_{ac}) \times \left(t^b\right)_{dg} \times (\delta_{de}\delta_{fg}) = \left(t^b\right)_{ac}$

adjoint representation:
$\sim (\delta_{af}\delta_{ec} + \delta_{ae}\delta_{fc} + \delta_{ac}\delta_{fe}) \times \left(f^{bdg}\right) \times (\delta_{de}\delta_{fg}) = \left(f^{bca} - f^{bca}\right) = 0$

The diagrams appearing in the DSEs of the 4-point functions are more complicated. According to [43], a 4-point function in adjoint representation can be decomposed into a sum of ten different tree-level diagrams that correspond to invariant tensor structures. Fortunately, not all of them are independent. Using the Jacobi identity and some other relations only six independent tree level diagrams are left. The same decomposition can be done for a 4-point function in fundamental representation and for a 4-point function that has two adjoint and two fundamental legs. This leads to a basis of four and five components, respectively.

These tensor structures form a basis that is not orthogonal. In this thesis an orthogonal basis was constructed from these tensors for convenience. The only condition imposed was that the first component is the tree-level colour structure of the vertex in question. This is due to the fact that the tree-level contribution is leading in the ultraviolet regime and the same is assumed for the infrared. An investigation to which extent this applies can be found in [47]. The other components consist of linear combinations of the tensor structures mentioned before. Since there are different possibilities to realize that, the basis used in this work is given below.

4-legs-adjoint basis:

1^{st} component: $\left(f^{eac}f^{ebd} + f^{ead}f^{ebc}\right)$
2^{nd} component: $\left(f^{eac}f^{ebd} - f^{ead}f^{ebc}\right)$
3^{rd} component: $\left(\delta_{ab}\delta_{cd} + \delta_{ad}\delta_{bc} + \delta_{ac}\delta_{bd}\right)$
4^{th} component: $\left(f^{eac}f^{ebd} - f^{ead}f^{ebc} + C_A(N_A-1)\delta_{ac}\delta_{bd} + C_A(1-N_A)\delta_{ad}\delta_{bc}\right)$
5^{th} component: $\left(f^{eac}f^{ebd} + f^{ead}f^{ebc} - \frac{2}{3}C_A(N_A+1)\delta_{ab}\delta_{cd} + \frac{1}{3}C_A(N_A+1)\delta_{ad}\delta_{bc} + \right.$
$\left. + \frac{1}{3}C_A(N_A+1)\delta_{ac}\delta_{bd}\right)$
6^{th} component: $\left(\delta_{ab}\delta_{cd} + \delta_{ad}\delta_{bc} + \delta_{ac}\delta_{bd} + \frac{24(N_A+2)}{T_R(C_A-6C_R)}d^{abcd}\right)$

After comparing these expressions to appendix B, it can be seen that the first component of the adjoint basis is the tree-level colour structure of the 2-scalar-2-gluon vertex. The third component corresponds to the adjoint 4-scalar vertex.

Still, the first and the third components of the this basis were switched for the calculation of the adjoint 4-scalar vertex. This was done because in every table in appendix C the first expression should correspond to the tree-level contribution for convenience.

As far as the 4-gluon vertex is concerned, the order of the 4-legs-adjoint basis is the same as for the 2-scalar-2-gluon vertex.

Similarly, the first components of the 2-legs-adjoint-2-legs-fundamental basis and the 4-legs-fundamental basis can be identified with the tree-level colour structures of the 2-scalar-2-gluon and the fundamental 4-scalar vertex, respectively.

2-legs-adjoint-2-legs-fundamental basis:

1^{st} component: $\left(\left(t^a\right)^\dagger_{ik}\left(t^b\right)_{kj} + \left(t^b\right)^\dagger_{ik}\left(t^a\right)_{kj}\right)$
2^{st} component: $\left(\left(t^a\right)^\dagger_{ik}\left(t^b\right)_{kj} - \left(t^b\right)^\dagger_{ik}\left(t^a\right)_{kj}\right)$

3^{rd} component: $\left((t^a)^\dagger_{ik}\left(t^b\right)_{kj}+\left(t^b\right)^\dagger_{ik}(t^a)_{kj}-T_R(1+N_A)\delta_{ab}\delta_{cd}\right)$
4^{th} component: $\left(C_A\,(t^a)^\dagger_{ik}\left(t^b\right)_{kj}-C_A\left(t^b\right)^\dagger_{ik}(t^a)_{kj}-2iT_R(N_A-1)f^{abc}\,(t^c)_{ij}\right)$
5^{th} component: $\left((t^a)^\dagger_{ik}\left(t^b\right)_{kj}+\left(t^b\right)^\dagger_{ik}(t^a)_{kj}-\frac{T_RN_A(-C_A+4C_R+T_R(1+N_A)(-4+N_R+N_AN_R))}{2N_Rd33(1+N_A)}\times\right.$
$\left.\times d^{abc}\,(t^c)_{ij}-\frac{C_A-4C_R-4T_R(N_A+1)}{N_R(N_A+1)}\delta_{ab}\delta_{cd}\right)$

4-legs-fundamental basis:

1^{st} component: $(\delta_{ab}\delta_{cd}+\delta_{ad}\delta_{bc})$
2^{nd} component: $(\delta_{ab}\delta_{cd}-\delta_{ad}\delta_{bc})$
3^{rd} component: $\left(-N_AT_R\delta_{ab}\delta_{cd}-N_AT_R\delta_{ad}\delta_{bc}+N_R(N_R+1)\,(t^a)_{ji}\,(t^a)_{lk}+\right.$
$\left.+N_R(N_R+1)\left(t^b\right)_{jk}\left(t^b\right)_{li}\right)$
4^{th} component: $\left(-N_AT_R\delta_{ab}\delta_{cd}+N_AT_R\delta_{ad}\delta_{bc}-N_R(N_R-1)\,(t^a)_{ji}\,(t^a)_{lk}+\right.$
$\left.+N_R(N_R-1)\left(t^b\right)_{jk}\left(t^b\right)_{li}\right)$

The full results for every diagram for all DSEs including the ones for the non tree-level vertices can be found in appendix C.

All the results were calculated and checked with the help of the symbolic manipulation system FORM developed by J. A. M. Vermaseren [48]. There is a very useful FORM package named 'color' written by T. van Ritbergen, A.N. Schellekens and J.A.M. Vermaseren [25], which is able to calculate the colour structure of diagrams containing up to 16 vertices. The package is also sensitive to different representations and calculates the colour factor in terms of the group invariants N_A, N_R, C_A, C_R and T_R. More details can be found in the paper associated with the FORM package 'color' [25].

5. Results

In the previous chapters the colour structure analysis was motivated, the necessary tools were developed and an example was given in terms of group invariants to illustrate the procedure.

In this chapter the leading diagrams of each DSE according to power counting will be presented and their colour structure will be evaluated for both the adjoint and the fundamental representation. In addition the results will be applied to the gauge groups $SU(2)$, $SU(3)$ and $G(2)$.

A distinction between the massive and the massless scalar case will be made as well as the quenched and the unquenched system. Differences are pointed out and possible implications and consequences will be discussed.

A short note on the difference between the chosen gauge groups and in non-leading diagrams will close this chapter.

5.1. Propagator DSEs

Up to now every colour factor was calculated in terms of group invariants. Their values for the groups of most interest here are given in Table 5.1. As mentioned before the value for T_R is $\frac{1}{2}$. At this point, we insert specific values of the former invariants into the results to see whether we find differences concerning the gauge groups.

We start by looking at the Dyson-Schwinger equations of the propagators, i.e. 2-point functions. The powercounting analysis required that the ghost propagator is infrared enhanced. Furthermore, the leading diagrams of the gluon and the scalar propagator DSE were identified as the ghost-loop diagram and the bare scalar

group invariant	SU(2)	SU(3)	G(2)
N_A	3	8	14
N_R	2	3	7
C_A	2	3	2
C_R	$\frac{3}{4}$	$\frac{4}{3}$	1
$d33$	0	$\frac{10}{3}$	0
$d44$	$\frac{5}{1024}$	$\frac{5}{192}$	$\frac{7}{384}$
$d444$	$\frac{55}{294912}$	$\frac{5}{3456}$	$\frac{77}{110592}$

Table 5.1.: Values for group invariants for $SU(2)$, $SU(3)$ and $G(2)$.

propagator, respectively.

Their colour factors are given in the figures below. There is no difference between the different representations since the ghost and the gluon are both in the adjoint representation and the propagator is always proportional to δ^{ab}.

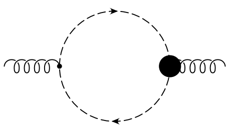

	group invariant	SU(2)	SU(3)	G(2)
adjoint	$C_A\delta^{ab}$	$2\delta^{ab}$	$3\delta^{ab}$	$2\delta^{ab}$

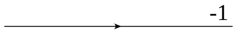

	group invariant	SU(2)	SU(3)	G(2)
adj.& fund.	δ^{ab}	δ^{ab}	δ^{ab}	δ^{ab}

5.2. 3-point Function DSEs in quenched Approximation

Continuing the analysis from before the results for the 3-point functions in quenched approximation are given. There are three tree-level vertices containing three external legs: the ghost-gluon, the scalar-gluon and the 3-gluon vertex. First, the leading diagrams of the ghost-gluon vertex are presented as well as the results for their colour structure:

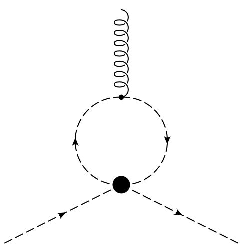

	group invariant	SU(2)	SU(3)	G(2)
adjoint	$C_A f^{abc}$	$2f^{abc}$	$3f^{abc}$	$2f^{abc}$

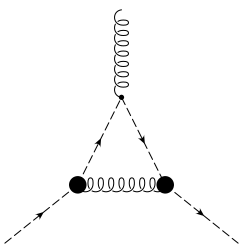

	group invariant	SU(2)	SU(3)	G(2)
adjoint	$-\frac{1}{2}C_A f^{abc}$	$-f^{abc}$	$-\frac{3}{2}f^{abc}$	$-f^{abc}$

However, no dependence on the gauge group can be observed in this case. Both diagrams are proportional to a product of the adjoint quadratic Casimir C_A and a generator of the adjoint representation f^{abc} modulo a prefactor. This is valid for the three groups in question and no qualitative difference can be seen.

Next, the leading contributions of the 3-gluon vertex DSE is given. There are two results presented for the diagram with the ghost-loop. As mentioned in the previous chapter, this is due to the fact that there are two possibilities for replacing the non tree-level 2-ghost-2-gluon vertex with tree-level diagrams.

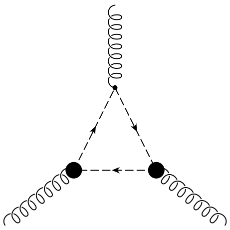

	group invariant	SU(2)	SU(3)	G(2)
adjoint	$\frac{1}{2}C_A f^{abc}$	f^{abc}	$\frac{3}{2}f^{abc}$	f^{abc}

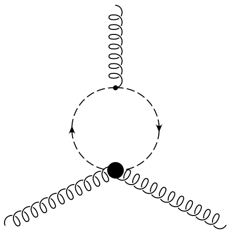

	group invariant	SU(2)	SU(3)	G(2)
L1	$\frac{1}{2}C_A f^{abc}$	f^{abc}	$\frac{3}{2}f^{abc}$	f^{abc}
L2	$-C_A f^{abc}$	$-2f^{abc}$	$-3f^{abc}$	$-2f^{abc}$

Still, no difference concerning the representations can be seen because, so far, there are no leading diagrams involving scalars. Additionally, no structural difference regarding the different gauge groups can be found.

We conclude this section with the result for the leading diagram in the scalar-gluon DSE given below.

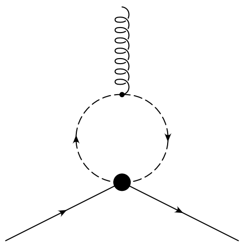

	group invariant	SU(2)	SU(3)	G(2)
adjoint	$-C_A f^{abc}$	$-2f^{abc}$	$-3f^{abc}$	$-2f^{abc}$
fund.	$\frac{1}{4}C_A\,(t^a)_{bc}$	$\frac{1}{2}\,(t^a)_{bc}$	$\frac{3}{4}\,(t^a)_{bc}$	$\frac{1}{2}\,(t^a)_{bc}$

Here too, no structural difference between the fundamental and the adjoint case can be observed.

5.3. 4-point Function DSE in the Yang-Mills Sector

As mentioned before, the 4-point functions are projected on bases including their own tree-level colour structure according to chapter 4. Again, the quenched case is considered.

The only tree-level 4-point function in the pure gauge sector is the 4-gluon vertex. Since the 4-gluon vertex is a pure Yang-Mills vertex, the leading diagrams are identified as those with a ghost loop or a ghost box and are given below. Again, there are two expressions for one of the diagrams stemming from the two tree-level possibilities of the 2-gluon-2-ghost vertex.

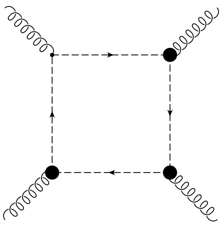

adj.	group invariant	SU(2)	SU(3)	G(2)
1^{st}	$\frac{1}{4}N_AC_A^3$	6	54	28
2^{nd}	$-\frac{1}{4}N_AC_A^3$	-6	-54	-28
3^{rd}	$\frac{5}{2}N_AC_A^2$	30	180	140
4^{th}	$\frac{1}{4}N_AC_A^3(2N_A-3)$	18	702	700
5^{th}	$-\frac{(1)}{12}N_AC_A^3(-2N_A+1)$	-10	-270	-252
6^{th}	$\frac{1}{2T_R(C_A-6C_R)}\,(5N_AT_R\times$ $\times C_A^2(C_A-6C_R)+$ $+12\text{ d44}(2+N_A))$	$\frac{3825}{128}$	$\frac{1435}{8}$	$\frac{1113}{8}$

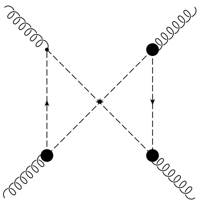

adj.	group invariant	SU(2)	SU(3)	G(2)
1^{st}	$-\frac{1}{2}N_AC_A^3$	-12	-108	-56
2^{nd}	0	0	0	0
3^{rd}	$\frac{5}{2}N_AC_A^2$	30	180	140
4^{th}	0	0	0	0
5^{th}	$\frac{(1)}{6}N_AC_A^3(2N_A-1)$	20	540	504
6^{th}	$\frac{1}{2T_R(C_A-6C_R)}\,(5N_AT_RC_A^2\times$ $\times(C_A-6C_R)+$ $+12\text{ d44}(2+N_A))$	$\frac{3825}{128}$	$\frac{1435}{8}$	$\frac{1113}{8}$

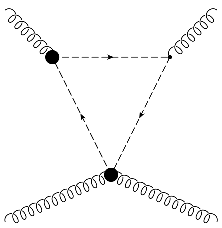

L_1	group invariant	SU(2)	SU(3)	G(2)
1^{st}	$\frac{1}{4}N_AC_A^3$	6	54	28
2^{nd}	$-\frac{1}{4}N_AC_A^3$	-6	-54	-28
3^{rd}	$\frac{5}{2}N_AC_A^2$	30	180	140
4^{th}	$\frac{1}{4}N_AC_A^3(2N_A-3)$	18	702	700
5^{th}	$\frac{1}{12}N_AC_A^3(-2N_A+1)$	-10	-270	-252
6^{th}	$\frac{1}{2T_R(C_A-6C_R)}\,(5N_AT_RC_A^2\times$ $\times(C_A-6C_R)+$ $+12\text{ d44}(2+N_A))$	$\frac{3825}{128}$	$\frac{1435}{8}$	$\frac{1113}{8}$

L_2	group invariant	SU(2)	SU(3)	G(2)
1^{st}	$-\frac{3}{4}N_AC_A^3$	-18	-162	-84
2^{nd}	$\frac{1}{4}N_AC_A^3$	6	54	28
3^{rd}	0	0	0	0
4^{th}	$\frac{1}{4}N_AC_A^3(-2N_A+3)$	-18	-702	-700
5^{th}	$\frac{1}{4}N_AC_A^3(2N_A-1)$	30	810	756
6^{th}	0	0	0	0

For these three diagrams no qualitative difference can be observed as far as the different gauge groups are concerend.

5.4. 4-point Function DSEs including Scalars

Since the two remaining tree-level vertices involve scalar fields, again a distinction between a massless and a massive scalar has to be made. In addition, differences regarding the adjoint and the fundamental representation are most likely to be found here.

Looking for the leading contributions, the 2-scalar-2-gluon vertex DSE is insensitive to whether the scalar carries a mass or not. In both cases the same two diagrams are the leading ones: the ghost-triangle diagram and one higher order graph containing a 5-point function and a ghost loop.

The results of the ghost triangle diagram are given here.

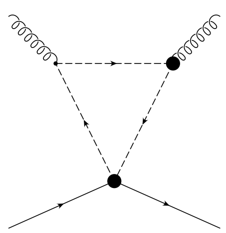

adj.	group invariant	SU(2)	SU(3)	G(2)
1^{st}	0	0	0	0
2^{nd}	$-\frac{1}{2}N_A C_A^3$	-12	-108	-56
3^{rd}	0	0	0	0
4^{th}	$\frac{1}{2}N_A C_A^3(2N_A - 3)$	36	1404	1400
5^{th}	0	0	0	0
6^{th}	0	0	0	0

fund.	group invariant	SU(2)	SU(3)	G(2)
1^{st}	$-\frac{1}{8}N_A T_R\,(3C_A^2 - 10C_A C_R + {} +8C_R^2)$	$-\frac{9}{32}$	$-\frac{11}{18}$	0
2^{nd}	0	0	0	0
3^{rd}	$\frac{1}{8}N_A T_R\,(-3C_A^2 + 10C_A C_R + {} +4C_R(-2C_R + T_R + T_R N_A))$	$\frac{27}{32}$	$\frac{205}{18}$	$\frac{105}{4}$
4^{th}	0	0	0	0
5^{th}	$\frac{1}{8}N_A T_R\,(-3C_A^2 + 10C_A C_R + {} +4C_R(-2C_R + T_R + T_R N_A))$	$\frac{27}{32}$	$\frac{205}{18}$	$\frac{105}{4}$

This is the first evidence for the differences we have been looking for. First of all, there is a structural difference in the tree-level component of this specific diagram. In the adjoint case the colour structure is zero, even when calculated in group invariants. On the other hand, the fundamental colour structure is proportional to a finite value.

Looking at all components, another detail can be observed. If the 6^{th} component of the adjoint case is excluded, the zero-components of the adjoint and the fundamental representation seem to be switched. Those components that have a finite value for the adjoint representation are zero for the fundamental case and vice versa. However, this fact should not be overemphasized because the order of components of the basis is an arbitrary choice. Still, an underlying structure can be seen.

The third difference that can be found in this diagram concerns the gauge groups. Going back to the tree-level component of the fundamental case, it should be noted that the explicit values for $SU(2)$ and $SU(3)$ are finite, while it is zero for $G(2)$.

Since it was stated in chapter 2 that there is a structural difference between $SU(N)$ and $G(2)$, one is looking for details that might be important for an underlying mechanism. This indicates that there is one.

The second leading contribution in the 2-scalar-2-gluon DSE is an higher-order diagram containing a 5-point function. As it was shown in [41], a skeleton expansion can be applied to get rid of the 5-point function. This results in two diagrams of two-loop order that are given below. It should be emphasized once more that these diagrams are the leading contributions of the 2-scalar-2-gluon DSE for both the massless and the massive case.

In the first of the diagrams steming from the skeleton expansion, no structural difference between the adjoint and the fundamental representation can be seen. The switching of the components like in the last diagram is also not repeated here. However, the tree-level component deserves some attention in the fundamental case. Again, the value for G_2 is zero whereas those for $SU(2)$ and $SU(3)$ are finite.

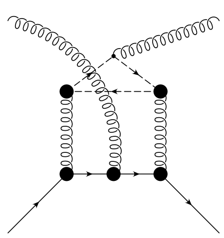

adj.	group invariant	SU(2)	SU(3)	G(2)
1^{st}	$-\frac{1}{8}N_A C_A^4$	-6	-81	-28
2^{nd}	$-\frac{1}{8}N_A C_A^4$	-6	-81	-28
3^{rd}	$-\frac{5}{4}N_A C_A^3$	-30	-270	-140
4^{th}	$\frac{1}{8}N_A C_A^4(2N_A-3)$	18	1053	700
5^{th}	$\frac{1}{24}N_A C_A^4(-1+2N_A)$	10	405	252
6^{th}	$-\frac{C_A}{4T_R(C_A-6C_R)}(5N_AT_RC_A^2\times$ $\times(C_A-6C_R)+$ $+12\ \mathrm{d44}(2+N_A))$	$-\frac{3825}{128}$	$-\frac{4305}{16}$	$-\frac{1113}{8}$

fund.	group invariant	SU(2)	SU(3)	G(2)
1^{st}	$-\frac{1}{4}iN_AT_RC_A^2(C_A-2C_R)$	$-\frac{3i}{4}$	$-3i$	0
2^{nd}	0	0	0	0
3^{rd}	$\frac{1}{4}iN_AT_RC_A^2(-C_A+2C_R+$ $+T_R+T_RN_A)$	$\frac{9i}{4}$	$-\frac{75i}{2}$	$-\frac{105i}{2}$
4^{th}	0	0	0	0
5^{th}	$\frac{iN_AT_RC_A^2}{4N_R(1+N_A)}(-C_A(-1+N_R+$ $+N_AN_R)+2(2T_R(1+N_A))+$ $+C_R(-2+N_R+N_AN_R))$	$\frac{9i}{16}$	$\frac{20i}{9}$	$\frac{28i}{15}$

Next, the second diagram resulting from the skeleton expansion is given. Here, neither a qualitative difference regarding the representations can be observed, nor between $SU(N)$ and $G(2)$. Nevertheless, it should be noted, that the 4^{th} component for fundamental representation bears a difference within the $SU(N)$. While there is a finite value in case of $SU(3)$, it reduces to zero for $SU(2)$.

adj.	group invariant	SU(2)	SU(3)	G(2)
1^{st}	$-\frac{1}{8}N_A C_A^4$	-6	-81	-28
2^{nd}	$\frac{1}{8}N_A C_A^4$	6	81	28
3^{rd}	$-\frac{5}{4}N_A C_A^3$	-30	-270	-140
4^{th}	$\frac{1}{8}N_A C_A^4(-2N_A+3)$	-18	-1053	-700
5^{th}	$\frac{1}{24}N_A C_A^4(-1+2N_A)$	10	405	252
6^{th}	$-\frac{C_A}{4T_R(C_A-6C_R)}\,(5N_A T_R C_A^2\times$ $\times(C_A-6C_R)+$ $+12\ \mathrm{d44}(2+N_A))$	$-\frac{3825}{128}$	$-\frac{4305}{16}$	$-\frac{1113}{8}$

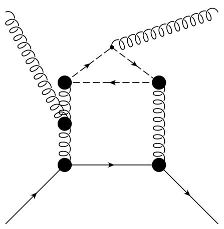

fund.	group invariant	SU(2)	SU(3)	G(2)
1^{st}	$\frac{1}{8}N_A T_R C_A^3$	$\frac{3}{2}$	$\frac{27}{2}$	7
2^{nd}	$\frac{1}{8}N_A T_R C_A^3$	$\frac{3}{2}$	$\frac{27}{2}$	7
3^{rd}	$\frac{1}{8}N_A T_R C_A^2(C_A-4T_R(1+N_A))$	$-\frac{9}{2}$	$-\frac{135}{2}$	-98
4^{th}	$-\frac{1}{8}N_A T_R C_A^3\,(C_A-2T_R\times$ $\times(-1+N_A))$	0	54	77
5^{th}	$\frac{N_A T_R C_A^2}{8N_R(1+N_A)}\,(8C_R+C_A\times$ $\times(-2+N_R+N_R N_A)+$ $-2T_R\,(N_A^2 N_R+4+N_R+$ $+2N_A(1+N_R)))$	$-\frac{45}{16}$	$-\frac{290}{9}$	$-\frac{1021}{30}$

Continuing with the 4-scalar vertex DSE, the distinction between a massless and a massive scalar has to be taken into account.

In the first case, where the scalar does not carry a mass, the leading diagram can be identified as the bare 4-scalar vertex. The colour structure of this diagram can be read off from appendix B, since the same colour structure for bare and dressed vertices is assumed.

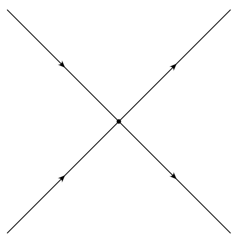

$\sim (\delta_{ab}\delta_{cd}+\delta_{ac}\delta_{bd}+\delta_{ad}\delta_{bc})$ adjoint

$\sim (\delta_{ab}\delta_{cd}+\delta_{ad}\delta_{bc})$ fundamental

If the scalar is massive, the leading contribution contains a 5-point function. This diagram can again be skeleton expanded. The resulting graph is of 3-loop order and its colour structure is given below.

adj.	group invariant	SU(2)	SU(3)	G(2)
1^{st}	$\frac{1}{24}\left(48 \text{ d44} + 25N_A C_A^4\right)$	$\frac{25605}{512}$	$\frac{64805}{96}$	$\frac{44807}{192}$
2^{nd}	$\frac{1}{144}C_A\left(-96 \text{ d44} + 13N_A C_A^4\right)$	$\frac{2217}{256}$	$\frac{16893}{96}$	$\frac{11641}{288}$
3^{rd}	$-\frac{1}{144}C_A\left(96 \text{ d44} + 5N_A C_A^4\right)$	$-\frac{855}{256}$	$-\frac{6485}{96}$	$-\frac{4487}{288}$
4^{th}	$\frac{1}{144}C_A\left(-48 \text{ d44}(3N_A - 1) + \right.$ $\left. 5N_A C_A^4(30N_A - 31)\right)$	$\frac{12585}{64}$	$\frac{2708525}{192}$	$\frac{3485153}{576}$
5^{th}	$\frac{1}{144}C_A\left(-48 \text{ d44}(3N_A + 1) + \right.$ $\left. N_A C_A^4(38N_A - 51)\right)$	$\frac{28155}{256}$	$\frac{920105}{192}$	$\frac{1044617}{576}$
6^{th}	$\frac{1}{24T_R(C_A - 6C_R)}\left(48 \text{ d44} C_A T_R + \right.$ $+N_A T_R C_A^4(25C_A - 150C_R) +$ $+20C_A^2 \text{ d44}(2 + N_A)$ $144\left(-2C_R T_R \text{ d44} + \right.$ $\left.\left. + \text{ d444}(2 + N_A)\right)\right)$	$\frac{204555}{4096}$	$\frac{48545}{72}$	$\frac{178829}{768}$

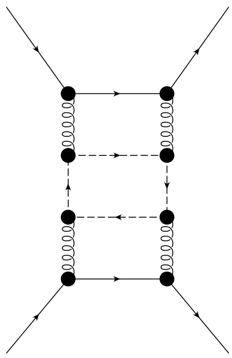

fund.	group invariant	SU(2)	SU(3)	G(2)
1^{st}	$\frac{1}{12}\left(12 \text{ d44} + N_A T_R C_A^2(C_A + 12T_R)\right)$	$\frac{4101}{1024}$	27	$\frac{56}{3}$
2^{nd}	$\frac{1}{12}\left(12 \text{ d44} + N_A T_R C_A^2(C_A - 12T_R)\right)$	$-\frac{2043}{1024}$	-9	$-\frac{28}{3}$
3^{rd}	$\frac{1}{48}\left(-48 \text{ d44}\left(T_R N_A + (C_A - C_R)\times\right.\right.$ $\left.\times N_R(1 + N_R)\right) +$ $+C_A^2\left(-4C_A^2 T_R N_A N_R(1 + N_R)\right) +$ $+12\left(T_R^3 N_A^2 + \text{ d33} N_R(1 + N_R) +\right)$ $C_A T_R N_A\left(4C_R N_R(1 + N_R) + \right.$ $\left.\left. +T_R(-4N_A + 3N_R(1 + N_R))\right)\right)$	$-\frac{11565}{1024}$	$-\frac{1265}{8}$	$-\frac{37779}{128}$
4^{th}	$\frac{1}{48}\left(-48 \text{ d44}\left(T_R N_A - (C_A - C_R)\times\right.\right.$ $\left.\times N_R(-1 + N_R)\right)) +$ $+C_A^2\left(-4C_A^2 T_R N_A N_R(-1 + N_R)\right) +$ $+12\left(T_R^3 N_A^2 + \text{ d33} N_R(-1 + N_R) +\right)$ $C_A T_R N_A\left(-4C_R N_R(-1 + N_R) + \right.$ $\left.\left. +T_R(-4N_A + 3N_R(-1 + N_R))\right)\right)$	$\frac{6405}{1024}$	$\frac{6125}{32}$	$\frac{128821}{384}$

5.5. quenched vs unquenched

In the next part of this chapter the difference between the quenched and the unquenched system is examined. As mentioned in chapter 2 the meaning of quenched in this context means that no contributions from sea particles are allowed. Therefore, all diagrams containing a closed scalar loops are ignored in this case.

Starting with the Dyson-Schwinger equations of the 3-point functions, the diagrams containing closed scalar loops are shown, along with their respective colour structure. Only one such diagram is found in each 3-point DSE.

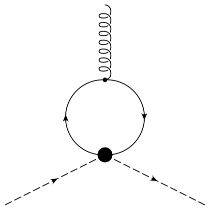

	group invariant	SU(2)	SU(3)	G(2)
adjoint	$-C_A f^{abc}$	$-2f^{abc}$	$-3f^{abc}$	$-2f^{abc}$
fundamental	$T_R f^{abc}$	$\frac{1}{2}f^{abc}$	$\frac{1}{2}f^{abc}$	$\frac{1}{2}f^{abc}$

In case of the ghost-gluon vertex, it should be noted that in the adjoint representation the colour structure is proportional to the adjoint Casimir operator. On the other hand, in fundamental representation it is proprotional to the index constant T_R that is fixed by the normalization and has the same value for every group.

However, no qualitative difference can be seen if this diagram is excluded.

Next, the corresponding diagram of the 3-gluon vertex DSE is given. A difference can indeed be seen here. The colour structure of this swordfish diagram is zero for the adjoint and proportional to d^{abc} for the fundamental representation. The quantity d^{abc} is non-vanishing for $SU(3)$, but zero for $SU(2)$ and $G(2)$.

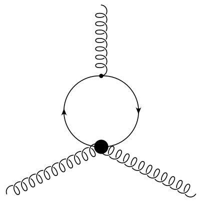

	group invariant	SU(2)	SU(3)	G(2)
adjoint	0	0	0	0
fundamental	$\frac{1}{2}d^{acb}$	0	$\frac{1}{2}d^{acb}$	0

The results so far support the assumption that the pure Yang-Mills sector is basically not affected whether one considers the quenched or the unquenched case.

The remaining 3-point function DSE is the one of the scalar-gluon vertex. The diagram corresponding to this equation is shown below. Here, we also see a difference between the two representations: the colour structure is proportional to a generator in the fundamental case, but cancels for the adjoint.

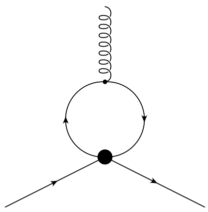

	group invariant	SU(2)	SU(3)	G(2)
adjoint	0	0	0	0
fundamental	$\frac{1}{6}\left(t^a\right)_{bc}$	$\frac{1}{6}\left(t^a\right)_{bc}$	$\frac{1}{6}\left(t^a\right)_{bc}$	$\frac{1}{6}\left(t^a\right)_{bc}$

This is again the kind of difference we have been looking for. As stated in the introduction, the aim of this thesis was to see whether these representation-dependent differences can be seen on the level of correlation functions. Knowing that there has to be a distiction between the two representations, these results provide a starting point for a deeper analysis.

However, the diagrams are subleading in the infrared. This requires that cancellations occur if this should be relevant.

Proceeding with the 4-point DSEs, their diagrams containing scalar loops do not show a similar difference regarding the representation. This is expected for the 4-gluon DSE since it belongs to the pure Yang-Mills sector and therefore, should be unaffected by this. The diagrams of interest are the first, the seventh and last two graphs in appendix C.7.

Likewise, the corresponding diagrams of the 4-scalar and the 2-scalar-2-gluon DSE do not exhibit a qualitative difference concerning their colour structure. Regarding the 4-scalar vertex, the only quenched diagram is the second graph in appendix C.9. In case of the 2-scalar-2-gluon vertex there are two quenched diagrams which are the first two listed in appendix C.8. This seems to hint that the main contribution to this behaviour stems from the 3-point functions, more precisely from the scalar-gluon DSE.

5.6. SU(N) vs G(2)

A few more words on the differences between different gauge groups are in order.

As explained in chapter 2, the main reason for being interested in the group $G(2)$ in this context is the fact that there is a structural difference between $SU(N)$ and $G(2)$. In contrast to the group $SU(N)$, $G(2)$ has a trivial center. This has consequences on how confinement is realized in these groups.

Starting to look at the tree-level component of the colour structure of the various diagrams from this point of view, it can be seen that there are several diagrams whose colour structures have finite values for $SU(N)$ but are zero for $G(2)$. This was already pointed out in the previous section, where the leading diagrams were presented. It should be emphasized that this kind of difference is not obeserved in the diagrams steming from the Dyson-Schwinger equations of the pure Yang-Mills sector. Furthermore, this behaviour occurs only in the fundamental representation.

Concerning the scalar-gluon DSE, the diagrams of interest are the third and the fifth in appendix C.6. In the 2-scalar-2-gluon DSE we find four diagrams exhibiting this behaviour (diagrams 6, 7, 11, 12 in appendix C.8) additional to the leading ones discussed in section 5.4. This kind of difference is not found in the tree-level components of any diagram in the 4-scalar vertex DSE. However, it can be seen in the second component of both the first and the third diagram in appendix C.9.

Indeed, there seems to be a pattern behind this, and one can speculate, that contributions showing this behaviour might be important to the building of the string tension.

5.7. Non-leading Differences

To close this chapter, a few other differences in non-leading and unquenched diagrams are pointed out.

Starting with the difference between the two representations, there is one diagram (diagram 8 in appendix C.8) from the 2-scalar-2-gluon DSE that deserves attention. In this case, the colour structure of the adjoint representation is proportional to a product of group invariants while it is zero for fundamental representation. This is somehow inverse to the cases discussed in the previous sections, where it is always the adjoint case that reduces to zero.

There is another diagram (fifth diagram in appendix C.8) belonging to the 2-scalar-2-gluon vertex DSE that shows the same behaviour, although only in case of $SU(2)$.

Next, there are two diagrams of the 3-gluon DSE that are proportional to d^{abc}: the quenched diagram dicussed in a previous section and the scalar-triangle graph (diagram 5 in appendix C.5). Since d^{abc} is zero for $SU(2)$ and $G(2)$, there is a difference between those two groups and $SU(3)$.

The last peculiar detail in this section concerns a diagram of the 2-gluon-2-ghost veretx DSE. As mentioned before there are two possibilities to replace the non-tree level 2-gluon-2-ghost vertex, denoted by L_1 and L_2. This makes a difference for the third graph in appendix C.11, where the colour structure has a finite value when using L_1 but cancels in case of L_2.

6. Summary

In this last part of this thesis the results will be summarized.

In this thesis a charged scalar field coupled to a Landau-gauge Yang-Mills theory has been investigated. Among others, the confinement problem serves as a motivation. The strong interaction force can be described by an attractive potential. This potential depends on the gauge group as well as on the representation chosen for the scalar. In this case, the adjoint and the fundamental representation are considered. The aim of this thesis was to examine whether these differences can be seen on the level of correlation functions.

To this end, the Dyson-Schwinger equations for both systems were derived first. As expected, they turn out to be topologically equivalent and no difference can be seen.

Next, an infrared powercounting analysis was performed on the adjoint and the fundamental case. The leading diagrams of each DSE were identified and their infrared exponents were evaluated. In addition, the possible phases of the system were discussed, along with the mathematically possible solutions. However, the IREs of both systems are identical and lead to the same solutions in both cases.

To gain further insight, the colour structure of the diagrams appearing in the DSEs was analysed. Since the Dyson-Schwinger equations are an infinite tower of equations, a one-loop truncation was applied. Only DSEs to the order of four were taken into account and all diagrams involving a n-point function where $n = 5$ or higher were ignored. The tree-level vertices were left bare and the appearing non tree-level vertices were approximated by diagrams containing tree-level vertices. The colour structures of the remaining diagrams were calculated in terms of group invariants and later the values for the groups $SU(2)$, $SU(3)$ and $G(2)$ were inserted. To get results for the DSEs of the 4-point functions, a basis orthogonal to the respective tree-level colour factor was developped.

In the following, the results for the leading diagrams identified with the help of the powercounting analysis before are presented. No qualitative differences can be seen in the pure Yang-Mills sector. The same is true for the leading diagram of the scalar-gluon DSE.

However, when considering the leading triangle graph of the 2-scalar-2-gluon DSE, a difference concerning the representation is found. The tree-level component of this specific diagram is zero in the adjoint and is proportional to a product of group invariants in the fundamental case. Additionally, the fundamnetal tree-level component exhibits another difference regarding the gauge groups of interest. It has a finite value for $SU(2)$ and $SU(3)$ but is zero for $G(2)$.

The other leading diagrams do not show this difference concerning the representation, but the discrepancy between $SU(N)$ and $G(2)$ can be observed in a number of other leading as well as subleading diagrams of the 2-scalar-2-gluon DSE. One might speculate that these contributions are important for the building of the string tension.

Next, the quenched and the unquenched system are considered. In this context, the term 'quenched' refers to the fact that all diagrams containing a closed scalar loop are excluded. As expected, there is no qualitative difference for the ghost-gluon DSE. On the other hand, the corresponding diagrams of the scalar-gluon DSE and the 3-gluon DSE reveal a distinction. The colour factor is proportional to a fixed value in the fundamental case, but cancels for the adjoint. This behaviour is not seen in the DSEs of the 4-point functions which backs the conjecture that the 4-point functions might not be important for this mechanism.

At the end, the differences occuring in non-leading contributions are discussed. There is one subleading diagram of the 2-scalar-2-gluon DSE that shows a structural difference between the adjoint and the fundamental representation. A second one exhibits this difference only in case of $SU(2)$.
In addition the colour structure of a diagram steming from the 2-gluon-2-ghost vertex turns out to be qualitatively different, depending on which possibility to replace the non tree-level 2-gluon-2-ghost vertex is chosen.

By identifying the contributions that are sensitive to different gauge groups one provides the basis to identify the mechanism by more sophisticated treatments, in particular self-consistent extensions. In particular, this gives reason to believe that the qualitatively different behaviour of the string tension could be embodied in (low-n) correlation functions.

A. Dyson-Schwinger Equations

This appendix consists of a graphic representation of the truncated Dyson-Schwinger equations of the propagators and the tree-level and non-tree-level vertices. All DSEs were derived with the help of the Mathematica package DoDSE [33]. For the sake of brevity only the truncated versions employed here are shown.

A.1. Propagator Equations

A.1.1. Ghost Propagator DSE

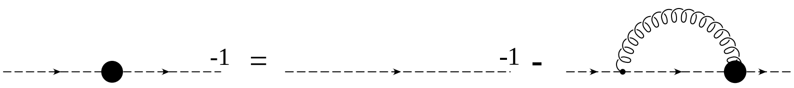

A.1.2. Gluon Propagator DSE

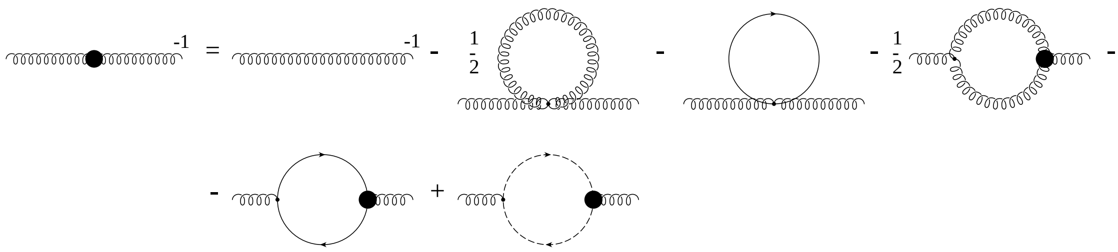

A.1.3. Scalar Propagator DSE

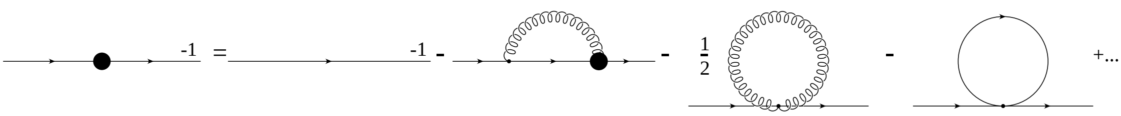

A.2. tree-level Vertex Equations

A.2.1. Ghost-gluon Vertex DSE

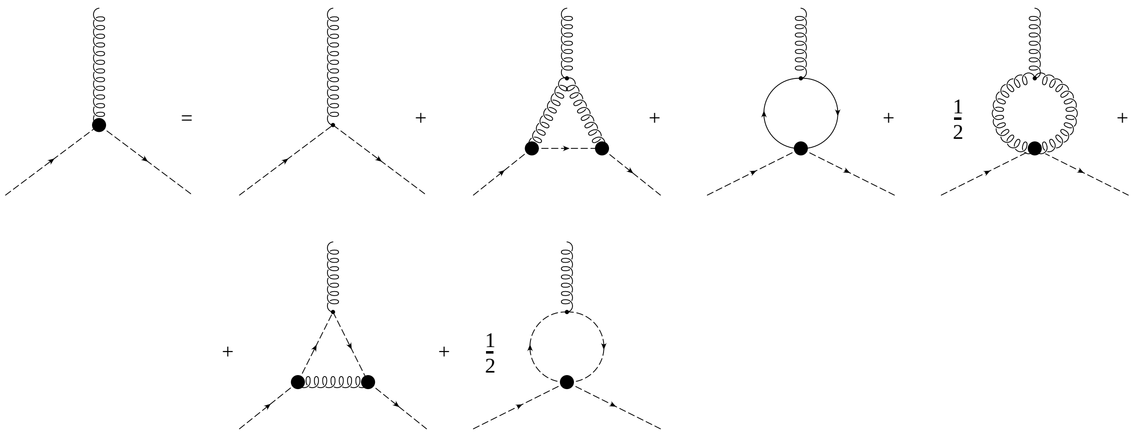

A.2.2. 3-gluon Vertex DSE

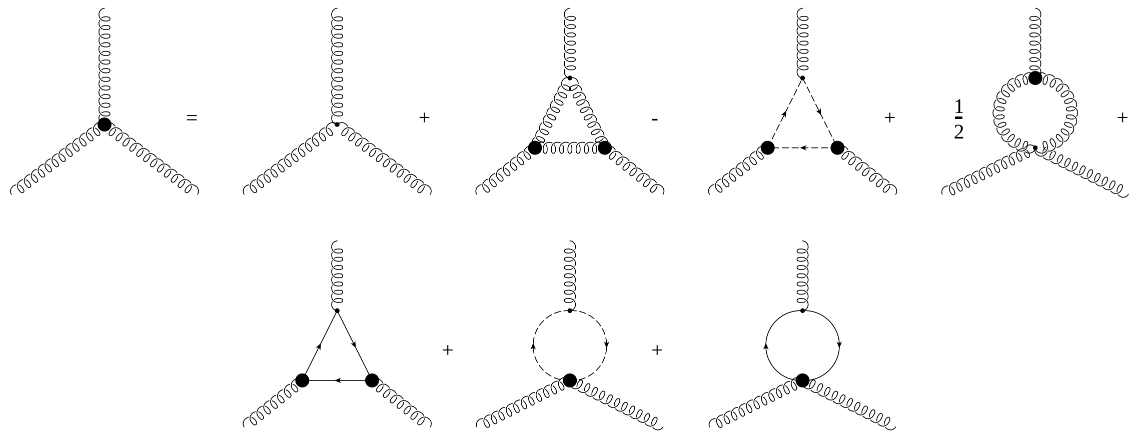

A.2.3. Scalar-gluon Vertex DSE

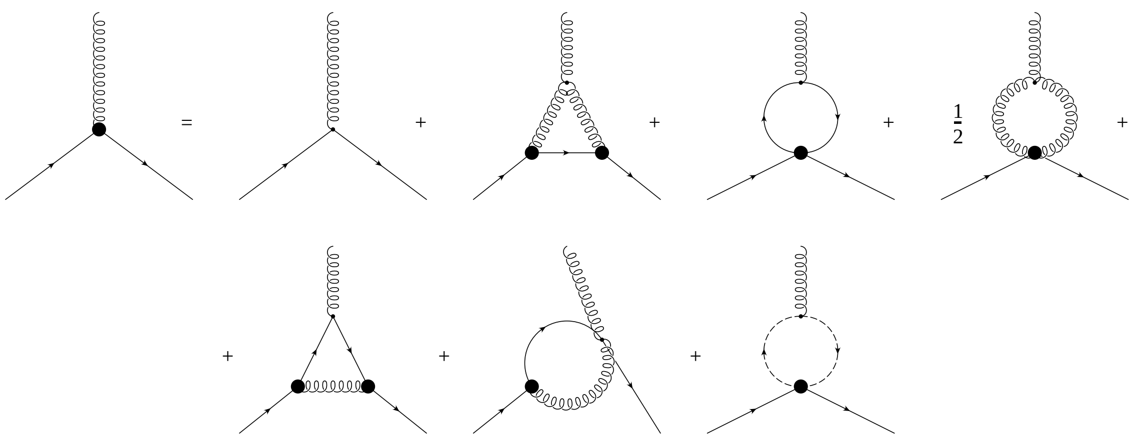

A.2.4. 4-gluon Vertex DSE

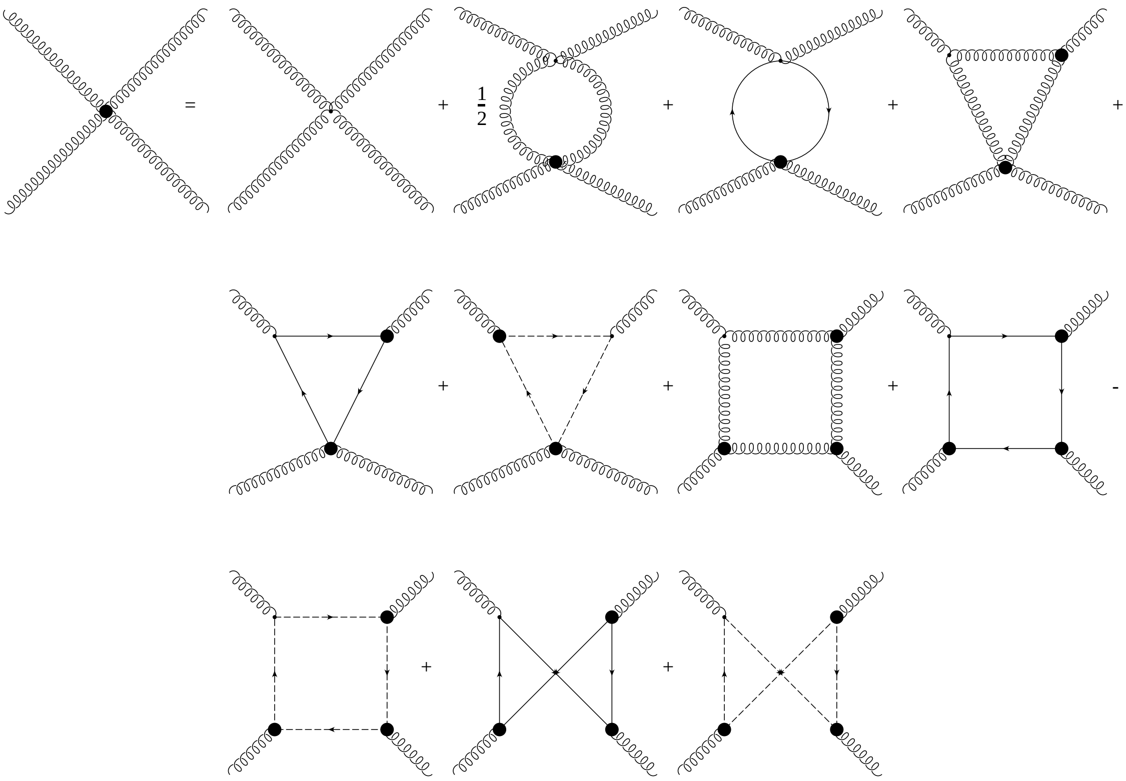

A.2.5. 2-scalar-2-gluon Vertex DSE

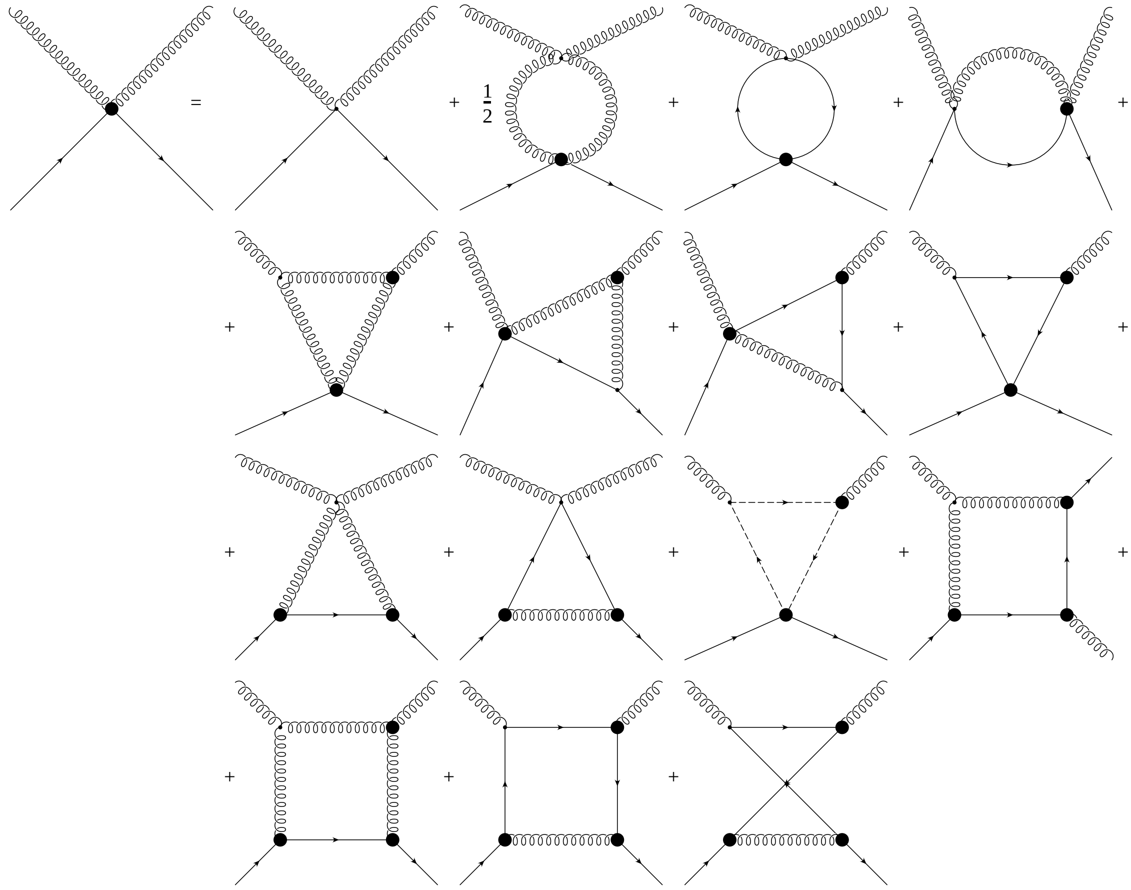

A.2.6. 4-scalar Vertex DSE

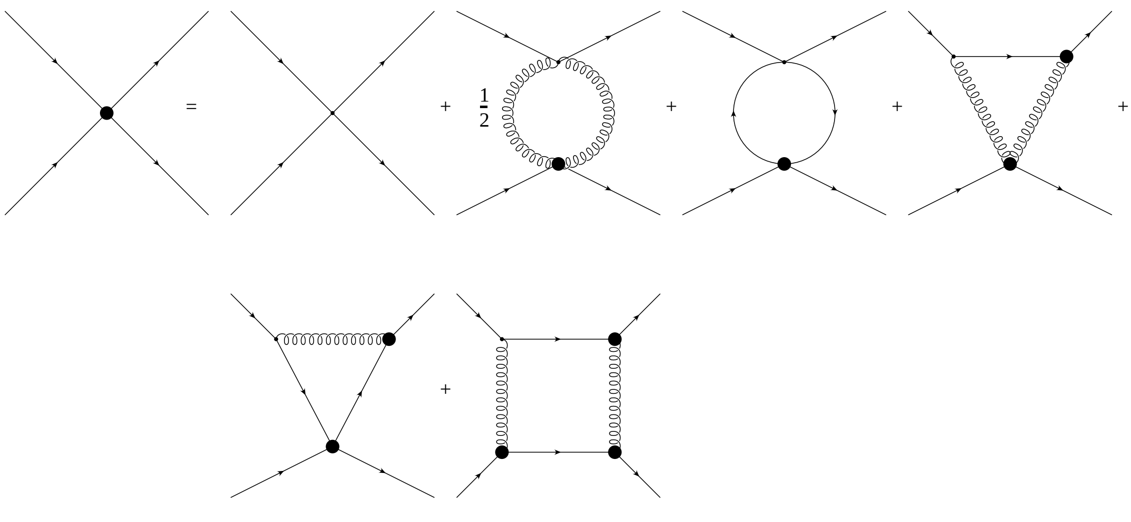

A.3. non tree-level Vertex Equations

For the sake of completeness the Dyson-Schwinger equations of the three appearing non tree-level vertices are given below.

A.3.1. 4-ghost Vertex DSE

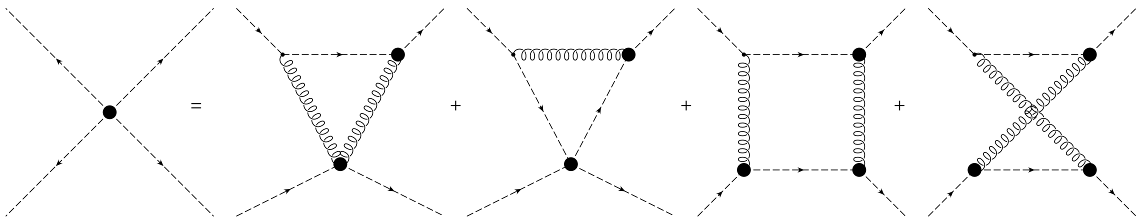

A.3.2. 2-ghost-2-gluon Vertex DSE

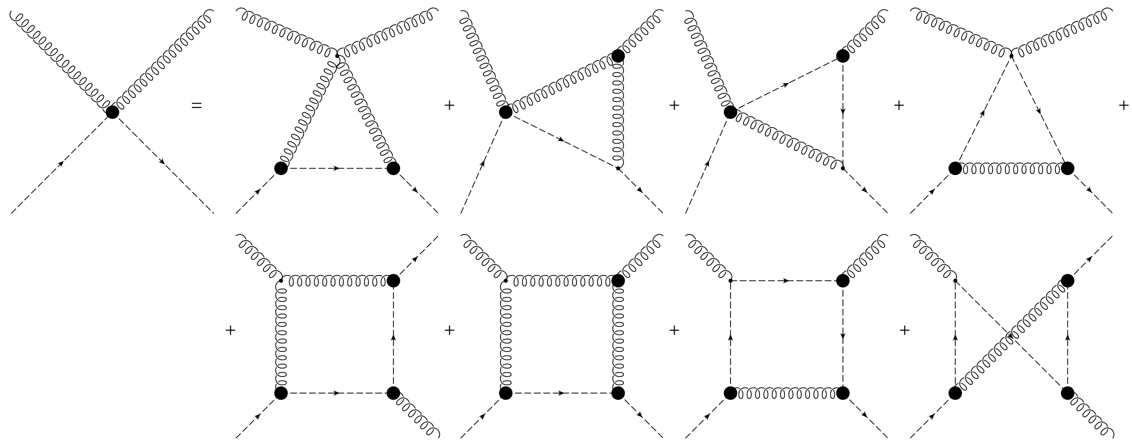

A.3.3. 2-scalar-2-ghost Vertex DSE

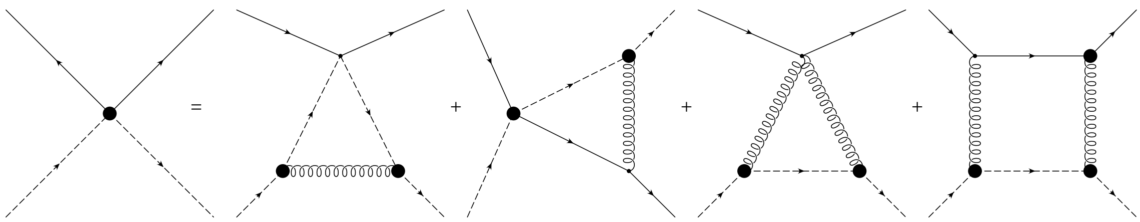

B. Colour structure of Feynman Diagrams

B.1. Vertex Conventions

In this chapter the expressions of the colour structures of the tree-level vertices are summarized. These factors can be read off from the Dyson-Schwinger equations calculated before. Greek letters refer to Lorentz and latin letters to colour indices.

i	imaginary unit
g	coupling constant of the gauge sector
h	coupling constant between scalars
f^{abc}	structure constants
(t^a_{ij})	generators of fundamental representation
p_μ, q_ν, k_σ	momentum tensors

B.1.1. pure Yang-Mills vertices

ghost-gluon vertex:

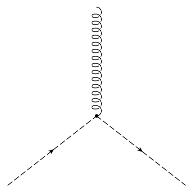

$$\sim igf^{abc}p^\mu$$

3-gluon vertex:

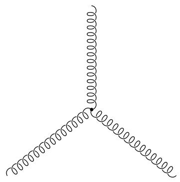

$$\sim -igf^{abc}\left((q-k)_\mu\delta_{\nu\rho} + (k-p)_\nu\delta_{\mu\rho} + (p-q)_\rho\delta_{\mu\nu}\right)$$

4-gluon vertex:

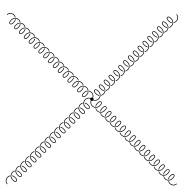

$$\begin{aligned}\sim g^2(&f^{eab}f^{ecd}(\delta_{\mu\sigma}\delta_{\nu\rho}-\delta_{\mu\rho}\delta_{\nu\sigma})+f^{eac}f^{ebd}(\delta_{\mu\nu}\delta_{\sigma\rho}-\delta_{\mu\rho}\delta_{\nu\sigma})\\ &+f^{ead}f^{ebc}(\delta_{\mu\nu}\delta_{\sigma\rho}-\delta_{\mu\sigma}\delta_{\nu\rho}))\\ &= g^2(f^{eab}f^{ecd}A + f^{eac}f^{ebd}B\\ &\quad +f^{ead}f^{ebc}C)\end{aligned}$$

B.1.2. vertices involving adjoint scalar fields

scalar-gluon vertex:

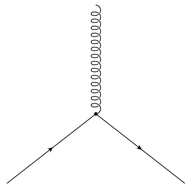

$$\sim igf^{abc}(q-k)_\mu$$

2-scalar-2-gluon vertex:

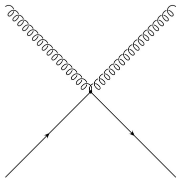

$$\sim g^2\left(f^{eac}f^{ebd}+f^{ead}f^{ebc}\right)\delta_{\mu\nu}$$

4-scalar vertex:

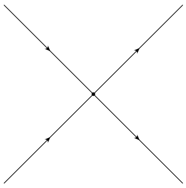

$$\sim 2h\left(\delta_{ab}\delta_{cd}+\delta_{ac}\delta_{bd}+\delta_{ad}\delta_{bc}\right)$$

B.1.3. vertices involving fundamental scalar fields

scalar-gluon vertex:

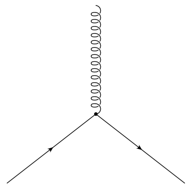

$$\sim ig(t^a)_{ij}q_\mu$$

2-scalar-2-gluon vertex:

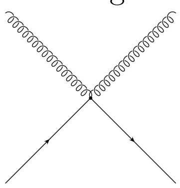

$$\sim g^2\left[\left(\tfrac{t^a}{2}\right)^\dagger_{ik}\left(\tfrac{t^b}{2}\right)_{kj}+\left(\tfrac{t^b}{2}\right)^\dagger_{ik}\left(\tfrac{t^a}{2}\right)_{kj}\right]\delta_{\mu\nu}$$

4-scalar vertex:

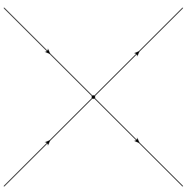

$$\sim -\tfrac{h}{3!}\left(\delta_{ab}\delta_{cd}+\delta_{ad}\delta_{bc}\right)$$

C. Results for colour structure of DSE diagrams

In this part the results of the colour contribution for all the diagrams are shown. In case of the DSEs of the 4-point function the results are projected on the basis given below. The structure of this chapter is as follows: The diagrams are classified by the DSEs they appear in. The colour structure of the tree-level diagrams can be found in appendix B. The remaining higher order diagrams are shown in the left column. The upper table of the right column contains the results for $SU(2)$, $SU(3)$ and $G(2)$ for the adjoint representation while the lower one corresponds to the fundamental representation.

The results of some diagrams contain factors A, B, ... F. They stem from the 4-gluon vertex whose tree-level colour structure does not factor from the Lorentz tensor structure. See appendix B.1.1 for details.

The 4-point functions are projected one the following basis:

- 4-legs-adjoint basis:

1^{st} component: $\left(f^{eac}f^{ebd} + f^{ead}f^{ebc}\right)$
2^{nd} component: $\left(f^{eac}f^{ebd} - f^{ead}f^{ebc}\right)$
3^{rd} component: $(\delta_{ab}\delta_{cd} + \delta_{ad}\delta_{bc} + \delta_{ac}\delta_{bd})$
4^{th} component: $\left(f^{eac}f^{ebd} - f^{ead}f^{ebc} + C_A(N_A-1)\delta_{ac}\delta_{bd} + C_A(1-N_A)\delta_{ad}\delta_{bc}\right)$
5^{th} component: $\left(f^{eac}f^{ebd} + f^{ead}f^{ebc} - \frac{2}{3}C_A(N_A+1)\delta_{ab}\delta_{cd} + \frac{1}{3}C_A(N_A+1)\delta_{ad}\delta_{bc} + \right.$
$\left. + \frac{1}{3}C_A(N_A+1)\delta_{ac}\delta_{bd}\right)$
6^{th} component: $\left(\delta_{ab}\delta_{cd} + \delta_{ad}\delta_{bc} + \delta_{ac}\delta_{bd} + \frac{24(N_A+2)}{T_R(C_A-6C_R)}d^{abcd}\right)$

Note that for appendix C.9 the first and the third component of the 4-legs-adjoint basis are interchanged.

- 2-legs-adjoint-2-legs fundamental basis:

1^{st} component: $\left((t^a)^\dagger_{ik}\left(t^b\right)_{kj} + \left(t^b\right)^\dagger_{ik}(t^a)_{kj}\right)$
2^{st} component: $\left((t^a)^\dagger_{ik}\left(t^b\right)_{kj} - \left(t^b\right)^\dagger_{ik}(t^a)_{kj}\right)$
3^{rd} component: $\left((t^a)^\dagger_{ik}\left(t^b\right)_{kj} + \left(t^b\right)^\dagger_{ik}(t^a)_{kj} - T_R(1+N_A)\delta_{ab}\delta_{cd}\right)$
4^{th} component: $\left(C_A(t^a)^\dagger_{ik}\left(t^b\right)_{kj} - C_A\left(t^b\right)^\dagger_{ik}(t^a)_{kj} - 2iT_R(N_A-1)f^{abc}(t^c)_{ij}\right)$
5^{th} component: $\left((t^a)^\dagger_{ik}\left(t^b\right)_{kj} + \left(t^b\right)^\dagger_{ik}(t^a)_{kj} - \frac{T_R N_A(-C_A+4C_R+T_R(1+N_A)(-4+N_R+N_AN_R))}{2N_R d33(1+N_A)}\times\right.$

$\times d^{abc} \left(t^c\right)_{ij} - \frac{C_A - 4C_R - 4T_R(N_A+1)}{N_R(N_A+1)} \delta_{ab}\delta_{cd} \Big)$

• 4-legs-fundamental basis:

1^{st} component: $(\delta_{ab}\delta_{cd} + \delta_{ad}\delta_{bc})$
2^{nd} component: $(\delta_{ab}\delta_{cd} - \delta_{ad}\delta_{bc})$
3^{rd} component: $\Big(-N_A T_R \delta_{ab}\delta_{cd} - N_A T_R \delta_{ad}\delta_{bc} + N_R(N_R+1) \left(t^a\right)_{ji} \left(t^a\right)_{lk} +$
$+ N_R(N_R+1) \left(t^b\right)_{jk} \left(t^b\right)_{li}\Big)$
4^{th} component: $\Big(-N_A T_R \delta_{ab}\delta_{cd} + N_A T_R \delta_{ad}\delta_{bc} - N_R(N_R-1) \left(t^a\right)_{ji} \left(t^a\right)_{lk} +$
$+ N_R(N_R-1) \left(t^b\right)_{jk} \left(t^b\right)_{li}\Big)$

C.1. ghost propagator DSE

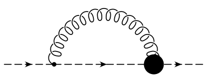

	group invariant	SU(2)	SU(3)	G(2)
adjoint	$C_A\delta^{ab}$	$2\delta^{ab}$	$3\delta^{ab}$	$2\delta^{ab}$

C.2. gluon propagator DSE

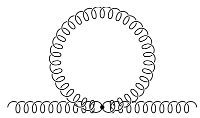

	group invariant	SU(2)	SU(3)	G(2)
adjoint	$2C_A\delta^{ab}$	$4\delta^{ab}$	$6\delta^{ab}$	$4\delta^{ab}$

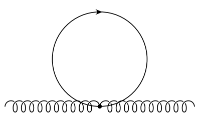

	group invariant	SU(2)	SU(3)	G(2)
adjoint	$2C_A\delta^{ab}$	$4\delta^{ab}$	$6\delta^{ab}$	$4\delta^{ab}$
fundamental	$T_R\delta^{ab}$	$\frac{1}{2}\delta^{ab}$	$\frac{1}{2}\delta^{ab}$	$\frac{1}{2}\delta^{ab}$

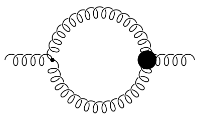

	group invariant	SU(2)	SU(3)	G(2)
adjoint	$C_A\delta^{ab}$	$2\delta^{ab}$	$3\delta^{ab}$	$2\delta^{ab}$

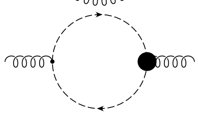

	group invariant	SU(2)	SU(3)	G(2)
adjoint	$C_A\delta^{ab}$	$2\delta^{ab}$	$3\delta^{ab}$	$2\delta^{ab}$

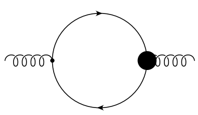

	group invariant	SU(2)	SU(3)	G(2)
adjoint	$C_A\delta^{ab}$	$2\delta^{ab}$	$3\delta^{ab}$	$2\delta^{ab}$
fundamental	$-T_R\delta^{ab}$	$-\frac{1}{2}\delta^{ab}$	$-\frac{1}{2}\delta^{ab}$	$-\frac{1}{2}\delta^{ab}$

C.3. scalar propagator DSE

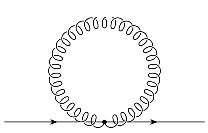

	group invariant	SU(2)	SU(3)	G(2)
adjoint	$2C_A\delta^{ab}$	$4\delta^{ab}$	$6\delta^{ab}$	$4\delta^{ab}$
fundamental	$\frac{1}{2}C_R\delta^{ab}$	$\frac{3}{8}\delta^{ab}$	$\frac{4}{6}\delta^{ab}$	$\frac{1}{2}\delta^{ab}$

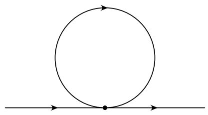

	group invariant	SU(2)	SU(3)	G(2)
adjoint	$2\,(N_A+2)\,\delta^{ab}$	$10\delta^{ab}$	$20\delta^{ab}$	$32\delta^{ab}$
fundamental	$(N_R+1)\delta^{ab}$	$3\delta^{ab}$	$4\delta^{ab}$	$8\delta^{ab}$

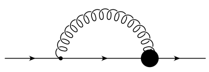

	group invariant	SU(2)	SU(3)	G(2)
adjoint	$C_A\delta^{ab}$	$2\delta^{ab}$	$3\delta^{ab}$	$2\delta^{ab}$
fundamental	$-C_R\delta^{ab}$	$-\frac{3}{4}\delta^{ab}$	$-\frac{4}{3}\delta^{ab}$	$-\delta^{ab}$

C.4. ghost-gluon Vertex DSE

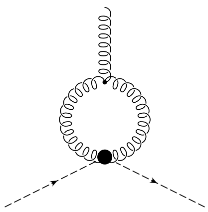

	group invariant	SU(2)	SU(3)	G(2)
L1	$-\frac{1}{2}C_A f^{abc}$	$-f^{abc}$	$\frac{3}{2}f^{abc}$	$-f^{abc}$
L2	$C_A f^{abc}$	$2f^{abc}$	$3f^{abc}$	$2f^{abc}$

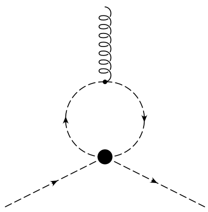

	group invariant	SU(2)	SU(3)	G(2)
adjoint	$C_A f^{abc}$	$2f^{abc}$	$3f^{abc}$	$2f^{abc}$

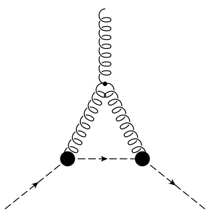

	group invariant	SU(2)	SU(3)	G(2)
adjoint	$-\frac{1}{2}C_A f^{abc}$	$-f^{abc}$	$\frac{3}{2}f^{abc}$	$-f^{abc}$

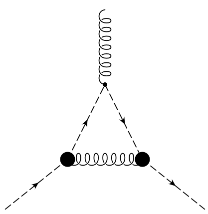

	group invariant	SU(2)	SU(3)	G(2)
adjoint	$-\frac{1}{2}C_A f^{abc}$	$-f^{abc}$	$-\frac{3}{2}f^{abc}$	$-f^{abc}$

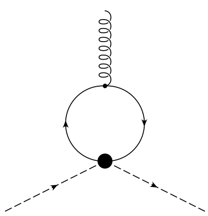

	group invariant	SU(2)	SU(3)	G(2)
adjoint	$-C_A f^{abc}$	$-2f^{abc}$	$-3f^{abc}$	$-2f^{abc}$
fundamental	$T_R f^{abc}$	$\frac{1}{2}f^{abc}$	$\frac{1}{2}f^{abc}$	$\frac{1}{2}f^{abc}$

C.5. 3-gluon vertex DSE

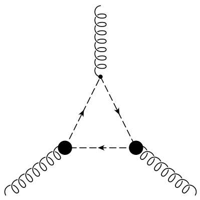

	group invariant	SU(2)	SU(3)	G(2)
	$\frac{1}{2}C_A f^{abc}$	f^{abc}	$\frac{3}{2}f^{abc}$	f^{abc}

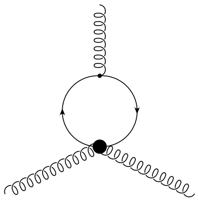

	group invariant	SU(2)	SU(3)	G(2)
adjoint	0	0	0	0
fundamental	$\frac{1}{2}d^{acb}$	0	$\frac{1}{2}d^{acb}$	0

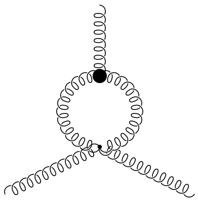

	group invariant	SU(2)	SU(3)	G(2)
	$\frac{D}{2}C_A f^{abc}\times$ $\times(A-B+$ $-2C)$	$f^{abc}D\times$ $\times(A-B+$ $-2C)$	$\frac{3}{2}Df^{abc}\times$ $\times(A-B+$ $-2C)$	$f^{abc}D\times$ $\times(A-B+$ $-2C)$

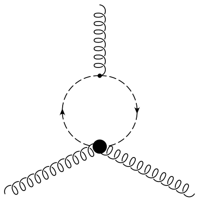

	group invariant	SU(2)	SU(3)	G(2)
L1	$\frac{1}{2}C_A f^{abc}$	f^{abc}	$\frac{3}{2}f^{abc}$	f^{abc}
L2	$-C_A f^{abc}$	$-2f^{abc}$	$-3f^{abc}$	$-2f^{abc}$

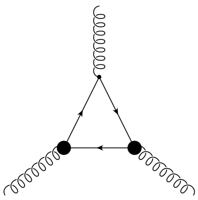

	group invariant	SU(2)	SU(3)	G(2)
adjoint	$\frac{1}{2}C_A f^{abc}$	f^{abc}	$\frac{3}{2}f^{abc}$	f^{abc}
fundamental	$-d^{abc}+$ $+\frac{1}{2}f^{abc}T_R$	$+\frac{1}{4}f^{abc}$	$-d^{abc}+$ $+\frac{1}{4}f^{abc}$	$+\frac{1}{4}f^{abc}$

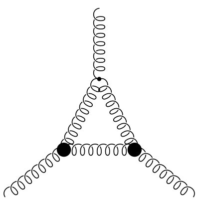

	group invariant	SU(2)	SU(3)	G(2)
	$-\frac{1}{2}C_A f^{abc}$	$-f^{abc}$	$-\frac{3}{2}f^{abc}$	$-f^{abc}$

C.6. scalar-gluon DSE

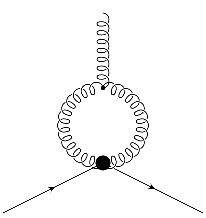

	group invariant	SU(2)	SU(3)	G(2)
adjoint	0	0	0	0
fundamental	0	0	0	0

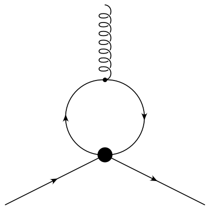

	group invariant	SU(2)	SU(3)	G(2)
adjoint	0	0	0	0
fundamental	$\frac{1}{6}\left(t^a\right)_{bc}$	$\frac{1}{6}\left(t^a\right)_{bc}$	$\frac{1}{6}\left(t^a\right)_{bc}$	$\frac{1}{6}\left(t^a\right)_{bc}$

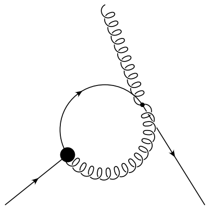

	group invariant	SU(2)	SU(3)	G(2)
adjoint	$\frac{3}{2}C_A f^{abc}$	$3f^{abc}$	$\frac{9}{2}f^{abc}$	$3f^{abc}$
fund.	$\frac{1}{2}\left(C_R - \frac{1}{2}C_A\right)$	$-\frac{1}{8}$	$-\frac{1}{12}$	0

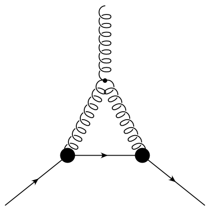

	group invariant	SU(2)	SU(3)	G(2)
adjoint	$-\frac{1}{2}C_A f^{abc}$	$-f^{abc}$	$-\frac{3}{2}f^{abc}$	$-f^{abc}$
fund.	$-\frac{1}{8}C_A$	$-\frac{1}{4}$	$-\frac{3}{8}$	$-\frac{1}{4}$

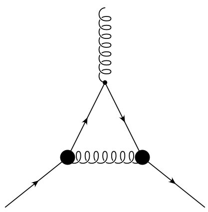

	group invariant	SU(2)	SU(3)	G(2)
adjoint	$\frac{1}{2}C_A f^{abc}$	f^{abc}	$\frac{3}{2}f^{abc}$	f^{abc}
fund.	$C_R - \frac{1}{2}C_A$	$-\frac{1}{4}$	$-\frac{1}{6}$	0

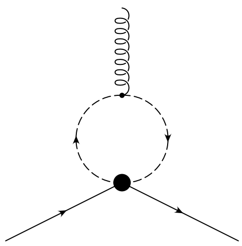

	group invariant	SU(2)	SU(3)	G(2)
adjoint	$-C_A f^{abc}$	$-2f^{abc}$	$-3f^{abc}$	$-2f^{abc}$
fund.	$\frac{1}{4}C_A\left(t^a\right)_{bc}$	$\frac{1}{2}\left(t^a\right)_{bc}$	$\frac{3}{4}\left(t^a\right)_{bc}$	$\frac{1}{2}\left(t^a\right)_{bc}$

C.7. 4-gluon vertex DSE

adj.	group invariant	SU(2)	SU(3)	G(2)
1^{st}	$-\frac{1}{2}N_A C_A^3$	-12	-108	-56
2^{nd}	$-\frac{1}{2}N_A C_A^3$	-12	-108	-56
3^{rd}	$10 N_A C_A^2$	120	720	560
4^{th}	$\frac{1}{2}N_A C_A^3(2N_A-3)$	36	1404	1400
5^{th}	$\frac{1}{6}N_A C_A^3(2N_A-1)$	20	540	504
6^{th}	$\frac{2}{T_R(C_A-6C_R)}\left(5N_A T_R C_A^2\times\right.$ $\left.\times(C_A-6C_R)+12\ \mathrm{d44}(2+N_A)\right)$	$\frac{3825}{32}$	$\frac{1435}{2}$	$\frac{1113}{2}$

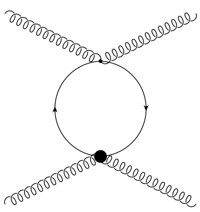

fund.	group invariant	SU(2)	SU(3)	G(2)
1^{st}	$-\frac{1}{16}N_A T_R C_A^2$	$-\frac{3}{8}$	$-\frac{9}{4}$	$-\frac{7}{4}$
2^{nd}	$-\frac{1}{16}N_A T_R C_A^2$	$-\frac{3}{8}$	$-\frac{9}{4}$	$-\frac{7}{4}$
3^{rd}	$-\frac{1}{4}N_A T_R(C_A-6C_R)$	$\frac{15}{16}$	5	7
4^{th}	$\frac{1}{16}N_A T_R C_A^2(2N_A-3)$	$\frac{9}{8}$	$\frac{117}{4}$	$\frac{175}{4}$
5^{th}	$\frac{1}{48}N_A T_R C_A^2(2N_A-1)$	$\frac{5}{8}$	$\frac{45}{4}$	$\frac{63}{4}$
6^{th}	$\frac{1}{192T_R(C_A-6C_R)}\left(48\ \mathrm{d44}(2+N_A)+\right.$ $+N_A T_R\left(-59C_A^3(2+N_A)+\right.$ $+576C_R^2\left(-3T_R+C_R(2+N_A)\right)$ $-72C_A C_R\left(-8T_R+9C_R(2+N_A)\right)+$ $\left.\left.+6C_A^2(-8T_R+51C_R(2+N_A))\right)\right)$	$\frac{2235}{1024}$	$\frac{3425}{576}$	$-\frac{455}{192}$

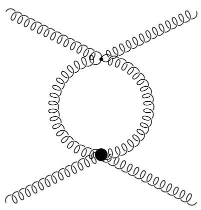

adj.	group invariant	SU(2)
1^{st}	$\frac{N_A C_A^3}{4}\left(A(D-3F-3G)+\right.$ $+3C(-D+2F+G)+$ $\left.+B(-2D+3F+G)\right)$	$6\left(A(D-3F-3G)+\right.$ $+3C(-D+2F+G)+$ $\left.+B(-2D+3F+G)\right)$
2^{nd}	$-\frac{1}{2}N_A C_A^3\left(A(D-F)+\right.$ $+B(G+F)+$ $\left.+C(-D+G+2F)\right)$	$-6\left(A(D-F)+\right.$ $+B(G+F)+$ $\left.+C(-D+G+2F)\right)$
3^{rd}	$\frac{5}{2}N_A C_A^2(A+B)(D+G)$	$30(A+B)(D+G)$
4^{th}	$\frac{1}{4}N_A C_A^3(2N_A-3)\left(A(D-F)+\right.$ $\left.+B(G+F)+C(-D+G+2F)\right)$	$18\left(A(D-F)+B(G+F)+\right.$ $\left.+C(-D+G+2F)\right)$
5^{th}	$-\frac{1}{12}N_A C_A^3(2N_A-1)\times$ $\times\left(A(D-2G-3F)+\right.$ $+3C(-D+G+2F)+$ $\left.+B(-2D+G+3F)\right)$	$-10\left(A(D-2G-3F)+\right.$ $+3C(-D+G+2F)+$ $\left.+B(-2D+G+3F)\right)$
6^{th}	$\frac{(A+B)(D+G)}{2T_R(C_A-6C_R)}\left(5N_A T_R C_A^2\times\right.$ $\left.\times(C_A-6C_R)+12\,\mathrm{d44}(2+N_A)\right)$	$\frac{3825}{128}(A+B)(D+G)$

	SU(3)	G(2)
1^{st}	$54\left(A(D-3F-3G)+\right.$ $+3C(-D+2F+G)+$ $\left.+B(-2D+3F+G)\right)$	$28\left(A(D-3F-3G)+\right.$ $+3C(-D+2F+G)+$ $\left.+B(-2D+3F+G)\right)$
2^{nd}	$-54\left(A(D-F)+\right.$ $+B(G+F)+$ $\left.+C(-D+G+2F)\right)$	$-28\left(A(D-F)+\right.$ $+B(G+F)+$ $\left.+C(-D+G+2F)\right)$
3^{rd}	$180(A+B)(D+G)$	$140(A+B)(D+G)$
4^{th}	$702\left(A(D-F)+B(G+F)+\right.$ $\left.+C(-D+G+2F)\right)$	$700\left(A(D-F)+B(G+F)+\right.$ $\left.+C(-D+G+2F)\right)$
5^{th}	$-270\left(A(D-2G-3F)+\right.$ $+3C(-D+G+2F)+$ $\left.+B(-2D+G+3F)\right)$	$-252\left(A(D-2G-3F)+\right.$ $+3C(-D+G+2F)+$ $\left.+B(-2D+G+3F)\right)$
6^{th}	$\frac{1435}{8}(A+B)(D+G)$	$\frac{1113}{8}(A+B)(D+G)$

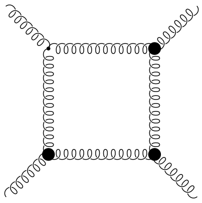

adj.	group invariant	SU(2)	SU(3)	G(2)
1^{st}	$\frac{1}{4}N_A C_A^3$	6	54	28
2^{nd}	$-\frac{1}{4}N_A C_A^3$	-6	-54	-28
3^{rd}	$\frac{5}{2}N_A C_A^2$	30	180	140
4^{th}	$\frac{1}{4}N_A C_A^3(2N_A-3)$	18	702	700
5^{th}	$-\frac{(1)}{12}N_A C_A^3(-2N_A+1)$	-10	-270	-252
6^{th}	$\frac{1}{2T_R(C_A-6C_R)}\left(5N_A T_R C_A^2\times\right.$ $\left.\times(C_A-6C_R)+12\,\mathrm{d44}(2+N_A)\right)$	$\frac{3825}{128}$	$\frac{1435}{8}$	$\frac{1113}{8}$

C. *Results for colour structure of DSE diagrams*

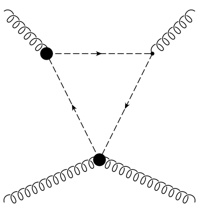

L_1	group invariant	SU(2)	SU(3)	G(2)
1^{st}	$\frac{1}{4}N_A C_A^3$	6	54	28
2^{nd}	$-\frac{1}{4}N_A C_A^3$	-6	-54	-28
3^{rd}	$\frac{5}{2}N_A C_A^2$	30	180	140
4^{th}	$\frac{1}{4}N_A C_A^3(2N_A - 3)$	18	702	700
5^{th}	$\frac{1}{12}N_A C_A^3(-2N_A + 1)$	-10	-270	-252
6^{th}	$\frac{1}{2T_R(C_A-6C_R)}\,(5N_A T_R C_A^2 \times$ $\times(C_A - 6C_R)+$ $+12\ \mathrm{d44}(2 + N_A))$	$\frac{3825}{128}$	$\frac{1435}{8}$	$\frac{1113}{8}$

L_2	group invariant	SU(2)	SU(3)	G(2)
1^{st}	$-\frac{3}{4}N_A C_A^3$	-18	-162	-84
2^{nd}	$\frac{1}{4}N_A C_A^3$	6	54	28
3^{rd}	0	0	0	0
4^{th}	$\frac{1}{4}N_A C_A^3(-2N_A + 3)$	-18	-702	-700
5^{th}	$\frac{1}{4}N_A C_A^3(2N_A - 1)$	30	810	756
6^{th}	0	0	0	0

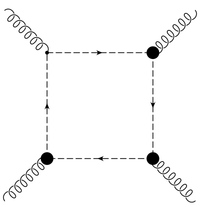

adj.	group invariant	SU(2)	SU(3)	G(2)
1^{st}	$\frac{1}{4}N_A C_A^3$	6	54	28
2^{nd}	$-\frac{1}{4}N_A C_A^3$	-6	-54	-28
3^{rd}	$\frac{5}{2}N_A C_A^2$	30	180	140
4^{th}	$\frac{1}{4}N_A C_A^3(2N_A - 3)$	18	702	700
5^{th}	$-\frac{1}{12}N_A C_A^3(-2N_A + 1)$	-10	-270	-252
6^{th}	$\frac{1}{2T_R(C_A-6C_R)}\,(5N_A T_R \times$ $\times C_A^2(C_A - 6C_R)+$ $+12\ \mathrm{d44}(2 + N_A))$	$\frac{3825}{128}$	$\frac{1435}{8}$	$\frac{1113}{8}$

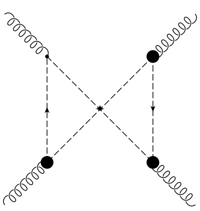

adj.	group invariant	SU(2)	SU(3)	G(2)
1^{st}	$-\frac{1}{2}N_A C_A^3$	-12	-108	-56
2^{nd}	0	0	0	0
3^{rd}	$\frac{5}{2}N_A C_A^2$	30	180	140
4^{th}	0	0	0	0
5^{th}	$\frac{1}{6}N_A C_A^3(2N_A - 1)$	20	540	504
6^{th}	$\frac{1}{2T_R(C_A-6C_R)}\,(5N_A T_R C_A^2 \times$ $\times(C_A - 6C_R)+$ $+12\ \mathrm{d44}(2 + N_A))$	$\frac{3825}{128}$	$\frac{1435}{8}$	$\frac{1113}{8}$

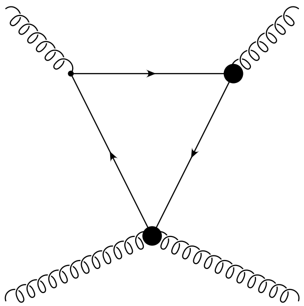

adj.	group invariant	SU(2)	SU(3)	G(2)
1^{st}	$-\frac{1}{4}N_A C_A^3$	-6	-54	-28
2^{nd}	$-\frac{1}{4}N_A C_A^3$	-6	-54	-28
3^{rd}	$5N_A C_A^2$	60	360	280
4^{th}	$\frac{1}{4}N_A C_A^3(2N_A - 3)$	18	702	700
5^{th}	$\frac{1}{12}N_A C_A^3(2N_A - 1)$	10	270	252
6^{th}	$\frac{1}{T_R(C_A-6C_R)}\left(5N_A T_R C_A^2\times\right.$ $\left.\times(C_A - 6C_R) + 12\ \mathrm{d44}(2 + N_A)\right)$	$\frac{3825}{64}$	$\frac{1435}{4}$	$\frac{1113}{4}$

fund.	group invariant	SU(2)	SU(3)	G(2)
1^{st}	$\frac{1}{16}N_A T_R C_A^2$	$\frac{3}{8}$	$\frac{9}{4}$	$\frac{7}{4}$
2^{nd}	$\frac{1}{16}N_A T_R C_A^2$	$\frac{3}{8}$	$\frac{9}{4}$	$\frac{7}{4}$
3^{rd}	$\frac{1}{4}N_A T_R(C_A - 6C_R)$	$-\frac{15}{16}$	-5	-7
4^{th}	$\frac{1}{16}N_A T_R C_A^2(-2N_A + 3)$	$-\frac{9}{8}$	$-\frac{117}{4}$	$-\frac{175}{4}$
5^{th}	$\frac{1}{48}N_A T_R C_A^2(-2N_A + 1)$	$-\frac{5}{8}$	$-\frac{45}{4}$	$-\frac{63}{4}$
6^{th}	$\frac{1}{96T_R(C_A-6C_R)}\left(-24\ \mathrm{d44}(2 + N_A) + N_A T_R\times\right.$ $(31C_A^3(2 + N_A) - 288C_R^2\left(-3T_R + C_R(2 + N_A)\right) +$ $+48C_A C_R\left(-6T_R + 7C_R(2 + N_A)\right) +$ $\left.-6C_A^2(-4T_R + 27C_R(2 + N_A)))\right)$	$-\frac{2139}{1024}$	$-\frac{3089}{576}$	$\frac{455}{192}$

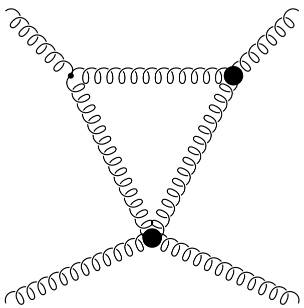

adj.	group invariant	SU(2)	SU(3)	G(2)
1^{st}	$\frac{(A-2B-3C)}{4} N_A C_A^3$	$6\,(A-2B+$ $-3C)$	$54\,(A-2B+$ $-3C)$	$28\,(A-2B+$ $-3C)$
2^{nd}	$\frac{(C-A)}{4} N_A C_A^3$	$6(C-A)$	$54(C-A)$	$28(C-A)$
3^{rd}	$\frac{5}{2} N_A C_A^2 (A+B)$	$30(A+B)$	$180(A+B)$	$140(A+B)$
4^{th}	$\frac{(A-C)}{4} N_A C_A^3 (2N_A-3)$	$18(A-C)$	$702(A-C)$	$700(A-C)$
5^{th}	$-\frac{(A-2B-3C)}{12} N_A C_A^3 \times$ $\times(2N_A-1)$	$-10\,(A+$ $-2B-3C)$	$-270\,(A+$ $-2B-3C)$	$-252\,(A+$ $-2B-3C)$
6^{th}	$\frac{(A+B)}{2T_R(C_A-6C_R)} \times$ $\times\,(5N_A T_R C_A^2$ $\times(C_A-6C_R)+$ $+12\ \mathrm{d44}(2+N_A))$	$\frac{3825}{128}(A+B)$	$\frac{1435}{8}(A+B)$	$\frac{1113}{8}(A+B)$

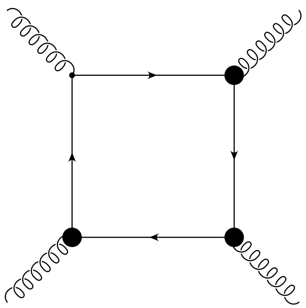

adj.	group invariant	SU(2)	SU(3)	G(2)
1^{st}	$\frac{1}{4}N_A C_A^3$	6	54	28
2^{nd}	$-\frac{1}{4}N_A C_A^3$	-6	-54	-28
3^{rd}	$\frac{5}{2}N_A C_A^2$	30	180	140
4^{th}	$\frac{1}{4}N_A C_A^3(2N_A-3)$	18	702	700
5^{th}	$-\frac{1}{12}N_A C_A^3(-2N_A+1)$	-10	-270	-252
6^{th}	$\frac{1}{2T_R(C_A-6C_R)}\left(5N_A T_R C_A^2\times\right.$ $\left.\times(C_A-6C_R)+12\ \mathrm{d44}(2+N_A)\right)$	$\frac{3825}{128}$	$\frac{1435}{8}$	$\frac{1113}{8}$

fund.	group invariant	SU(2)	SU(3)	G(2)
1^{st}	$\frac{1}{4}N_A T_R C_A^2$	$\frac{3}{2}$	9	7
2^{nd}	$-\frac{1}{4}N_A T_R C_A^2$	$-\frac{3}{2}$	-9	-7
3^{rd}	$-\frac{1}{2}N_A T_R(C_A-6C_R)$	$\frac{15}{8}$	10	14
4^{th}	$\frac{1}{4}N_A T_R C_A^2(2N_A-3)$	$\frac{9}{2}$	117	175
5^{th}	$\frac{1}{12}N_A T_R C_A^2(-2N_A+1)$	$-\frac{5}{2}$	-45	-63
6^{th}	$\frac{1}{12T_R(C_A-6C_R)}\left(12\ \mathrm{d44}(2+N_A)+N_A T_R\times\right.$ $(-35C_A^3(2+N_A)+72C_R^2\left(-3T_R+C_R(2+N_A)\right)+$ $+18C_A C_R\left(-4T_R+9C_R(2+N_A)\right)+$ $\left.+6C_A^2(-T_R+20C_R(2+N_A))))\right.$	$\frac{9675}{256}$	$-\frac{39505}{144}$	$\frac{12313}{48}$

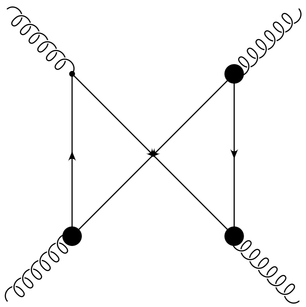

adj.	group invariant	SU(2)	SU(3)	G(2)
1^{st}	$-\frac{1}{2}N_A C_A^3$	-12	-108	-56
2^{nd}	0	0	0	0
3^{rd}	$\frac{5}{2}N_A C_A^2$	30	180	140
4^{th}	0	0	0	0
5^{th}	$\frac{1}{6}N_A C_A^3(2N_A-1)$	20	540	504
6^{th}	$\frac{1}{2T_R(C_A-6C_R)}\left(5N_A T_R C_A^2\times\right.$ $\left.\times(C_A-6C_R)+12\ \mathrm{d44}(2+N_A)\right)$	$\frac{3825}{128}$	$\frac{1435}{8}$	$\frac{1113}{8}$

fund.	group invariant	SU(2)	SU(3)	G(2)
1^{st}	$-\frac{1}{2}N_A T_R C_A^2$	-3	-18	-14
2^{nd}	0	0	0	0
3^{rd}	$-\frac{1}{2}N_A T_R(C_A-6C_R)$	$\frac{15}{8}$	10	14
4^{th}	0	0	0	0
5^{th}	$\frac{1}{6}N_A T_R C_A^2(2N_A-1)$	5	90	126
6^{th}	$\frac{1}{2T_R(C_A-6C_R)}\left(12\ \mathrm{d44}(2+N_A)+N_A T_R\times\right.$ $(-35C_A^3(2+N_A)+72C_R^2\left(-3T_R+C_R(2+N_A)\right)+$ $+18C_A C_R\left(-4T_R+9C_R(2+N_A)\right)+$ $\left.+6C_A^2(-T_R+20C_R(2+N_A))))\right.$	$\frac{225}{128}$	$-\frac{75}{8}$	$\frac{105}{8}$

C.8. 2-scalar-2-gluon vertex DSE

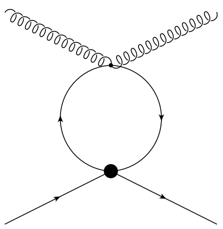

adj.	group invariant	SU(2)	SU(3)	G(2)
1^{st}	$20N_AC_A^2$	240	1440	1120
2^{nd}	0	0	0	0
3^{rd}	$4N_AC_A(N_A+2)$	120	960	1792
4^{th}	0	0	0	0
5^{th}	$-\frac{4}{3}N_AC_A^2(2N_A^2+6N_A-11)$	-400	-15840	-34720
6^{th}	0	0	0	0

fund.	group invariant	SU(2)	SU(3)	G(2)
1^{st}	$\frac{1}{24}N_AT_R(C_A-4(C_R+T_R))$	$-\frac{3}{16}$	$-\frac{13}{18}$	$-\frac{7}{6}$
2^{nd}	0	0	0	0
3^{rd}	$\frac{1}{24}N_AT_R\left(C_A+2\left(-2C_R+\right.\right.$ $\left.\left.+T_R(N_A+N_R+N_AN_R-1)\right)\right)$	$\frac{9}{16}$	$\frac{95}{18}$	$\frac{203}{6}$
4^{th}	0	0	0	0
5^{th}	$\frac{1}{24(1+N_A)}N_AT_R\left((3+N_A)\times\right.$ $\left.\times(C_A+2(-2C_R+T_R+T_RN_A))\right)$	$\frac{9}{32}$	$\frac{110}{81}$	$\frac{1547}{360}$

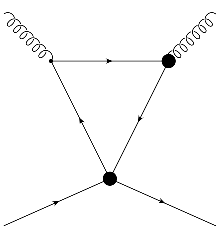

adj.	group invariant	SU(2)	SU(3)	G(2)
1^{st}	$10N_AC_A^2$	120	720	560
2^{nd}	0	0	0	0
3^{rd}	$2N_AC_A(N_A+2)$	60	480	896
4^{th}	0	0	0	0
5^{th}	$-\frac{2}{3}N_AC_A^2(2N_A^2+6N_A-11)$	-200	-7920	-17360
6^{th}	0	0	0	0

fund.	group invariant	SU(2)	SU(3)	G(2)
1^{st}	$\frac{1}{12}N_AT_R(-C_A+4(C_R+T_R))$	$\frac{3}{8}$	$\frac{13}{9}$	$\frac{7}{3}$
2^{nd}	$\frac{1}{12}N_AT_RC_A$	$\frac{1}{4}$	1	$\frac{7}{6}$
3^{rd}	$-\frac{1}{12}N_AT_R\left(C_A+2(-2C_R+\right.$ $\left.+T_R(N_A+N_R+N_AN_R-1))\right)$	$-\frac{9}{8}$	$-\frac{95}{9}$	$-\frac{203}{3}$
4^{th}	$-\frac{1}{12}N_AT_RC_A(C_A-2T_R(N_A-1))$	0	4	$\frac{77}{6}$
5^{th}	$-\frac{3+N_A}{12(1+N_A)}N_AT_R\left(C_A+2(-2C_R+\right.$ $\left.+T_R+T_RN_A)\right)$	$-\frac{9}{16}$	$-\frac{220}{81}$	$-\frac{1547}{180}$

C. Results for colour structure of DSE diagrams

adj.	group invariant	SU(2)	SU(3)	G(2)
1^{st}	0	0	0	0
2^{nd}	$-\frac{1}{2}N_A C_A^3$	-12	-108	-56
3^{rd}	0	0	0	0
4^{th}	$\frac{1}{2}N_A C_A^3(2N_A - 3)$	36	1404	1400
5^{th}	0	0	0	0
6^{th}	0	0	0	0

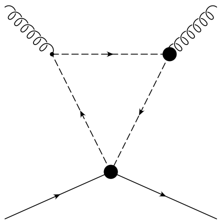

fund.	group invariant	SU(2)	SU(3)	G(2)
1^{st}	$-\frac{1}{8}N_A T_R\,(3C_A^2 - 10C_A C_R +$ $+8C_R^2)$	$-\frac{9}{32}$	$-\frac{11}{18}$	0
2^{nd}	0	0	0	0
3^{rd}	$\frac{1}{8}N_A T_R\,(-3C_A^2 + 10C_A C_R +$ $+4C_R(-2C_R + T_R + T_R N_A))$	$\frac{27}{32}$	$\frac{205}{18}$	$\frac{105}{4}$
4^{th}	0	0	0	0
5^{th}	$\frac{1}{8}N_A T_R\,(-3C_A^2 + 10C_A C_R +$ $+4C_R(-2C_R + T_R + T_R N_A))$	$\frac{27}{32}$	$\frac{205}{18}$	$\frac{105}{4}$

adj.	group invariant	SU(2)	SU(3)	G(2)
1^{st}	$\frac{1}{2}N_A C_A^3$	12	108	56
2^{nd}	0	0	0	0
3^{rd}	$5N_A C_A^2$	60	360	280
4^{th}	$\frac{1}{6}N_A C_A^3(1 - 2N_A)$	-20	-540	-504
5^{th}	0	0	0	0
6^{th}	$\frac{1}{T_R(C_A - 6C_R)}\,(5N_A T_R C_A^2 \times$ $\times(C_A - 6C_R) +$ $+12\ \mathrm{d44}(2 + N_A))$	$\frac{3825}{64}$	$\frac{1435}{4}$	$\frac{1113}{4}$

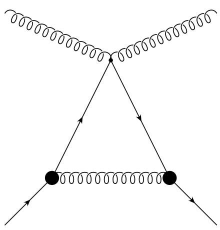

fund.	group invariant	SU(2)	SU(3)	G(2)
1^{st}	$-\frac{1}{4}N_A T_R C_A^2$	$-\frac{3}{2}$	-9	-7
2^{nd}	$-\frac{1}{4}N_A T_R C_A^2$	$-\frac{3}{2}$	-9	-7
3^{rd}	$-\frac{1}{4}N_A T_R C_A\,(C_A +$ $-4T_R(1 + N_A))$	$\frac{9}{2}$	45	98
4^{th}	$\frac{1}{4}N_A T_R C_A^3$	3	27	14
5^{th}	$-\frac{N_A T_R C_A}{4N_R(1+N_A)}\,(16\,(C_R +$ $-T_R(1 + N_A)) +$ $+C_A(N_R + N_A N_R - 4))$	$\frac{9}{8}$	$-\frac{55}{27}$	$-\frac{49}{15}$

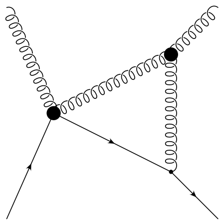

adj.	group invariant	SU(2)	SU(3)	G(2)
1^{st}	$-\frac{5}{4}N_A C_A^3$	-30	-270	-140
2^{nd}	$\frac{1}{4}N_A C_A^3$	6	54	28
3^{rd}	$\frac{5}{2}N_A C_A^2$	30	180	140
4^{th}	$\frac{1}{4}N_A C_A^3(3-2N_A)$	-18	-702	-700
5^{th}	$\frac{5}{12}N_A C_A^3(2N_A-1)$	50	1350	1260
6^{th}	$\frac{1}{2T_R(C_A-6C_R)}\left(5N_A T_R \times \times C_A^2(C_A-6C_R)+ +12\ \mathrm{d44}(2+N_A)\right)$	$\frac{3825}{128}$	$\frac{1435}{8}$	$\frac{1113}{8}$

fund.	group invariant	SU(2)	SU(3)	G(2)
1^{st}	$\frac{1}{16}iN_A T_R C_A(3C_A-8C_R)$	0	$-\frac{5i}{4}$	$-\frac{7i}{4}$
2^{nd}	$-\frac{1}{16}iN_A T_R C_A^2$	$-\frac{3i}{8}$	$-\frac{9i}{4}$	$-\frac{7i}{4}$
3^{rd}	$\frac{1}{16}iN_A T_R C_A(3C_A-8C_R)$	0	$-\frac{5i}{4}$	$-\frac{7i}{4}$
4^{th}	$\frac{1}{16}iN_A T_R C_A\left(C_A^2+ -4C_A T_R(N_A-1)+ +16C_R T_R(N_A-1)\right)$	$\frac{3i}{2}$	$\frac{125i}{4}$	$49i$
5^{th}	$\frac{1}{16}iN_A T_R C_A(3C_A-8C_R)$	0	$-\frac{5i}{4}$	$-\frac{7i}{4}$

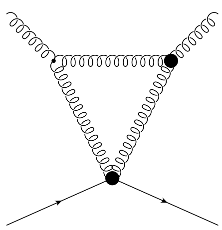

adj.	group invariant	SU(2)	SU(3)	G(2)
1^{st}	$-\frac{1}{2}N_A C_A^3$	-12	-108	-56
2^{nd}	0	0	0	0
3^{rd}	$-5N_A C_A^2$	-60	-360	-280
4^{th}	0	0	0	0
5^{th}	$\frac{1}{6}N_A C_A^3(2N_A-1)$	20	540	504
6^{th}	$-\frac{1}{T_R(C_A-6C_R)}\left(5N_A T_R C_A^2 \times \times(C_A-6C_R)+ +12\ \mathrm{d44}(2+N_A)\right)$	$-\frac{3825}{64}$	$-\frac{1435}{4}$	$-\frac{1113}{4}$

fund.	group invariant	SU(2)	SU(3)	G(2)
1^{st}	$-\frac{1}{2}iN_A T_R C_A(C_A-2C_R)$	$-\frac{3i}{4}$	$-2i$	0
2^{nd}	0	0	0	0
3^{rd}	$-\frac{1}{2}iN_A T_R C_A\left(C_A-2C_R-T_R+ -T_R N_A\right)$	$\frac{9i}{4}$	$25i$	$\frac{105i}{2}$
4^{th}	$-2iN_A T_R^2 C_A C_R(N_A-1)$	$-\frac{9i}{2}$	$-112i$	$-182i$
5^{th}	$-\frac{N_A T_R C_A}{2N_R(1+N_A)}\left(C_A(N_R+N_A N_R-1)+ -4T_R(1+N_A)+ +2C_R(N_R+N_A N_R-2)\right)$	$\frac{9i}{16}$	$\frac{40i}{27}$	$\frac{28i}{15}$

C. *Results for colour structure of DSE diagrams*

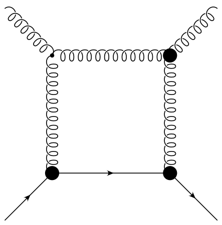

adj.	group invariant	SU(2)	SU(3)	G(2)
1^{st}	$-\frac{1}{4}N_AC_A^3$	-6	-54	-28
2^{nd}	$\frac{1}{4}N_AC_A^3$	6	54	28
3^{rd}	$-\frac{5}{2}N_AC_A^2$	-30	-180	-140
4^{th}	$\frac{1}{4}N_AC_A^3(3-2N_A)$	-18	-702	-700
5^{th}	$\frac{1}{12}N_AC_A^3(2N_A-1)$	10	270	252
6^{th}	$-\frac{1}{2T_R(C_A-6C_R)}\left(5N_AT_R\times\right.$ $\times C_A^2(C_A-6C_R)+$ $\left.+12\ \mathrm{d44}(2+N_A)\right)$	$-\frac{3825}{128}$	$-\frac{1435}{8}$	$-\frac{1113}{8}$

fund.	group invariant	SU(2)	SU(3)	G(2)
1^{st}	$\frac{1}{4}N_AT_R(3C_A^2-10C_AC_R+8C_R^2)$	$\frac{9}{16}$	$\frac{11}{9}$	0
2^{nd}	$-\frac{1}{4}N_AT_RC_A(C_A-2C_R)$	$-\frac{3}{8}$	-1	0
3^{rd}	$-\frac{1}{4}N_AT_R\left(-3C_A^2+10C_AC_R+\right.$ $\left.+4C_R(-2C_R+T_R+T_RN_A)\right)$	$-\frac{27}{16}$	$-\frac{205}{9}$	$-\frac{105}{2}$
4^{th}	$\frac{1}{4}N_AT_RC_A\left(C_A^2-2C_AC_R+\right.$ $\left.+4C_RT_R(N_A-1)\right)$	3	59	91
5^{th}	$-\frac{N_AT_R}{4}\left(-3C_A^2+10C_AC_R+\right.$ $\left.+4C_R(-2C_R+T_R+T_RN_A)\right)$	$-\frac{27}{16}$	$-\frac{205}{9}$	$-\frac{105}{2}$

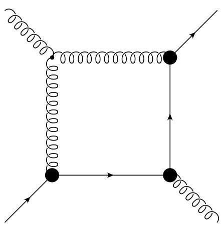

adj.	group invariant	SU(2)	SU(3)	G(2)
1^{st}	$\frac{1}{2}N_AC_A^3$	12	108	56
2^{nd}	0	0	0	0
3^{rd}	$-\frac{5}{2}N_AC_A^2$	-30	-180	-140
4^{th}	0	0	0	0
5^{th}	$\frac{1}{6}N_AC_A^3(1-2N_A)$	-20	-540	-504
6^{th}	$-\frac{1}{2T_R(C_A-6C_R)}\left(5N_AT_R\times\right.$ $\times C_A^2(C_A-6C_R)+$ $\left.+12\ \mathrm{d44}(2+N_A)\right)$	$-\frac{3825}{128}$	$-\frac{1435}{8}$	$-\frac{1113}{8}$

fund.	group invariant	SU(2)	SU(3)	G(2)
1^{st}	0	0	0	0
2^{nd}	$\frac{1}{2}iN_AT_RC_A^2$	$3i$	$18i$	$14i$
3^{rd}	0	0	0	0
4^{th}	$-\frac{1}{1}iN_AT_RC_A^2\left(C_A+\right.$ $\left.-2T_RN_A(N_A-1)\right)$	$12i$	$954i$	$2520i$
5^{th}	0	0	0	0

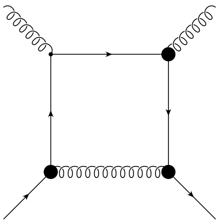

adj.	group invariant	SU(2)	SU(3)	G(2)
1^{st}	$\frac{1}{4}N_AC_A^3$	6	54	28
2^{nd}	$-\frac{1}{4}N_AC_A^3$	-6	-54	-28
3^{rd}	$\frac{5}{2}N_AC_A^2$	30	180	140
4^{th}	$\frac{1}{4}N_AC_A^3(2N_A-3)$	18	702	700
5^{th}	$\frac{1}{12}N_AC_A^3(1-2N_A)$	-10	-270	-252
6^{th}	$\frac{1}{2T_R(C_A-6C_R)}\,(5N_AT_R\times$ $\times C_A^2(C_A-6C_R)+$ $+12\ \mathrm{d44}(2+N_A))$	$\frac{3825}{128}$	$\frac{1435}{8}$	$\frac{1113}{8}$

fund.	group invariant	SU(2)	SU(3)	G(2)
1^{st}	$\frac{1}{8}N_AT_RC_A^2$	$\frac{3}{4}$	$\frac{9}{2}$	$\frac{7}{2}$
2^{nd}	0	0	0	0
3^{rd}	$\frac{1}{8}N_AT_RC_A(C_A-4T_R(1+N_A))$	$-\frac{9}{4}$	$-\frac{45}{2}$	-49
4^{th}	0	0	0	0
5^{th}	$\frac{N_AT_RC_A}{8N_R(1+N_A)}\,(16\,(C_R+$ $-T_R(1+N_A))+$ $+C_A(N_R+N_AN_R-4))$	$-\frac{9}{16}$	$\frac{55}{54}$	$\frac{49}{30}$

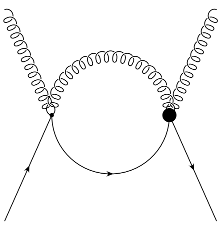

adj.	group invariant	SU(2)	SU(3)	G(2)
1^{st}	$\frac{13}{4}N_AC_A^3$	78	702	364
2^{nd}	$-\frac{5}{4}N_AC_A^3$	-30	270	-140
3^{rd}	$\frac{5}{2}N_AC_A^2$	30	180	140
4^{th}	$\frac{5}{4}N_AC_A^3(2N_A-3)$	90	3510	3500
5^{th}	$\frac{13}{12}N_AC_A^3(1-2N_A)$	-130	-3510	-3276
6^{th}	$\frac{1}{2T_R(C_A-6C_R)}\,(5N_AT_R\times$ $\times C_A^2(C_A-6C_R)+$ $+12\ \mathrm{d44}(2+N_A))$	$\frac{3825}{128}$	$\frac{1435}{8}$	$\frac{1113}{8}$

fund.	group invariant	SU(2)	SU(3)	G(2)
1^{st}	$\frac{1}{32}N_AT_R(5C_A^2-24C_AC_R+32C_R^2)$	$\frac{3}{32}$	$\frac{53}{72}$	$\frac{7}{8}$
2^{nd}	$\frac{1}{32}N_AT_RC_A(8C_R-3C_A)$	0	$\frac{5}{8}$	$\frac{7}{8}$
3^{rd}	$\frac{1}{32}N_AT_R\,(5C_A^2+$ $+4C_A(T_R+T_RN_A-6C_R)+$ $+16C_R(2C_R-T_R(1+N_A)))$	$-\frac{9}{32}$	$-\frac{325}{72}$	$-\frac{49}{4}$
4^{th}	$\frac{1}{32}N_AT_RC_A^2(-8C_R+3C_A)$	0	$-\frac{15}{8}$	$-\frac{7}{4}$
5^{th}	$\frac{1}{32(1+N_A)N_R}N_AT_R\times$ $\times(-16C_R(1+N_A)\times$ $\times(-2C_R+T_R+T_RN_A)+$ $+C_A^2(4+5N_R(1+N_A))+$ $-8C_A\,(-2T_R(1+N_A)+$ $+C_R(2+3N_R(1+N_A))))$	$-\frac{45}{64}$	$-\frac{2245}{216}$	$-\frac{2989}{120}$

C. Results for colour structure of DSE diagrams

adj.	group invariant	SU(2)	SU(3)	G(2)
1^{st}	$\frac{1}{4}N_AC_A^3$	6	54	28
2^{nd}	$\frac{1}{4}N_AC_A^3$	6	54	28
3^{rd}	$\frac{5}{2}N_AC_A^2$	30	180	140
4^{th}	$\frac{1}{4}N_AC_A^3(-2N_A+3)$	-18	-702	-700
5^{th}	$\frac{1}{12}N_AC_A^3(1-2N_A)$	-10	-270	-252
6^{th}	$\frac{1}{2T_R(C_A-6C_R)}\left(5N_AT_R\times \times C_A^2(C_A-6C_R)+ +12\ \mathrm{d44}(2+N_A)\right)$	$\frac{3825}{128}$	$\frac{1435}{8}$	$\frac{1113}{8}$

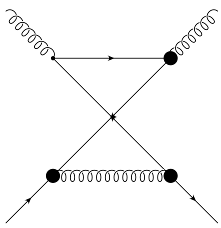

fund.	group invariant	SU(2)	SU(3)	G(2)
1^{st}	$\frac{1}{4}N_AT_R(3C_A^2-10C_AC_R+8C_R^2)$	$\frac{9}{16}$	$\frac{11}{9}$	0
2^{nd}	$\frac{1}{4}N_AT_RC_A(C_A-2C_R)$	$\frac{3}{8}$	1	0
3^{rd}	$-\frac{1}{4}N_AT_R\left(-3C_A^2+10C_AC_R+ +4C_R^2(-2C_R+T_R+T_RN_A)\right)$	$-\frac{27}{16}$	$-\frac{205}{9}$	$-\frac{105}{2}$
4^{th}	$-\frac{1}{4}N_AT_RC_A\left(C_A^2-2C_AC_R+ +4C_RT_R(N_A-1)\right)$	-3	-59	-91
5^{th}	$\frac{N_AT_RC_A}{8N_R(1+N_A)}\left(16(C_R-T_R(1+N_A))+ -\frac{1}{4}N_AT_R\left(-3C_A^2+10C_AC_R+ +4C_R^2(-2C_R+T_R+T_RN_A)\right)\right.$	$-\frac{27}{16}$	$-\frac{205}{9}$	$-\frac{105}{2}$

adj.	group invariant	SU(2)	SU(3)	G(2)
1^{st}	$-N_AC_A^3$	-24	-216	-112
2^{nd}	$\frac{1}{2}N_AC_A^3$	12	108	56
3^{rd}	$-\frac{5}{2}N_AC_A^2$	-30	-180	-140
4^{th}	$\frac{1}{2}N_AC_A^3(3-2N_A)$	-36	-1404	-1400
5^{th}	$\frac{1}{3}N_AC_A^3(2N_A-1)$	40	1080	1008
6^{th}	$-\frac{1}{2T_R(C_A-6C_R)}\left(5N_AT_R\times \times C_A^2(C_A-6C_R)+ +12\ \mathrm{d44}(2+N_A)\right)$	$-\frac{3825}{128}$	$-\frac{1435}{8}$	$-\frac{1113}{8}$

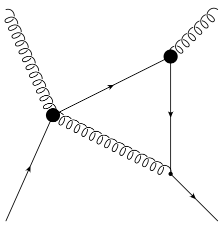

fund.	group invariant	SU(2)	SU(3)	G(2)
1^{st}	$-\frac{1}{4}N_AT_R(C_A-2C_R)^2$	$-\frac{3}{32}$	$-\frac{1}{9}$	0
2^{nd}	$\frac{1}{8}N_AT_RC_A(C_A-2C_R)$	$\frac{3}{16}$	$\frac{1}{2}$	0
3^{rd}	$-\frac{1}{8}N_AT_R\left(2C_A^2+ +C_A(-8C_R+T_R+T_RN_A)+ +4C_R(2C_R-T_R(1+N_A))\right)$	$\frac{9}{32}$	$\frac{185}{36}$	$\frac{105}{8}$
4^{th}	$-\frac{1}{8}N_AT_RC_A^2(C_A-2C_R)$	$-\frac{3}{8}$	$-\frac{3}{2}$	0
5^{th}	$-\frac{T_RN_A}{8N_R(1+N_A)}\left(4C_RN_R(1+N_A)\times \times\left(-2C_R+T_R+T_RN_A\right)+ -C_A^2\left(1+2(1+N_A)N_R\right)+ +4C_A(-T_R(1+N_A)+ +C_R(1+2N_R(1+N_A)))\right)$	$\frac{45}{64}$	$\frac{595}{54}$	$\frac{1547}{60}$

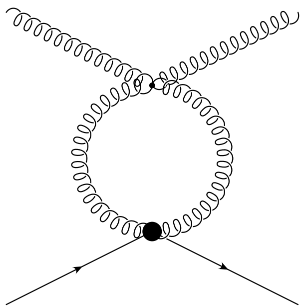

adj.	group invariant	SU(2)	SU(3)	G(2)
1^{st}	$-\frac{1}{2}N_A C_A^3(C+B)$	$12(C+B)$	$108(C+B)$	$56(C+B)$
2^{nd}	0	0	0	0
3^{rd}	$5N_A C_A^2(C+B)$	$60(C+B)$	$360(C+B)$	$280(C+B)$
4^{th}	0	0	0	0
5^{th}	$-\frac{1}{6}N_A C_A^3(2N_A-1)(B+C)$	$-20(C+B)$	$-540(C+B)$	$-504(C+B)$
6^{th}	$\frac{(C+B)}{T_R(C_A-6C_R)}(5N_A T_R C_A^2 \times$ $\times(C_A-6C_R)+12\ \mathrm{d44}(2+N_A))$	$\frac{3825}{64}(C+B)$	$\frac{1435}{4}(C+B)$	$\frac{1113}{4}(C+B)$

fund.	group invariant	SU(2)	SU(3)	G(2)
1^{st}	$-\frac{1}{8}N_A T_R C_A^2(A+B)$	$-\frac{3}{4}(A+B)$	$-\frac{9}{2}(A+B)$	$-\frac{7}{2}(A+B)$
2^{nd}	0	0	0	0
3^{rd}	$-\frac{1}{8}N_A T_R C_A(C_A-4T_R(1+N_A))$ $(A+B)$	$\frac{9}{4}(A+B)$	$\frac{45}{2}(A+B)$	$49(A+B)$
4^{th}	$\frac{1}{2}N_A T_R^2 C_A^2(N_A-1)C$	$3C$	$63C$	$91C$
5^{th}	$-\frac{A+B}{8N_R(1+N_A)}N_A T_R C_A \times$ $\times(16(C_R-T_R(1+N_A))+$ $+C_A(N_R+N_R N_A-4))$	$\frac{9}{16}(A+B)$	$-\frac{55}{54}(A+B)$	$-\frac{49}{30}(A+B)$

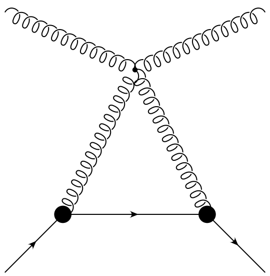

adj.	group invariant	SU(2)	SU(3)	G(2)
1^{st}	$-\frac{1}{4}N_A C_A^3(A+B)$	-6(A+B)	-54(A+B)	-28(A+B)
2^{nd}	$\frac{1}{4}N_A C_A^3(A-B-2C)$	6(A-B-2C)	54(A-B-2C)	28(A-B-2C)
3^{rd}	$-\frac{5}{2}N_A C_A^2(A+B)$	-30(A+B)	-180(A+B)	-140(A+B)
4^{th}	$-\frac{1}{4}N_A C_A^3(2N_A-3)(A-B-2C)$	18(A-B-2C)	-702(A-B-2C)	-700(A-B-2C)
5^{th}	$\frac{1}{12}N_A C_A^3(2N_A-1)(A+B)$	10(A+B)	270(A+B)	252(A+B)
6^{th}	$-\frac{(A+B)}{2T_R(C_A-6C_R)}\left(5N_A T_R C_A^2\times\right.$ $\left.\times(C_A-6C_R)+12\,\mathrm{d44}(2+N_A)\right)$	$-\frac{3825}{128}(A+B)$	$-\frac{1435}{8}(A+B)$	$-\frac{1113}{8}(A+B)$

fund.	group invariant	SU(2)	SU(3)	G(2)
1^{st}	$\frac{1}{4}N_A T_R C_A^2(A+B)$	$\frac{3}{2}(A+B)$	$9(A+B)$	$7(A+B)$
2^{nd}	$\frac{1}{4}N_A T_R C_A^2(A-B-2C)$	$\frac{3}{2}(A-B-2C)$	$9(A-B-2C)$	$7(A-B-2C)$
3^{rd}	$\frac{1}{4}N_A T_R C_A\,(C_A+$ $-4T_R(1+N_A))\,(A+B)$	$-\frac{9}{2}(A+B)$	$-45(A+B)$	$-98(A+B)$
4^{th}	$\frac{1}{4}N_A T_R C_A^3(B-A+2C)$	$3(B-A+2C)$	$27(-A+B+2C)$	$14(-A+B+2C)$
5^{th}	$\frac{T_R N_A C_A}{4N_R(1+N_A)}\times$ $\times(16\,(C_R-T_R(1+N_A))+$ $+C_A(-4+N_R+N_R N_A))$	$-\frac{9}{8}(A+B)$	$\frac{55}{27}(A+B)$	$\frac{49}{15}(A+B)$

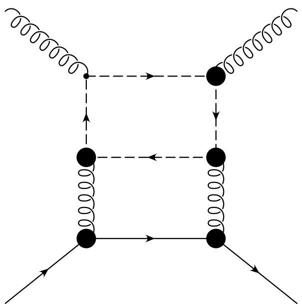

adj.	group invariant	SU(2)	SU(3)	G(2)
1^{st}	$\frac{1}{24}(N_A C_A^4 + 48\ \mathrm{d44})$	$\frac{1029}{512}$	$\frac{2597}{96}$	$\frac{1799}{192}$
2^{nd}	$-\frac{1}{8} N_A C_A^4$	-6	-81	-28
3^{rd}	$\frac{5}{4} N_A C_A^3$	30	270	140
4^{th}	$\frac{1}{8} N_A C_A^4 (2N_A - 3)$	18	1053	700
5^{th}	$\frac{1}{24}(N_A C_A^4 (13 + 14 N_A) + 48\ \mathrm{d44})$	$-\frac{56315}{512}$	$-\frac{323995}{96}$	$-\frac{374521}{192}$
6^{th}	$\frac{C_A}{4T_R(C_A - 6C_R)}\left(5 N_A T_R C_A^2 (C_A - 6C_R) + \right.$ $\left. +12\ \mathrm{d44}(2 + N_A)\right)$	$\frac{3825}{128}$	$\frac{4305}{16}$	$\frac{1113}{8}$

fund.	group invariant	SU(2)	SU(3)	G(2)
1^{st}	$-\frac{1}{24}(N_A T_R C_A^3 + 48\ \mathrm{d44})$	$-\frac{261}{512}$	$-\frac{437}{96}$	$-\frac{455}{192}$
2^{nd}	$-\frac{1}{8} N_A T_R C_A^3$	$-\frac{3}{2}$	$\frac{27}{2}$	-7
3^{rd}	$-\frac{1}{24}(N_A T_R C_A^2 (C_A - 24 T_R (1 + N_A)) +$ $+48\ \mathrm{d44})$	$\frac{5883}{512}$	$\frac{15115}{96}$	$\frac{39865}{192}$
4^{th}	$\frac{1}{8} N_A T_R C_A^3 (C_A - 4T_R(N_A - 1))$	-3	$-\frac{297}{2}$	-168
5^{th}	$\frac{1}{24 N_R (1+N_A)}\left(-48\ \mathrm{d44} N_R (1 + N_A) - N_A T_R C_A^3 (N_R + \right.$ $+ N_A N_R - 18) + 6 C_A^2 N_A T_R (-12 C_R + T_R (1 + N_A) \times$ $\left. \times (12 + N_R + N_A N_R))\right)$	$\frac{3291}{512}$	$\frac{4955}{96}$	$\frac{53501}{960}$

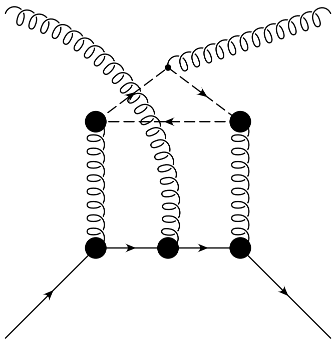

adj.	group invariant	SU(2)	SU(3)	G(2)
1^{st}	$-\frac{1}{8}N_A C_A^4$	-6	-81	-28
2^{nd}	$-\frac{1}{8}N_A C_A^4$	-6	-81	-28
3^{rd}	$-\frac{5}{4}N_A C_A^3$	-30	-270	-140
4^{th}	$\frac{1}{8}N_A C_A^4(2N_A - 3)$	18	1053	700
5^{th}	$\frac{1}{24}N_A C_A^4(-1 + 2N_A)$	10	405	252
6^{th}	$-\frac{C_A}{4T_R(C_A-6C_R)}(5N_A T_R C_A^2(C_A - 6C_R)+$ $+12\ \mathrm{d44}(2 + N_A))$	$-\frac{3825}{128}$	$-\frac{4305}{16}$	$-\frac{1113}{8}$

fund.	group invariant	SU(2)	SU(3)	G(2)
1^{st}	$-\frac{1}{4}iN_A T_R C_A^2(C_A - 2C_R)$	$-\frac{3i}{4}$	$-3i$	0
2^{nd}	0	0	0	0
3^{rd}	$\frac{1}{4}iN_A T_R C_A^2(-C_A + 2C_R + T_R + T_R N_A)$	$\frac{9i}{4}$	$-\frac{75i}{2}$	$-\frac{105i}{2}$
4^{th}	0	0	0	0
5^{th}	$\frac{iN_A T_R C_A^2}{4N_R(1+N_A)}(-C_A(-1 + N_R + N_A N_R)+$ $+2(2T_R(1 + N_A)) + C_R(-2 + N_R + N_A N_R)))$	$\frac{9i}{16}$	$\frac{20i}{9}$	$\frac{28i}{15}$

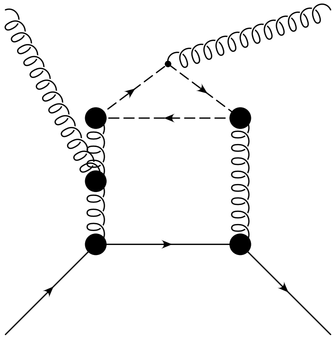

adj.	group invariant	SU(2)	SU(3)	G(2)
1^{st}	$-\frac{1}{8}N_A C_A^4$	-6	-81	-28
2^{nd}	$\frac{1}{8}N_A C_A^4$	6	81	28
3^{rd}	$-\frac{5}{4}N_A C_A^3$	-30	-270	-140
4^{th}	$\frac{1}{8}N_A C_A^4(-2N_A+3)$	-18	-1053	-700
5^{th}	$\frac{1}{24}N_A C_A^4(-1+2N_A)$	10	405	252
6^{th}	$-\frac{C_A}{4T_R(C_A-6C_R)}(5N_A T_R C_A^2(C_A-6C_R)+$ $+12\text{ d44}(2+N_A))$	$-\frac{3825}{128}$	$-\frac{4305}{16}$	$-\frac{1113}{8}$

fund.	group invariant	SU(2)	SU(3)	G(2)
1^{st}	$\frac{1}{8}N_A T_R C_A^3$	$\frac{3}{2}$	$\frac{27}{2}$	7
2^{nd}	$\frac{1}{8}N_A T_R C_A^3$	$\frac{3}{2}$	$\frac{27}{2}$	7
3^{rd}	$\frac{1}{8}N_A T_R C_A^2(C_A-4T_R(1+N_A))$	$-\frac{9}{2}$	$-\frac{135}{2}$	-98
4^{th}	$-\frac{1}{8}N_A T_R C_A^3(C_A-2T_R(-1+N_A))$	0	54	77
5^{th}	$\frac{N_A T_R C_A^2}{8N_R(1+N_A)}(8C_R+C_A(-2+N_R+N_R N_A)+$ $-2T_R(N_A^2 N_R+4+N_R+2N_A(1+N_R)))$	$-\frac{45}{16}$	$-\frac{290}{9}$	$-\frac{1021}{30}$

C.9. 4-scalar vertex

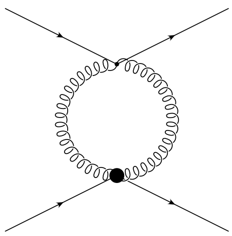

adj.	group invariant	SU(2)	SU(3)	G(2)
1^{st}	$10N_AC_A^2$	120	720	560
2^{nd}	$-\frac{1}{2}N_AC_A^3$	-12	-108	-56
3^{rd}	$-\frac{1}{2}N_AC_A^3$	-12	-108	-56
4^{th}	$-\frac{1}{2}N_AC_A^3(2N_A-3)$	36	1404	1400
5^{th}	$\frac{1}{6}N_AC_A^3(2N_A-1)$	20	540	504
6^{th}	$\frac{2}{T_R(C_A-6C_R)}(5N_AT_R\times$ $\times C_A^2(C_A-6C_R)+$ $+12\,\mathrm{d44}(2+N_A))$	$\frac{3825}{32}$	$\frac{1435}{2}$	$\frac{1113}{2}$

fund.	group invariant	SU(2)	SU(3)	G(2)
1^{st}	$\frac{1}{8}N_AT_R(-C_A+4(C_R+T_R))$	$\frac{9}{16}$	$\frac{13}{6}$	$\frac{7}{2}$
2^{nd}	$-\frac{1}{8}N_AT_R(-C_A-4(C_R-T_R))$	$-\frac{3}{16}$	$\frac{1}{6}$	0
3^{rd}	$-\frac{1}{8}N_AT_R\,(4C_RT_RN_A+4T_R^2N_A+$ $-4C_R^2N_R(1+N_R)+$ $+C_A(-T_RN_A+C_RN_R(1+N_R)))$	0	10	$\frac{147}{2}$
4^{th}	$\frac{1}{8}N_AT_R\,(-4C_RT_RN_A+4T_R^2N_A+$ $-4C_R^2N_R(-1+N_R)+$ $+C_A(T_RN_A+C_RN_R(-1+N_R)))$	0	-10	$-\frac{147}{2}$

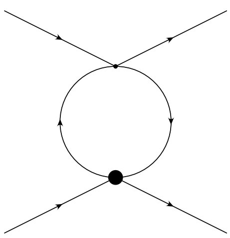

adj.	group invariant	SU(2)	SU(3)	G(2)
1^{st}	$4N_A(16+10N_A+N_A^2)$	660	5120	19712
2^{nd}	$-4N_AC_A(2+N_A)$	-120	-960	-1792
3^{rd}	$-4N_AC_A(2+N_A)$	-120	-960	-1792
4^{th}	$-4N_A^2C_A(-4+N_A^2)$	360	46080	301056
5^{th}	$\frac{4}{3}N_AC_A(-2+N_A)(2+N_A)^2$	200	19200	114688
6^{th}	0	0	0	0

fund.	group invariant	SU(2)	SU(3)	G(2)
1^{st}	$\frac{1}{36}N_R(3+4N_R+N_R^2)$	$\frac{5}{6}$	2	$\frac{140}{9}$
2^{nd}	$-\frac{1}{36}N_R(-1+N_R^2)$	$-\frac{1}{6}$	$-\frac{2}{3}$	$-\frac{28}{3}$
3^{rd}	0	0	0	0
4^{th}	0	0	0	0

adj.	group invariant	SU(2)	SU(3)	G(2)
1^{st}	$5N_AC_A^2$	60	360	280
2^{nd}	$-\frac{1}{4}N_AC_A^3$	-6	-54	-28
3^{rd}	$-\frac{1}{4}N_AC_A^3$	-6	-54	-28
4^{th}	$\frac{1}{4}N_AC_A^3(2N_A-3)$	18	702	700
5^{th}	$\frac{1}{12}N_AC_A^3(2N_A-1)$	10	270	252
6^{th}	$\frac{1}{T_R(C_A-6C_R)}\left(5N_AT_R\times\right.$ $\times C_A^2(C_A-6C_R)+$ $\left.+12\ \mathrm{d44}(2+N_A)\right)$	$\frac{3825}{64}$	$\frac{1435}{4}$	$\frac{1113}{4}$

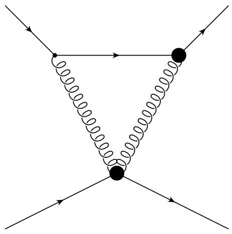

fund.	group invariant	SU(2)	SU(3)	G(2)
1^{st}	$\frac{1}{8}N_AT_R(C_A-4(C_R+T_R))$	$-\frac{9}{16}$	$-\frac{13}{6}$	$-\frac{7}{2}$
2^{nd}	$\frac{1}{8}N_AT_R(C_A-4(C_R-T_R))$	$\frac{3}{16}$	$-\frac{1}{6}$	0
3^{rd}	$-\frac{1}{16}\left(3N_AT_RN_RC_A^2(1+N_R)+\right.$ $+2N_AT_RC_A\left(N_AT_R+\right.$ $\left.-5N_RC_R(1+N_R)\right)+$ $+8\left(-N_A^2T_R^2C_R-N_A^2T_R^3+\right.$ $+\ \mathrm{d33}N_R(1+N_R)+$ $\left.\left.+N_AT_RN_RC_R^2(1+N_R)\right)\right)$	0	-15	0
4^{th}	$\frac{1}{16}\left(3N_AT_RN_RC_A^2(-1+N_R)+\right.$ $-2N_AT_RC_A\left(N_AT_R+\right.$ $\left.+5N_RC_R(-1+N_R)\right)+$ $+8\left(-N_A^2T_R^2C_R-N_A^2T_R^3+\right.$ $-\ \mathrm{d33}N_R(-1+N_R)+$ $\left.\left.+N_AT_RN_RC_R^2(-1+N_R)\right)\right)$	0	$-\frac{15}{2}$	0

adj.	group invariant	SU(2)	SU(3)	G(2)
1^{st}	$2N_AC_A(2+N_A)$	60	480	896
2^{nd}	$-5N_AC_A^2$	-60	-360	-280
3^{rd}	$-5N_AC_A^2$	-6	-360	-280
4^{th}	$N_AC_A^2(2N_A^2+2N_A-9)$	180	9720	23016
5^{th}	$\frac{1}{3}N_AC_A^2(2N_A^2+6N_A-11)$	100	3960	8680
6^{th}	0	0	0	0

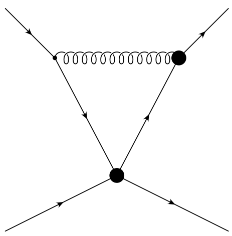

fund.	group invariant	SU(2)	SU(3)	G(2)
1^{st}	$-\frac{1}{6}N_AT_R(2+N_R)$	-1	$-\frac{10}{3}$	$-\frac{21}{2}$
2^{nd}	$\frac{1}{6}N_AT_RN_R$	$\frac{1}{2}$	2	$\frac{49}{6}$
3^{rd}	$\frac{1}{12}N_AT_R(N_R\left(C_A-4C_R\right)\times$ $\times(1+N_R)+$ $-2N_AT_R(-2+N_R^2))$	$-\frac{3}{2}$	-28	$-\frac{2695}{6}$
4^{th}	$\frac{1}{12}N_AT_R\left(2N_AT_R(-2+N_R)+\right.$ $\left.+C_A(-1+N_R)\right)$	$\frac{1}{2}$	14	$\frac{2009}{6}$

C. *Results for colour structure of DSE diagrams*

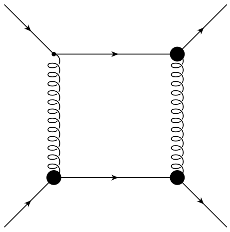

adj.	group invariant	SU(2)	SU(3)	G(2)
1^{st}	$\frac{5}{2}N_A C_A^2$	30	180	140
2^{nd}	$\frac{1}{4}N_A C_A^3$	6	54	28
3^{rd}	$-\frac{1}{4}N_A C_A^3$	-6	-54	-28
4^{th}	$-\frac{1}{4}N_A C_A^3(2N_A - 3)$	18	702	700
5^{th}	$-\frac{1}{12}N_A C_A^3(1 - N_A)$	-10	-270	-252
6^{th}	$\frac{1}{2T_R(C_A-6C_R)}\,(5N_A T_R\times$ $\times C_A^2(C_A - 6C_R)+$ $+12\ \mathrm{d44}(2 + N_A))$	$\frac{3825}{128}$	$\frac{1435}{8}$	$\frac{1113}{8}$

fund.	group invariant	SU(2)	SU(3)	G(2)
1^{st}	$N_A T_R(C_R + T_R)$	$\frac{15}{8}$	$\frac{22}{3}$	$\frac{21}{2}$
2^{nd}	$N_A T_R(-C_R + T_R)$	$-\frac{3}{8}$	$-\frac{10}{3}$	$-\frac{7}{2}$
3^{rd}	$-\frac{1}{2}N_A T_R\,(2T_R^2 N_A+$ $-2C_R^2 N_R(1 + N_R)+$ $+C_R(2T_R N_A + C_A N_R(1 + N_R)))$	$-\frac{9}{2}$	-40	$-\frac{147}{2}$
4^{th}	$-\frac{1}{2}N_A T_R\,(2T_R^2 N_A+$ $-2C_R^2 N_R(-1 + N_R)+$ $+C_R(-2T_R N_A+$ $+C_A N_R(-1 + N_R)))$	0	8	$\frac{49}{2}$

adj.	group invariant	SU(2)	SU(3)	G(2)
1^{st}	$\frac{1}{24}\left(48\ \mathrm{d44}+25N_AC_A^4\right)$	$\frac{25605}{512}$	$\frac{64805}{96}$	$\frac{44807}{192}$
2^{nd}	$\frac{1}{144}C_A\left(-96\ \mathrm{d44}+13N_AC_A^4\right)$	$\frac{2217}{256}$	$\frac{16893}{96}$	$\frac{11641}{288}$
3^{rd}	$-\frac{1}{144}C_A\left(96\ \mathrm{d44}+5N_AC_A^4\right)$	$-\frac{855}{256}$	$-\frac{6485}{96}$	$-\frac{4487}{288}$
4^{th}	$\frac{1}{144}C_A\left(-48\ \mathrm{d44}(3N_A-1)+\right.$ $\left.5N_AC_A^4(30N_A-31)\right)$	$\frac{12585}{64}$	$\frac{2708525}{192}$	$\frac{3485153}{576}$
5^{th}	$\frac{1}{144}C_A\left(-48\ \mathrm{d44}(3N_A+1)+\right.$ $\left.N_AC_A^4(38N_A-51)\right)$	$\frac{28155}{256}$	$\frac{920105}{192}$	$\frac{1044617}{576}$
6^{th}	$\frac{1}{24T_R(C_A-6C_R)}\left(48\ \mathrm{d44}C_AT_R+\right.$ $+N_AT_RC_A^4(25C_A-150C_R)+$ $+20C_A^2\ \mathrm{d44}(2+N_A)$ $144\left(-2C_RT_R\ \mathrm{d44}+\right.$ $\left.\left.+\ \mathrm{d444}(2+N_A)\right)\right)$	$\frac{204555}{4096}$	$\frac{48545}{72}$	$\frac{178829}{768}$

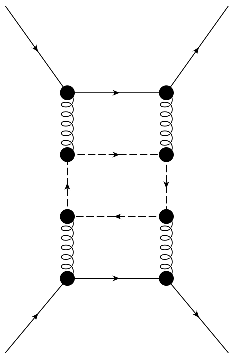

fund.	group invariant	SU(2)	SU(3)	G(2)
1^{st}	$\frac{1}{12}\left(12\ \mathrm{d44}+N_AT_RC_A^2(C_A+12T_R)\right)$	$\frac{4101}{1024}$	27	$\frac{56}{3}$
2^{nd}	$\frac{1}{12}\left(12\ \mathrm{d44}+N_AT_RC_A^2(C_A-12T_R)\right)$	$-\frac{2043}{1024}$	-9	$-\frac{28}{3}$
3^{rd}	$\frac{1}{48}\left(-48\ \mathrm{d44}\left(T_RN_A+(C_A-C_R)\times\right.\right.$ $\left.\times N_R(1+N_R)\right)+$ $+C_A^2\left(-4C_A^2T_RN_AN_R(1+N_R)\right)+$ $+12\left(T_R^3N_A^2+\ \mathrm{d33}N_R(1+N_R)+\right)$ $C_AT_RN_A\left(4C_RN_R(1+N_R)+\right.$ $\left.\left.+T_R(-4N_A+3N_R(1+N_R))\right)\right)$	$-\frac{11565}{1024}$	$-\frac{1265}{8}$	$-\frac{37779}{128}$
4^{th}	$\frac{1}{48}\left(-48\ \mathrm{d44}\left(T_RN_A-(C_A-C_R)\times\right.\right.$ $\left.\times N_R(-1+N_R)\right))+$ $+C_A^2\left(-4C_A^2T_RN_AN_R(-1+N_R)\right)+$ $+12\left(T_R^3N_A^2+\ \mathrm{d33}N_R(-1+N_R)+\right)$ $C_AT_RN_A\left(-4C_RN_R(-1+N_R)+\right.$ $\left.\left.+T_R(-4N_A+3N_R(-1+N_R))\right)\right)$	$\frac{6405}{1024}$	$\frac{6125}{32}$	$\frac{128821}{384}$

C.10. 4-ghost vertex DSE

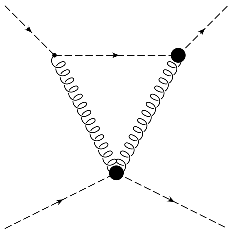

L_1	group invariant	SU(2)	SU(3)	G(2)
1^{st}	$\frac{1}{4}N_A C_A^3$	6	54	28
2^{nd}	$-\frac{1}{4}N_A C_A^3$	-6	-54	-28
3^{rd}	$\frac{5}{2}N_A C_A^2$	30	180	140
4^{th}	$\frac{1}{4}N_A C_A^3(2N_A - 3)$	18	702	700
5^{th}	$\frac{1}{12}N_A C_A^3(1 - 2N_A)$	-10	-270	-252
6^{th}	$\frac{1}{2T_R(C_A-6C_R)}\,(5N_A T_R \times$ $\times C_A^2(C_A - 6C_R)+$ $+12\ \mathrm{d44}(2 + N_A))$	$\frac{3825}{128}$	$\frac{1435}{8}$	$\frac{1113}{8}$

L_2	group invariant	SU(2)	SU(3)	G(2)
1^{st}	$-\frac{3}{4}N_A C_A^3$	-18	-162	-84
2^{nd}	$\frac{1}{4}N_A C_A^3$	6	54	28
3^{rd}	0	0	0	0
4^{th}	$\frac{1}{4}N_A C_A^3(-2N_A + 3)$	-18	-702	-700
5^{th}	$\frac{1}{4}N_A C_A^3(-1 + 2N_A)$	30	810	756
6^{th}	0	0	0	0

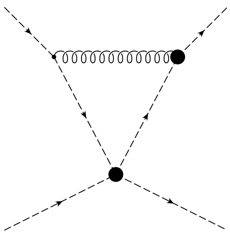

adj.	group invariant	SU(2)	SU(3)	G(2)
1^{st}	$\frac{3}{4}N_A C_A^3$	18	162	84
2^{nd}	$-\frac{1}{4}N_A C_A^3$	-6	-54	-28
3^{rd}	0	0	0	0
4^{th}	$\frac{1}{4}N_A C_A^3(2N_A - 3)$	18	702	700
5^{th}	$\frac{1}{4}N_A C_A^3(1 - 2N_A)$	-30	-810	-756
6^{th}	0	0	0	0

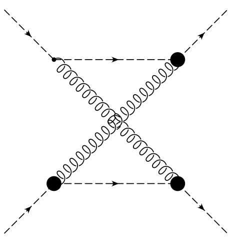

adj.	group invariant	SU(2)	SU(3)	G(2)
1^{st}	$-\frac{1}{2}N_A C_A^3$	-12	-108	-56
2^{nd}	0	0	0	0
3^{rd}	$\frac{5}{2}N_A C_A^2$	30	180	140
4^{th}	0	0	0	0
5^{th}	$\frac{1}{6}N_A C_A^3(-1 + 2N_A)$	20	540	504
6^{th}	$\frac{1}{2T_R(C_A-6C_R)}\,(5N_A T_R C_A^2(C_A - 6C_R)+$ $+12\ \mathrm{d44}(2 + N_A))$	$\frac{3825}{128}$	$\frac{1435}{8}$	$\frac{1113}{8}$

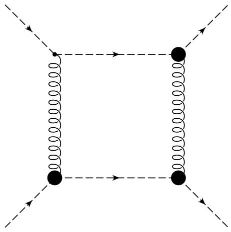

adj.	group invariant	SU(2)	SU(3)	G(2)
1^{st}	$\frac{1}{4}N_AC_A^3$	6	54	28
2^{nd}	$-\frac{1}{4}N_AC_A^3$	-6	-54	-28
3^{rd}	$\frac{5}{2}N_AC_A^2$	30	180	140
4^{th}	$\frac{1}{4}N_AC_A^3(2N_A-3)$	18	702	700
5^{th}	$\frac{1}{12}N_AC_A^3(1-2N_A)$	-10	-270	-252
6^{th}	$\frac{1}{2T_R(C_A-6C_R)}(5N_AT_RC_A^2(C_A-6C_R)+$ $+12\ \mathrm{d44}(2+N_A))$	$\frac{3825}{128}$	$\frac{1435}{8}$	$\frac{1113}{8}$

C.11. 2-gluon-2-ghost vertex DSE

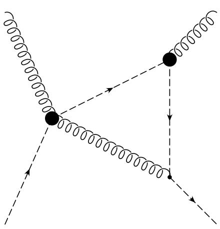

L_1	group invariant	SU(2)	SU(3)	G(2)
1^{st}	$\frac{3}{4}N_AC_A^3$	18	162	84
2^{nd}	$-\frac{1}{4}N_AC_A^3$	-6	-54	-28
3^{rd}	0	0	0	0
4^{th}	$\frac{1}{4}N_AC_A^3(2N_A-3)$	18	702	700
5^{th}	$\frac{1}{4}N_AC_A^3(1-2N_A)$	-30	-810	-756
6^{th}	0	0	0	0

L_2	group invariant	SU(2)	SU(3)	G(2)
1^{st}	$-\frac{1}{2}N_AC_A^3$	-12	-108	-56
2^{nd}	0	0	0	0
3^{rd}	$\frac{5}{2}N_AC_A^2$	30	180	140
4^{th}	0	0	0	0
5^{th}	$\frac{1}{6}N_AC_A^3(1-2N_A)$	20	540	504
6^{th}	$\frac{1}{2T_R(C_A-6C_R)}(5N_AT_R\times$ $C_A^2(C_A-6C_R)+$ $+12\ \mathrm{d44}(2+N_A))$	$\frac{3825}{128}$	$\frac{1435}{8}$	$\frac{1113}{8}$

C. *Results for colour structure of DSE diagrams*

L_1	group invariant	SU(2)	SU(3)	G(2)
1^{st}	$\frac{3}{4}N_A C_A^3$	18	162	84
2^{nd}	$-\frac{1}{4}N_A C_A^3$	-6	-54	-28
3^{rd}	0	0	0	0
4^{th}	$\frac{1}{4}N_A C_A^3(2N_A - 3)$	18	702	700
5^{th}	$\frac{1}{4}N_A C_A^3(1 - 2N_A)$	-30	-810	-756
6^{th}	0	0	0	0

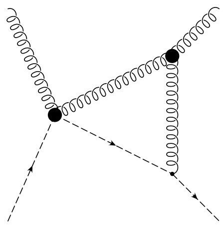

L_2	group invariant	SU(2)	SU(3)	G(2)
1^{st}	$-\frac{1}{4}N_A C_A^3$	-6	-54	-28
2^{nd}	$-\frac{5}{2}N_A C_A^2$	-30	-180	-140
3^{rd}	$\frac{1}{4}N_A C_A^3$	6	54	28
4^{th}	$\frac{1}{4}N_A C_A^3(-2N_A + 3)$	-18	-702	-700
5^{th}	$\frac{1}{12}N_A C_A^3(-1 + 2N_A)$	10	270	252
6^{th}	$-\frac{1}{2T_R(C_A-6C_R)}(5N_A T_R\times$ $\times C_A^2(C_A - 6C_R)+$ $+12\text{ d44}(2 + N_A))$	$-\frac{3825}{128}$	$-\frac{1435}{8}$	$-\frac{1113}{8}$

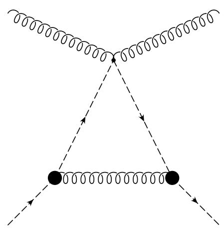

L_1	group invariant	SU(2)	SU(3)	G(2)
1^{st}	$\frac{1}{4}N_A C_A^3$	6	54	28
2^{nd}	$-\frac{1}{4}N_A C_A^3$	-6	-54	-28
3^{rd}	$\frac{5}{2}N_A C_A^2$	30	180	140
4^{th}	$\frac{1}{4}N_A C_A^3(2N_A - 3)$	18	702	700
5^{th}	$\frac{1}{12}N_A C_A^3(1 - 2N_A)$	-10	-270	-252
6^{th}	$\frac{1}{2T_R(C_A-6C_R)}(5N_A T_R\times$ $\times C_A^2(C_A - 6C_R)+$ $+12\text{ d44}(2 + N_A))$	$\frac{3825}{128}$	$\frac{1435}{8}$	$\frac{1113}{8}$

L_2	group invariant	SU(2)	SU(3)	G(2)
1^{st}	0	0	0	0
2^{nd}	$\frac{1}{2}N_A C_A^3$	12	108	56
3^{rd}	0	0	0	0
4^{th}	$\frac{1}{2}N_A C_A^3(-2N_A + 3)$	-36	-1404	-1400
5^{th}	0	0	0	0
6^{th}	0	0	0	0

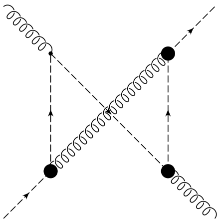

adj.	group invariant	SU(2)	SU(3)	G(2)
1^{st}	$\frac{1}{4}N_A C_A^3$	6	54	28
2^{nd}	$\frac{1}{4}N_A C_A^3$	6	54	28
3^{rd}	$\frac{5}{2}N_A C_A^2$	30	180	140
4^{th}	$\frac{1}{4}N_A C_A^3(-2N_A+3)$	-18	-702	-700
5^{th}	$\frac{1}{12}N_A C_A^3(1-2N_A)$	-10	-270	-252
6^{th}	$\frac{1}{2T_R(C_A-6C_R)}\,(5N_A T_R\times$ $\times C_A^2(C_A-6C_R)+$ $+12\text{ d44}(2+N_A))$	$\frac{3825}{128}$	$\frac{1435}{8}$	$\frac{1113}{8}$

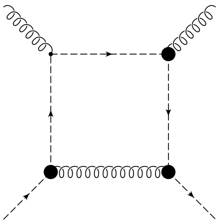

adj.	group invariant	SU(2)	SU(3)	G(2)
1^{st}	$\frac{1}{4}N_A C_A^3$	6	54	28
2^{nd}	$-\frac{1}{4}N_A C_A^3$	-6	-54	-28
3^{rd}	$\frac{5}{2}N_A C_A^2$	30	180	140
4^{th}	$\frac{1}{4}N_A C_A^3(2N_A-3)$	18	702	700
5^{th}	$\frac{1}{12}N_A C_A^3(1-2N_A)$	-10	-270	-252
6^{th}	$\frac{1}{2T_R(C_A-6C_R)}\,(5N_A T_R\times$ $\times C_A^2(C_A-6C_R)+$ $+12\text{ d44}(2+N_A))$	$\frac{3825}{128}$	$\frac{1435}{8}$	$\frac{1113}{8}$

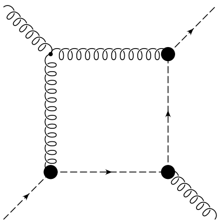

adj.	group invariant	SU(2)	SU(3)	G(2)
1^{st}	$\frac{1}{2}N_A C_A^3$	12	108	56
2^{nd}	0	0	0	0
3^{rd}	$-\frac{5}{2}N_A C_A^2$	-30	-180	-140
4^{th}	0	0	0	0
5^{th}	$\frac{1}{6}N_A C_A^3(1-2N_A)$	-20	-540	-504
6^{th}	$-\frac{1}{2T_R(C_A-6C_R)}\,(5N_A T_R\times$ $\times C_A^2(C_A-6C_R)+$ $+12\text{ d44}(2+N_A))$	$-\frac{3825}{128}$	$-\frac{1435}{8}$	$-\frac{1113}{8}$

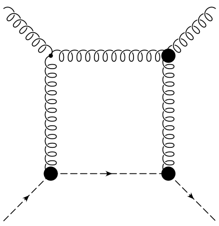

	group invariant	SU(2)	SU(3)	G(2)
1^{st}	$\frac{1}{4}N_A C_A^3$	6	54	28
2^{nd}	$-\frac{1}{4}N_A C_A^3$	-6	-54	-28
3^{rd}	$\frac{5}{2}N_A C_A^2$	30	180	140
4^{th}	$\frac{1}{4}N_A C_A^3(2N_A-3)$	18	702	700
5^{th}	$\frac{1}{12}N_A C_A^3(1-2N_A)$	-10	-270	-252
6^{th}	$\frac{1}{2T_R(C_A-6C_R)}\,(5N_A T_R\times$ $\times C_A^2(C_A-6C_R)+$ $+12\text{ d44}(2+N_A))$	$\frac{3825}{128}$	$\frac{1435}{8}$	$\frac{1113}{8}$

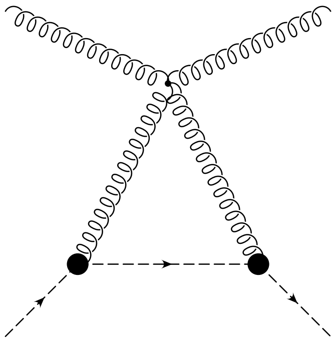

adj.	group invariant	SU(2)	SU(3)	G(2)
1^{st}	$\frac{B+C}{4} N_A C_A^3$	$6(B+C)$	$54(B+C)$	$28(B+C)$
2^{nd}	$\frac{2A+B-C}{4} N_A C_A^3$	$6\,(2A+$ $+B-C)$	$-54\,(2A+$ $+B-C)$	$28\,(2A+$ $+B-C)$
3^{rd}	$\frac{5(B+C)}{2} N_A C_A^2$	$30(B+C)$	$180(B+C)$	$140(B+C)$
4^{th}	$-\frac{2A+B-C}{4} N_A C_A^3 \times$ $\times(2N_A - 3)$	$-18\,(2A+$ $+B-C)$	$-702\,(2A+$ $+B-C)$	$-700\,(2A+$ $+B-C)$
5^{th}	$\frac{B+C}{12} N_A C_A^3 (1-2N_A)$	$-10(B+C)$	$-270(B+C)$	$-252(B+C)$
6^{th}	$\frac{B+C}{2T_R(C_A-6C_R)}\,(5N_A\times$ $\times T_R C_A^2 (C_A - 6C_R)+$ $+12\ \mathrm{d44}(2+N_A))$	$\frac{3825}{128}(B+C)$	$\frac{1435}{8}(B+C)$	$\frac{1113}{8}(B+C)$

C.12. 2-scalar-2ghost vertex DSE

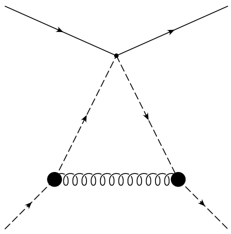

adj.	group invariant	SU(2)	SU(3)	G(2)
1^{st}	0	0	0	0
2^{nd}	$-\frac{1}{2}N_A C_A^3$	-12	-108	-56
3^{rd}	0	0	0	0
4^{th}	$\frac{1}{2}N_A C_A^3(2N_A-3)$	36	1404	1400
5^{th}	0	0	0	0
6^{th}	0	0	0	0

fund.	group invariant	SU(2)	SU(3)	G(2)
1^{st}	0	0	0	0
2^{nd}	$\frac{1}{2}iN_A T_R C_A^2$	$3i$	$18i$	$14i$
3^{rd}	0	0	0	0
4^{th}	$\frac{1}{2}iN_A T_R C_A^2(C_A+2T_R(N_A-1))$	$12i$	$180i$	$210i$
5^{th}	0	0	0	0

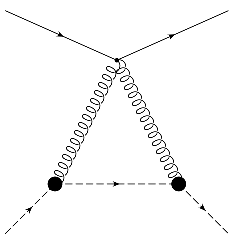

adj.	group invariant	SU(2)	SU(3)	G(2)
1^{st}	$\frac{1}{2}N_A C_A^3$	12	108	56
2^{nd}	0	0	0	0
3^{rd}	$5N_A C_A^2$	60	360	280
4^{th}	0	0	0	0
5^{th}	$\frac{1}{6}N_A C_A^3(1-2N_A)$	-20	-540	-504
6^{th}	$\frac{1}{T_R(C_A-6C_R)}\,(5N_A T_R\times$ $\times C_A^2(C_A-6C_R)+$ $+12\ \mathrm{d44}(2+N_A))$	$\frac{3825}{64}$	$\frac{1435}{4}$	$\frac{1113}{4}$

fund.	group invariant	SU(2)	SU(3)	G(2)
1^{st}	$-\frac{1}{2}N_A T_R C_A^2$	-3	-18	-14
2^{nd}	0	0	0	0
3^{rd}	$-\frac{1}{2}N_A T_R C_A\,(C_A+$ $-4T_R(N_A+1))$	9	90	196
4^{th}	0	0	0	0
5^{th}	$-\frac{N_A T_R C_A}{2N_R(1+N_A)}\,(8C_R+$ $+C_A(-2+N_R+N_A N_R)+$ $-2T_R(1+N_A)\times$ $\times(4+N_R+N_A N_R))$	$\frac{45}{8}$	$\frac{1160}{27}$	$\frac{1421}{15}$

C. *Results for colour structure of DSE diagrams*

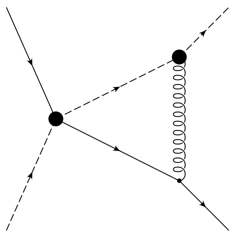

adj.	group invariant	SU(2)	SU(3)	G(2)
1^{st}	$\frac{1}{4}N_A C_A^3$	6	54	28
2^{nd}	$-\frac{1}{4}N_A C_A^3$	-6	-54	-28
3^{rd}	$\frac{5}{2}N_A C_A^2$	30	180	140
4^{th}	$\frac{1}{4}N_A C_A^3(2N_A - 3)$	18	702	700
5^{th}	$\frac{1}{12}N_A C_A^3(1 - 2N_A)$	-10	-270	-252
6^{th}	$\frac{1}{2T_R(C_A-6C_R)}(5N_A T_R\times$ $\times C_A^2(C_A - 6C_R)+$ $+12\ \mathrm{d44}(2 + N_A))$	$\frac{3825}{128}$	$\frac{1435}{8}$	$\frac{1113}{8}$

fund.	group invariant	SU(2)	SU(3)	G(2)
1^{st}	$\frac{1}{4}N_A T_R C_A^2$	$\frac{3}{2}$	9	7
2^{nd}	$-\frac{1}{4}N_A T_R C_A^2$	$-\frac{3}{2}$	-9	-7
3^{rd}	$\frac{1}{4}N_A T_R C_A(C_A - 4T_R(N_A + 1))$	$-\frac{9}{2}$	-45	-98
4^{th}	$-\frac{1}{4}N_A T_R C_A^2(C_A + 2T_R(N_A - 1))$	-6	-90	-105
5^{th}	$\frac{N_A T_R C_A}{4N_R(1+N_A)}(8C_R+$ $+C_A(-2 + N_R + N_A N_R)+$ $-2T_R(1 + N_A)\times$ $\times(4 + N_R + N_A N_R))$	$-\frac{45}{16}$	$-\frac{580}{27}$	$-\frac{1421}{30}$

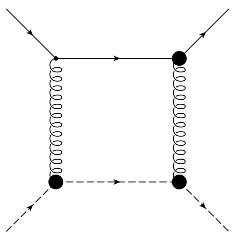

adj.	group invariant	SU(2)	SU(3)	G(2)
1^{st}	$\frac{1}{4}N_A C_A^3$	6	54	28
2^{nd}	$-\frac{1}{4}N_A C_A^3$	-6	-54	-28
3^{rd}	$\frac{5}{2}N_A C_A^2$	30	180	140
4^{th}	$\frac{1}{4}N_A C_A^3(2N_A - 3)$	18	702	700
5^{th}	$\frac{1}{12}N_A C_A^3(1 - 2N_A)$	-10	-270	-252
6^{th}	$\frac{1}{2T_R(C_A-6C_R)}(5N_A T_R\times$ $\times C_A^2(C_A - 6C_R)+$ $+12\ \mathrm{d44}(2 + N_A))$	$\frac{3825}{128}$	$\frac{1435}{8}$	$\frac{1113}{8}$

fund.	group invariant	SU(2)	SU(3)	G(2)
1^{st}	$-\frac{1}{4}N_A T_R C_A^2$	$-\frac{3}{2}$	-9	-7
2^{nd}	$\frac{1}{4}N_A T_R C_A^2$	$\frac{3}{2}$	9	7
3^{rd}	$-\frac{1}{4}N_A T_R C_A(C_A - 4T_R(N_A + 1))$	$\frac{9}{2}$	45	98
4^{th}	$\frac{1}{4}N_A T_R C_A^2(C_A + 2T_R(N_A - 1))$	6	90	105
5^{th}	$-\frac{N_A T_R C_A}{4N_R(1+N_A)}(8C_R+$ $+C_A(-2 + N_R + N_A N_R)+$ $-2T_R(1 + N_A)\times$ $\times(4 + N_R + N_A N_R))$	$\frac{45}{16}$	$\frac{580}{27}$	$\frac{1421}{30}$

Bibliography

[1] H. D. Politzer, *Reliable perturbative Results for Strong Interactions?*, *Phys. Rev. Lett.* **30** (1973) 1346–1349.

[2] D. J. Gross and F. Wilczek, *Ultraviolet Behaviour of non-Abelian Gauge Theories*, *Phys. Rev. Lett.* **30** (1973) 1343–1346.

[3] **Particle Data Group** Collaboration, C. Amsler *et al.*, *Review of particle physics*, *Phys. Lett.* **B667** (2008) 1.

[4] V. N. Gribov, *Quantization of non-Abelian gauge theories*, *Nucl. Phys.* **B139** (1978) 1.

[5] D. Zwanziger, *Renormalizability of the critical limit of lattice gauge theory by BRS invariance*, *Nucl. Phys.* **B399** (1993) 477–513.

[6] D. Zwanziger, *Vanishing of zero momentum lattice gluon propagator and color confinement*, *Nucl. Phys.* **B364** (1991) 127–161.

[7] T. Kugo and I. Ojima, *Local Covariant Operator Formalism of Nonabelian Gauge Theories and Quark Confinement Problem*, *Prog. Theor. Phys. Suppl.* **66** (1979) 1.

[8] M. Bohm, A. Denner, and H. Joos, *Gauge theories of the strong and electroweak interaction*,. Stuttgart, Germany: Teubner (2001) 784 p.

[9] M. E. Peskin and D. V. Schroeder, *An Introduction to quantum field theory*,. Reading, USA: Addison-Wesley (1995) 842 p.

[10] E. Seiler, *Gauge Theories as a Problem of Constructive Quantum Field Theory and Statistical Mechanics*, *Lect. Notes Phys.* **159** (1982) 1–192.

[11] J. Greensite, *The confinement problem in lattice gauge theory*, *Prog. Part. Nucl. Phys.* **51** (2003) 1, `arXiv:hep-lat/0301023`.

[12] G. S. Bali, *QCD forces and heavy quark bound states*, *Phys. Rept.* **343** (2001) 1–136, `arXiv:hep-ph/0001312`.

[13] C. S. Fischer, A. Maas, and J. M. Pawlowski, *On the infrared behavior of Landau gauge Yang-Mills theory*, *Annals Phys.* **324** (2009) 2408–2437, `arXiv:0810.1987 [hep-ph]`.

[14] C. S. Fischer and J. M. Pawlowski, *Uniqueness of infrared asymptotics in Landau gauge Yang- Mills theory*, *Phys. Rev.* **D75** (2007) 025012, `arXiv:hep-th/0609009`.

[15] C. S. Fischer and J. M. Pawlowski, *Uniqueness of infrared asymptotics in Landau gauge Yang- Mills theory II*, *Phys. Rev.* **D80** (2009) 025023, `arXiv:0903.2193 [hep-th]`.

[16] M. Q. Huber, K. Schwenzer, and R. Alkofer, *On the infrared scaling solution of SU(N) Yang-Mills theories in the maximally Abelian gauge*, `arXiv:0904.1873 [hep-th]`.

[17] T. Appelquist and R. D. Pisarski, *High-Temperature Yang-Mills Theories and Three-Dimensional Quantum Chromodynamics*, *Phys. Rev.* **D23** (1981) 2305.

[18] K. Kajantie, M. Laine, K. Rummukainen, and M. E. Shaposhnikov, *Generic rules for high temperature dimensional reduction and their application to the standard model*, *Nucl. Phys.* **B458** (1996) 90–136, `arXiv:hep-ph/9508379`.

[19] H.-C. Cheng, *2009 TASI Lecture – Introduction to Extra Dimensions*, `arXiv:1003.1162 [hep-ph]`.

[20] C.-N. Yang and R. L. Mills, *Conservation of isotopic spin and isotopic gauge invariance*, *Phys. Rev.* **96** (1954) 191–195.

[21] R. Alkofer, W. Detmold, C. S. Fischer, and P. Maris, *Analytic properties of the Landau gauge gluon and quark propagators*, *Phys. Rev.* **D70** (2004) 014014, `arXiv:hep-ph/0309077`.

[22] J. F. Cornwell, *Group Theory in Pysics. VOL. 1*,. London, Uk: Academic (1984) 399 P. (Techniques Of Physics, 7).

[23] J. F. Cornwell, *Group Theory in Pysics. VOL. 2*,. London, Uk: Academic (1984) 589 P. (Techniques Of Physics, 7).

[24] J. F. Cornwell, *Group Theory in Pysics. VOL. 3: Supersymmetries and infinite dimensional Algebras*,. London, UK: Academic (1989) 628 p. (Techniques of physics, 10).

[25] T. van Ritbergen, A. N. Schellekens, and J. A. M. Vermaseren, *Group theory factors for Feynman diagrams*, *Int. J. Mod. Phys.* **A14** (1999) 41–96, `arXiv:hep-ph/9802376`.

[26] M. Pepe, *Confinement and the center of the gauge group*, *PoS* **LAT2005** (2006) 017, `arXiv:hep-lat/0510013`.

[27] J. Greensite, K. Langfeld, S. Olejnik, H. Reinhardt, and T. Tok, *Color screening, Casimir scaling, and domain structure in G(2) and SU(N) gauge theories*, *Phys. Rev.* **D75** (2007) 034501, `arXiv:hep-lat/0609050`.

[28] C. Gattringer and C. B. Lang, *Quantum chromodynamics on the lattice*, *Lect. Notes Phys.* **788** (2010) 1–211.

[29] J. M. Pawlowski, *Aspects of the functional renormalisation group*, *Annals Phys.* **322** (2007) 2831–2915, `arXiv:hep-th/0512261`.

[30] L. von Smekal, R. Alkofer, and A. Hauck, *The infrared behavior of gluon and ghost propagators in Landau gauge QCD*, *Phys. Rev. Lett.* **79** (1997) 3591–3594, `arXiv:hep-ph/9705242`.

[31] F. J. Dyson, *The S matrix in quantum electrodynamics*, *Phys. Rev.* **75** (1949) 1736–1755.

[32] J. S. Schwinger, *On the Green's functions of quantized fields. 1*, *Proc. Nat. Acad. Sci.* **37** (1951) 452–455.

[33] R. Alkofer, M. Q. Huber, and K. Schwenzer, *Algorithmic derivation of Dyson-Schwinger Equations*, *Comput. Phys. Commun.* **180** (2009) 965–976, `arXiv:0808.2939 [hep-th]`.

[34] R. Alkofer, C. S. Fischer, and F. J. Llanes-Estrada, *Vertex functions and infrared fixed point in Landau gauge SU(N) Yang-Mills theory*, *Phys. Lett.* **B611** (2005) 279–288, `arXiv:hep-th/0412330`.

[35] R. Alkofer, C. S. Fischer, M. Q. Huber, F. J. Llanes-Estrada, and K. Schwenzer, *Confinement and Green functions in Landau-gauge QCD*, *PoS* **CONFINEMENT8** (2008) 019, `arXiv:0812.2896 [hep-ph]`.

[36] C. Lerche and L. von Smekal, *On the infrared exponent for gluon and ghost propagation in Landau gauge QCD*, *Phys. Rev.* **D65** (2002) 125006, `arXiv:hep-ph/0202194`.

[37] M. Q. Huber, *On gauge fixing aspects of the infrared behavior of Yang- Mills Green functions*, `arXiv:1005.1775 [hep-th]`.

[38] J. Braun, H. Gies, and J. M. Pawlowski, *Quark Confinement from Color Confinement*, *Phys. Lett.* **B684** (2010) 262–267, `arXiv:0708.2413 [hep-th]`.

[39] A. Maas, *Constructing non-perturbative gauges using correlation functions*, *Phys. Lett.* **B689** (2010) 107–111, `arXiv:0907.5185 [hep-lat]`.

[40] W. Caudy and J. Greensite, *On the Ambiguity of Spontaneously Broken Gauge Symmetry*, *Phys. Rev.* **D78** (2008) 025018, `arXiv:0712.0999 [hep-lat]`.

[41] L. Fister, *Infrared Behaviour of Landau Gauge Yang-Mills Theory with a Fundamentally Charged Scalar Field*, `arXiv:1002.1649 [hep-th]`.

[42] L. Fister, R. Alkofer, and K. Schwenzer, *On the Infrared Behavior of Landau Gauge Yang-Mills Theory with a Fundamentally Charged Scalar Field*, *Phys. Lett.* **B688** (2010) 237–243, `arXiv:1003.1668 [hep-th]`.

[43] P. Cvitanovic, *Group Theory: Birdtracks, Lie's, and Exceptional Groups*. Princeton University Press, 2010.

[44] A. Cucchieri, A. Maas, and T. Mendes, *Exploratory study of three-point Green's functions in Landau-gauge Yang-Mills theory*, *Phys. Rev.* **D74** (2006) 014503, `arXiv:hep-lat/0605011`.

[45] A. Cucchieri, A. Maas, and T. Mendes, *Three-point vertices in Landau-gauge Yang-Mills theory*, *Phys. Rev.* **D77** (2008) 094510, `arXiv:0803.1798 [hep-lat]`.

[46] A. Maas, *Two- and three-point Green's functions in two-dimensional Landau-gauge Yang-Mills theory*, *Phys. Rev.* **D75** (2007) 116004, `arXiv:0704.0722 [hep-lat]`.

[47] C. Kellermann and C. S. Fischer, *The running coupling from the four-gluon vertex in Landau gauge Yang-Mills theory*, *Phys. Rev.* **D78** (2008) 025015, `arXiv:0801.2697 [hep-ph]`.

[48] J. A. M. Vermaseren, *New features of FORM*, `arXiv:math-ph/0010025`.